박 사 학 위 논 문

Ph.D. Dissertation

토양-수분-하이드로겔 상호작용을 고려한 바이오폴리머 처리토의 특성파악

Characterization of Biopolymer-Treated Soils Considering Soil-Water-Hydrogel Interaction

2019

An Thi Phuong TRAN

한 국 과 학 기 술 원

Korea Advanced Institute of Science and Technology

박 사 학 위 논 문

Characterization of Biopolymer-Treated Soil Considering Soil-Water-Hydrogel Interaction

2019

An Thi Phuong TRAN

한 국 과 학 기 술 원

건설 및 환경공학과

Characterization of Biopolymer-Treated Soil Considering Soil-Water-Hydrogel Interaction

An Thi Phuong TRAN

위 논문은 한국과학기술원 박사학위논문으로
학위논문 심사위원회의 심사를 통과하였음

2019년 05월 29일

심사위원장 조 계 춘 (인)
심 사 위 원 이 승 래 (인)
심 사 위 원 김 동 수 (인)
심 사 위 원 권 태 혁 (인)
심 사 위 원 정 문 경 (인)
심 사 위 원 장 일 한 (인)

Characterization of Biopolymer-Treated Soil Considering Soil-Water-Hydrogel Interaction

An Thi Phuong TRAN

Advisor: Gye-Chun Cho
Joint-Advisor: Ilhan Chang

A dissertation/thesis submitted to the faculty of
Korea Advanced Institute of Science and Technology in
partial fulfillment of the requirements for the degree of
Doctor of Philosophy in Electrical Engineering

Daejeon, Korea

May 29, 2019

Approved by

Gye-Chun Cho, KAIST
Professor of Civil and Environmental Engineering

Ilhan Chang, UNSW
Senior lecturer, School of Engineering and Information Technology (SEIT)

The study was conducted in accordance with Code of Research Ethics[1)].

1) Declaration of Ethical Conduct in Research**:** I, as a graduate student of Korea Advanced Institute of Science and Technology, hereby declare that I have not committed any act that may damage the credibility of my research. This includes, but is not limited to, falsification, thesis written by someone else, distortion of research findings, and plagiarism. I confirm that my dissertation contains honest conclusions based on my own careful research under the guidance of my advisor.

CEE
20145586

토양-수분-하이드로겔 상호작용을 고려한 바이오폴리머 처리토의 특성파악. 건설및환경공학과. 2019년. 127+viii 쪽. 지도교수: 조계춘. (영문 논문)

An Thi Phuong TRAN. Characterizaion of Biopolymer-treated Soil Considering Soil-Water-Hydrogel Interaction. Department of Civil and Environmental Engineering. 2019. 127+viii pages. Advisor: Gye-Chun Cho. (Text in English)

초 록

최근 미생물 기반 바이오폴리머를 이용한 흙 처리와 지반 보강 기술이 활발히 연구되고 있다. 바이오폴리머 처리토는 토양-수분-하이드로겔 상호작용으로 인해 강도 증진, 투수계수 감소, 비산먼지 및 표면 침식 억제 등의 공학적 거동을 갖는 것으로 알려져 있으나, 구체적인 연구는 이루어지지 않고 있는 실정이다. 바이오폴리머를 이용한 지반공학적 적용은 외부 환경(강우 및 온도)의 영향을 많이 받는 표층 및 천층을 주 대상으로 하고 있는 실정이다. 따라서 표층의 토양 함수 특성 변화에 따른 바이오폴리머 처리토의 강도와 기타 지반공학적 물성들의 거동에 대한 연구가 필요하다. 아울러 바이오폴리머 처리토의 투수계수 조절 기능에 대한 구체적인 이해를 통해 바이오폴리머 처리토의 적용 분야를 차수벽 또는 지반주입재로의 확장 가능성에 대한 타당성 검토 수행도 가능할 것으로 기대된다.

본 연구의 목표는 토양-수분-바이오폴리머 하이드로겔의 상호작용을 고려한 바이오폴리머 처리토의 토양-수분 특성과 투수성을 파악하는 것이다. 이를 위해 물 흡습 시 하이드로겔을 형성하는 바이오폴리머인 잔탄검과 젤란검을 주 재료로 사용하였다. 다양한 실내실험을 통해 바이오폴리머 처리토의 토양-수분 특성 곡선, 가압조건에서의 투수계수, 중금속 흡착능, 그리고 식생생장 거동을 평가하였다. 특히 실험결과를 통해 바이오폴리머 처리토를 매립지 등지에서 적용할 수 있는 타당성을 검토하였다. 또한 본 연구를 통해 토양-수분 관점에서 각 바이오폴리머 별 최적 적용 조건을 도출하였다.

건조 및 습윤 상태에서의 토양 - 수분 특성은 바이오폴리머가 흙의 흡습율과 수분 함유율을 증진시키는 특성과 동시에 토양의 모세관 전도성을 감소시킴을 보였다. 점토가 혼합된 흙의 경우 점토 종류에 따라 바이오폴리머 처리 토양이 매우 상이한 습윤 거동을 보임이 확인되었다. 높은 수압 조건에서도 열적젤화 된 바이오폴리머 고분자 처리토는 높은 수분 흡수 및 보유 능력은 물론 투수계수 저감 효과가 높음을 실험을 통해 밝혀냈다. 특히 카올린 점토와 바이오폴리머 간 형성되는 바이오폴리머-점토 매트릭스 더 높은 압력 조건에서도 우수한 투수계수 저감 효과가 있는 것이 확인되었다. 한편, 바이오폴리머의 이온 흡착능은 토양의 중금속 제거에도 효과가 있음이 실내 중금속 여과 실험을 통해 확인되었다. 표준 니켈 중금속 오염시액을 젤란검 처리된

사질토에 여과 시 니켈 중금속의 제거능은 바이오폴리머의 농도와 유효표면적이 증거함에 따라 높아짐이 확인되었다.

일반적으로 바이오폴리머 처리토의 토양-수분특성은 바이오폴리머를 활용한 토양 침식 억제, 식생 생장 증진, 강우 시 비탈면 안정화 증진 등 다양한 분야에 활용될 수 있을 것으로 기대된다. 아울러 중금속 흡착능은 지하수 처리 또는 폐기물 매립지 분야 등에서 활용 가능할 것으로 보여지고, 사막화 확산 방지 등 다양한 지속가능한 공학 분야로의 적용이 기대된다.

핵 심 낱 말 바이오폴리머 처리토, 토양-수분 특성 곡선, 가압조건에서의 투수계수, 중금속 흡착능, 식생생장 거동

Abstract

Microbial biopolymers have recently been introduced as a new material for soil treatment and ground improvement. The engineering properties of biopolymer-treated soil are determined by the soil-water-hydrogel interactions, which allows biopolymers to show excellent performances in soil strengthening, reduction in hydraulic conductivity, dust control, reduction in surface erosion, and so on. Typical applications of biopolymer are for surface treatment and building materials, which are sensitive to weathering conditions such as rainfall and temperature. Weathering conditions determine the water distribution in biopolymer-soils as well as the relationship between water content and strengthening effects of biopolymer-soils. Furthermore, with biopolymer-soils' controllability of water flow, it may be suggested as a hydraulic barrier or grouting material.

The aim of this study is to have an understanding of the water-related properties of biopolymer-treated soil, considering the effects of external conditions on the soil-water-hydrogel interaction. To meet the objective of this study, xanthan gum and gellan gum were used for this study. Soil-water characteristic, pressurized hydraulic conductivity, heavy metal adsorption were main laboratory tests conducted in this study. In order to introduce the applicability of biopolymer-treated soil, additional testing on vegetation growth in a controlled chamber and numerical modeling on rainfall-induced slope failure retention were carried out. Furthermore, based on the experimental data, a potential as a landfill material using of biopolymer-treated soil was also provided. Through the study, biopolymer types and optimal content were suggested for different geotechnical engineering purposes.

The drying and wetting soil-water characteristics show that biopolymer can improve the water storage in soil and reduce the capillary conductivity of soil via water absorbing and holding capacity. The presence of clay admixture can render different wetting behavior of biopolymer-treated soil corresponding to clay types. Even under a high water pressure, the water absorbing and holding capacity of thermo-gelatin biopolymers, allows the treated-soil to be able to hold its structure and restrict the water movement through the soil system. The biopolymer-kaolinite matrix enhances the hydraulic reduction performance of biopolymer. Furthermore, ion adsorbability of biopolymers enhances the heavy metal removability of soil. The metal removability from a contaminated flow increases proportionally with biopolymer concentration.

In general, the water-related properties of biopolymer-treated soil brings a promising future of using biopolymer to improve drought survivability of vegetation and rainfall-induced slope stabilization. In addition, the water flow controllability and ion removability of biopolymer allow biopolymer-treated soil can be used as a hydraulic barrier.

Keywords biopolymer-treated soil, soil-water characteristic, pressurized hydraulic conductivity, vegetation, heavy metal adsorption.

Table of Contents

List of Tables

List of Figures

Chapter 1. Introduction

1.1 Background of biopolymer–soils

The drastic increase in the global population is a major reason for the unprecedented rate of expansion for civil infrastructures. One of the developments of civil infrastructures tend to demand promising and sustainable methods of soil improvement, with more than 40,000 soil improvement projects being performed per year at a total cost exceeding US$6 billion/year worldwide (DeJong et al. 2010).

The primary purpose of soil improvement methods is to increase soil stiffness and reduce soil hydraulic permeability, water infiltration. There are four main categories in the soil improvement technique: (1) soil improvement without admixture, which is known as mechanical stabilization; (2) soil improvement with admixture (e.g. microbial methods and sand compaction piles, etc.); (3) soil improvement grouting type admixtures (e.g. chemical stabilization, deep mixing, etc.); and (4) earth reinforcement (e.g. ground anchors, vegetation methods, etc.) (Chu et al. 2009). Mechanical stabilization and earth reinforcement are not the main subjects of this thesis and will not be further discussed.

The majority of the admixture methods is that soil stabilization mainly depends on the chemical reaction between the additives, which are injected into the pore space of soil, and are mixed with the natural soil to achieve the desired effect (Makusa 2012) via binding soil particles together. Common additive and grouting materials are cement, fly ash, bituminous materials, and sodium silicate polyacrylamides (PAM), or a combination of these materials. However, these materials generally exhibit a negative influence on the. Fly ash and cement have significant environmental impacts associated with its production in terms of high-energy consumption and CO2 emissions (Gaafer et al. 2015). The production of bitumen is responsible for 90% human and eco toxicity (Mazumder et al. 2016). Additionally, the residual monomer of PAM is a reproductive and development in humans (Dearfield et al. 1988), and it can cause long-term effects on human breast tissue (Christensen et al. 2003), and skin (Igisu et al. 1975).

Recently, interest in the use of biomineralization technologies such as microbially induced calcite precipitation (MICP) and living microorganism induced polymer (i.e. biopolymers) in geotechnical engineering has been rising over the last decade. Several studies have attempted to explain the hydraulic reduction and strength improvement of MICP (Cheng et al. 2013; Soon et al. 2013; Whiffin et al. 2007) and biopolymers (Chang and Cho 2019; Chang et al. 2016; Khatami and O’Kelly 2012) in soils. MICP was presented as an alternative method of soil improvement; however, there are several drawbacks in the application of MICP. MICP is affected by many factors for bacterial

ureolysis and the subsequent calcium carbonate precipitation such as pH value (Ivanov and Stabnikov 2017), soil structure, and soil components (Rong et al. 2011). Furthermore, several by-products of urea hydrolysis is ammonium and ammonia that are toxic substances for workers, harmful for the aquatic environment and atmosphere, and increases the risk of corrosion due to its high pH (Pacheco-Torgal and Jalali 2011). Meanwhile, biopolymers have the advantages of direct in field applications compared to MICP since biopolymers can be produced off site. Biopolymers has been studied for soil strengthening, soil permeability control, and erosion reduction, dust control, and drinking water treatment (Chang et al. 2016; Chang et al. 2015a; Chang et al. 2015d; Chen et al. 2013a; Zemmouri et al. 2013).

1.2 Main objective of this study

The direct biological attempt using common commercial biopolymers: xanthan gum, gellan gum were used in this study. While gellan gum hydrogel can form hard gels through heating above 90° and cooling process, xanthan gum hydrogel does not change its properties with temperature. These biopolymers have been researched for soil strengthening (Chang and Cho 2019; Chang et al. 2015a; Chang et al. 2015c; Khatami and O'Kelly 2012; Kulshreshtha et al. 2017), and hydraulic reduction (Bouazza et al. 2009; Chang et al. 2016). However, the detailed understandings on the effects of xanthan gum and gellan gum via inducing soil-water-hydrogel interaction on geotechnical engineering properties of soils such as water retention behavior, hydraulic conductivity concerning external pressures, and ion control have not been deeply studied. Furthermore, the interaction mechanism of soil-water-hydrogel in the soil system and their optimized biopolymer condition has been undiscovered.

The standard jumujin sand of Korea is the main objective material used in this study. Furthermore, kaolinite and montmorillonite clay were used as admixture materials to observe the effects of clay particles on the performance of biopolymers on sand treatment. In this thesis, xanthan gum and gellan gum are introduced to improve the water-related properties of jumunjin sand. A series of experimental studies performed to investigate the soil-water-hydrogel interaction mechanisms was soil-water characteristic test, pressurized hydraulic conductivity, and heavy metal ion adsorption tests. In order to introduce the applicability of biopolymer-treated soils, additional testing on vegetation growth in a controlled chamber and numerical modeling on rainfall-induced slope failure retention were carried out. Furthermore, based on the experimental data, a potential as a landfill materials of using biopolymer-treated soils was also provided. Through the study, biopolymer types and optimal content were suggested for different geotechnical engineering purposes.

1.3 Scope – organization

The thesis consists of 7 chapters: starting with a brief Introduction (present chapter) followed by an extensive literature review (Chapter 2), which expresses commonly used biopolymer and their up-to-date applications in geotechnical engineering. The literature review also presents a brief introduction on unsaturation soil mechanics, hydrogels, hydraulic conductivity, ion-hydrogel interaction, and soil materials. This is followed by three experimental chapters (3 – 5) and a practical application chapter (6). Finally, in Chapter 7, the Conclusions, and Further Recommendations are presented.

Chapter 3 presents water absorbing and holding properties of sand treated by xanthan gum. Laboratory attempts on wetting, drying soil water characteristic testing are performed to discover water distribution in xanthan-treated sand. Furthermore, this chapter also provides the role of clay admixture – xanthan gum interaction in the water retention performance of xanthan gum–treated sand. Emphasis is placed on water holding performance concerning xanthan gum content and soil types, compared to untreated soil materials.

Chapter 4, extending from the knowledge on water absorbing and holding capacities of biopolymers gathered in Chapter 3, assesses the performance in flow control of biopolymer treated sand in consideration of external pressures (i.e., pore water pressure and effective stress). A reason for using gellan gum in this chapter is explained. Besides providing the role of soil particles – gellan gum hydrogel – water interaction in reducing hydraulic conductivity of sand via pore-clogging, the effect of kaolinite on the hydraulic conductivity behavior of gellan gum-treated sand is shown. Based on obtained results an empirical equation is suggested to predict the hydraulic conductivity of gellan gum–treated sand, and the optimized biopolymer concentration is indicated in this chapter.

Chapter 5 expresses the ability of gellan gum on improving the metal ion adsorption of sand. This chapter investigates on nickel removal capacity of gellan gum treated sand from a nickel contaminated solution. Besides providing an insight into the adsorption mechanisms of gellan gum-nickel and sand – nickel via adsorption isotherm, kinetic studies, and surface morphology, the role of pore-clogging effect on nickel adsorption is emphasized.

Chapter 6 addresses practical applications of biopolymer-treated soil. From wetting SWCC parameters obtained from Chapter 3, numerical modeling on slope stability during rainfall is developed. Water retention improvement for soil of xanthan gum brings out the idea of providing water storage in sand for perennial ryegrass, which is also mentioned in this chapter. Including results obtained from previous chapter, a potential in landfill materials of biopolymer- treated soil is provided.

Finally, salient conclusions and recommendations for further study were summarized in Chapter 7.

Chapter 2. Literature review

2.1 Application of microbial biopolymers in geotechnical engineering

2.1.1 Biopolymer materials used in geotechnical engineering

2.1.1.1 Agar gum

Agars, a seaweed biopolymer (Lee et al. 2017), are linear polymers based on a disaccharide repeat structure of 3-linked β-D-galactopyranosyl and 4-linked 3,6-anhydro-α-L-galactopyranosyl units (Araki 1966). The most important property of agar is its capable of forming reversible gels simply by cooling hot aqueous solutions without the need for further reactions with other products or the introduction of a counter-ion, unlike carrageenans and alginates (Imeson 2012).

Agar gum is widely used in gelling, thickening, and stabilizing food additive (Imeson 2012), and has medical-industrial applications such as drug delivery (Nakano et al. 1979), DNA information (Dumitriu 2004), and dermatophyte recovery (Adachi and Watanabe 2007). Furthermore, as agar gum has rheological properties, it recently has been used to improve the strength of cohesionless soil without causing environmental toxicity (Chang et al. 2015c; Khatami and O'Kelly 2012; Smitha and Sachan 2016).

2.1.1.2 Guar gum

Guar gum, which is extracted from the seeds of plant *Cyamopsis tetragonoloba* (Lapasin 2012), consists of a (1-4) – linked β-D-mannopyranose backbone with random branchpoints of α-D galactose units (Risica et al. 2005). Guar gum is applied in many industries such as food (Mudgil et al. 2014; Whistler and Hymowitz 1979), pharmacy (Chourasia and Jain 2004; Khullar et al. 1998), paper (Chudzikowski 1971), and textile (Parija et al. 2001).

To geotechnical engineering, guar gum can be used to stabilize mine tailings to improve impoundment stability and erosion resistance by enhancing the undrained shear of mine tailings (Chen et al. 2015). Guar gum is used for grouting stabilization of sand for construction works in desert areas (Gupta et al. 2009), and used as an installation aid for the permeable reactive barrier wall construction in Belgium, Canada (Velimirovic et al. 2014). Guar gum also shows potential in ion removing from wastewater (Mukherjee et al. 2018).

2.1.1.3 Gellan gum

Gellan gum is a linear anionic polysaccharide manufactured by microbial fermentation of *Sphingomonas paucimobilis* microorganism (Oliveira et al. 2010). The primary structure of gellan gum is a tetra-saccharide unit composed of α-$_L$-rhamnose, β-$_D$-glucose, and β-$_D$-glucuronate, in the molar ratios 1:2:1 (Jansson et al. 1983).

In general, gellan gum is used as a food additive because in the food industry (Giavasis et al. 2000), oral drug delivery in pharmaceutical technology, and in the biomedical application such as tissue engineering, surgery and wound healing (Osmałek et al. 2014). Furthermore, it can be used in bioremediation of soil, particularly in petroleum contaminated soil, because of its bio-degradative property (Giavasis et al. 2000). Recently, gellan gum has been researched in soil strengthening and hydraulic reducing (Chang and Cho 2019; Chang et al. 2016)

2.1.1.4 Dextran

Dextran, which is produced by bacteria of *Leuconostoc mesenteroid*, is consist of α(1,6)-linkages in their major chain (Myriam et al. 2005). Dextrans are mainly used for medical (Bouhadir et al. 2001; Kaplan 1998; Lévesque et al. 2005), analytical (Auerbach et al. 1988) applications, food industry as a soluble macromolecule emulsifier (Kato et al. 1988) and paper industry (Myriam et al. 2005). For geotechnical engineering, dextran is used to improve the workability of oil drilling muds (Horace et al. 1944) and cement mixtures (Kato et al. 1988). Dextrans can be used as potential soil conditioners (Pini et al. 1994).

2.1.1.5 β-1,3-glucan

The main chain consisting of (1,3)-linked β-D-glucopyranosyl units along which are randomly dispersed single β-D-glucopyranosyl units attached by (1,6) linkages, giving a comb-like structure, is a common structure of β - glucan (Bohn and BeMiller 1995). Curdlan amd Scleroglucan are popular biopolymers in this group, which have been subjected to experimental testing for geotechnical purposes.

Scleroglucan is produced by an aerobic submerged culture of a selected strain of the fungus *Sclerotium rolfsii* (Castillo et al. 2015). It is a multipurpose compound that is applicable in many industrial fields, including the oil industry (Survase et al. 2007), and pharmaceutical industry (Kulicke et al. 1997; Viñarta et al. 2007). Furthermore, in conventional building products, scleroglucan has found a niche application in asphalt emulsions (Kulicke et al. 1997; Pierre et al. 1993). Scleroglucan is also studied to improve water retention of soils (Chenu 1989).

Curdlan, which is produced by pathogenic *Alicagenes faecalis* bacteria (Poli et al. 2011), has many positive performances in the food industry (Kaplan 1998), biomedical application (Bohn and BeMiller 1995; Zhan et al. 2012), and cosmetical industry (Davis 1992; Takanabe et al. 2001). To geotechnical engineering application, curdlan effectively reduces residual contaminants (D'Cunha et al. 2009) and controls hydraulic conductivity as a pore-clogging agent (Ivanov and Stabnikov 2017). Furthermore, curdlan has been used as an additive in concrete mixtures as a superplasticizer to improve workability and prevent cement-aggregate separation (Tanaka et al. 1996).

2.1.1.6 Xanthan gum

Xanthan gum is an anionic water-soluble exopolysaccharide that is synthesized by the *Xanthomonas campestris* bacterium (Poli et al. 2011). Xanthan gum is composed mainly of D-glucose chains linked via β(1→4) bonds, with side chains consisting of D-mannose and D-glucuronic acid at a ratio of 2:1 (Babbar and Jain 2006; Candia and Deckwer 2002).

Xanthan gum has been popularly used as an emulsifier, suspension stabilizer, flocculant, and thickening agent in various industrial applications such as food, agriculture and petroleum production (García-Ochoa et al. 2000; Katzbauer 1998; Palaniraj and Jayaraman 2011). Recently, there are many researches on the applicability of xanthan gum in soil strengthening, soil binding improvement (Ayeldeen et al. 2016; Chang et al. 2015a; Latifi et al. 2016; Yang et al. 2007)

2.1.1.7 Chitosan

Chitosan is derived by deacetylation of biopolymer chitin, and it is also found in the cell wall of fungi (Chatterjee et al. 2005). Chitosan is composed of randomly distributed β-(1-4)-linked D-glucosamine and N-acetyl-D-glucosamine (Islam et al. 2017). The application of chitosan includes a variety of areas such as food preservation as active coating materials (Aider 2010), biomedical engineering (Islam et al. 2017), agriculture as biopesticides and fertilizers (Hirano et al. 1996), paper industry (Tang et al. 2016), and cosmetics (Jimtaisong and Saewan 2014).

Regarding geotechnical and geoenvironmental applications, chitosan has been used in wastewater treatment (Lee et al. 2014; Liu et al. 2002; Renault et al. 2009). Chitosan also shows promising potential in increasing the plugging effect of soil via reducing the hydraulic conductivity of sandy soil by coating the sand particles (Khachatoorian et al. 2003b).

2.1.1.8 Starch

Starches, which are mostly found in plants (Poli et al. 2011), are polysaccharides, composed of a number of monosaccharides or sugar molecules linked together with α-D-(1-4) and/or α-D-(1-6) linkages (Rodrigues and Emeje 2012). Starch is widely used in industries as diverse as food (Eliasson 2004), adhesives (Vishnuvarthanan and Rajeswari 2013), paper (Nachtergaele 1989) and pharmaceuticals (Rodrigues and Emeje 2012).

In geotechnical engineering, starches have been applied as an adhesive for drilling fluids (Francis et al. 1987), soil strengthening and permeability control (Ayeldeen et al. 2016). Furthermore, starch can reduce erosion by aggregating the soil particles (Lentz et al. 1992; Orts et al. 2000)

Table 2.1 provides source, structure and applications of these common biopolymers

Table 2.1 Source, structure and applications of biopolymers

Biopolymer	Source	Structure	Application
Agar gum	Isolated from red algae	3-linked β-D-galactopyranosyl and 4-linked 3,6-anhydro-α-L-galactopyranosyl units	Food industry: Food additive Medical industry: drug delivery system, dermatophyte recovery Geotechnical: Soil strengthening
Guar gum	Extracted from seeds of *Cyamopsis tetragonoloba*	(1,4) – linked β-D-mannopyranose backbone	Food industry: stabilizer, emulsifier, thickener Textile industry: gelling and thickening agent Pharmaceutical applications: thickening agent, release agent, emulsifier. Paper industry Geotechnical engineering: grouting stabilization, initialization aid, heavy metal adsorbent
Gellan gum	Produced by microbial fermentation of *Sphingomonas paucimobilis* microorganism	α-$_{L}$-rhamnose, β-$_{D}$-glucose, and β-$_{D}$-glucuronate	Food industry: food additive Pharmaceutical engineering: oral drug delivery Biomedical applications: tissue engineering, surgery and would healing Geotechnical engineering: soil strengthening, hydraulic reducing
Dextran	Produced by bacteria of *Leuconostoc mesenteroid* bacteria	α(1,6)-linkages	Food industry: emulsifier Medical industry: Blood plasma extender, industrial separation of plasma protein, tissue engineering Paper industry: explosives, deflocculants Geotechnical engineering: drilling muds, cement additive, soil conditioner
Scleroglucan	Produced by fungus *Sclerotium rolfsii* bacteria	(1,3)-linked β-D-glucopyranosyl units	Oil industry Pharmaceutical industry: drug delivery vehicle Cosmetic industry: thickener Geotechnical engineering: asphalt emulsions, soil water retention

Curdlan	Produced by pathogenic *Alicagenes faecalis* bacteria	(1,3)-linked β-D-glucopyranosyl units	Food industry: stabilizer, water binder and holder Biomedical technology: enzyme carrier Cosmetic industry: water holder Geotechnical engineering: pore-clogging agent, superplasticizer for cement
Xanthan gum	Synthesized by the *Xanthomonas campestris* bacterium	β(1,4)-linked D-glucose	Food industry: emulsion stabilizer Agriculture industry: stabilizer Petroleum production: slurry explosives Geotechnical engineering: soil binder
Chitosan	- derived by deacetylation of biopolymer chitin - found in cell wall of fungi	β-1,4-glucosamine	Food industry: coating materials Biomedical engineering: Paper industry: wound-healing management products, biocompatible materials Agriculture: biopesticides and fertilizers Geotechnical engineering: wastewater treatment, hydraulic reduction of soil
Starch	Found in plant	α-D-(1-4) and/or α-D-(1-6) linkages	Food industry: thickeners and stabilizers Pharmaceutical engineering: binder, diluent, disintegrant Paper industry: paper strengthening Geotechnical engineering: soil strengthening, soil erosion controller, hydraulic controller

2.1.2 Current biopolymer applications in geotechnical engineering practices

2.1.2.1 Soil strengthening purposes

Biopolymers increase the strength of soil via enhancing the binding ability between soil particles. Biopolymer can coat grain particles via forming thread or textile type matrices, while biopolymer interacts with clay particles directly via hydrogen bonding (Chang et al. 2015a). The hydrogen bonding is conducted by functional groups such as hydroxyls, carboxyl, and amino group, depending on biopolymer types.

Previous studies, through testing the compressive strength and shear strength of soil, have found that xanthan gum, starch, guar gum, agar gum, and gellan gum increase the shear strength of soil particles, especially cohesion (Ayeldeen et al. 2017; Chang and Cho 2012; Chang et al. 2016; Chang et al. 2015c; Khatami and O'Kelly 2012; Latifi et al. 2016). To sand, the biopolymers coat soil particles and may decrease the particle roughness, thereby, in some cases, leading to a minor decrease in the friction angle of sand (Fig. 2.1a). The results indicated that the friction angle of sand decreased from 32.3° to 17.5° as it is treated by agar-starch mixture (Khatami and O'Kelly 2012). Meanwhile, biopolymers increase the friction angle of clay via a strong biopolymer – clay matrix (Fig. 2.1b). The effect of biopolymer on cohesion and friction angle, in turn, affects the strengthening behavior of the soil system (Fig 2.2a & b). Furthermore, with a small amount of beta-glucan, the compressive strength of soil reaches 2,650 kPa, which is stronger than that of 10% cement-mixed soil (2,170 kPa) (Chang and Cho 2012). Therefore, biopolymer has strong potential for the use of soil or ground strengthening purposes.

2.1.2.2 Erosion resistance purposes

Many studies have been conducted to investigate the applicability to wind and water erosion using biopolymers (Chang et al. 2015d; Kavazanjian et al. 2009; Larson et al. 2012; Orts et al. 2007; Orts et al. 2000). Biopolymers improve the stability and surface erosion resistance of slope and dam construction based on interaction mechanism such as bio-aggregation, bio-crusting, bio-coating, bio-clogging, bio-cementation (Stabnikov et al. 2015)

Figure 2.3 shows the effectiveness of using biopolymer in soil erosion via laboratory tests. In which, xanthan gum and chitosan treated sand perform a significant erosion resistance where the amount of soil runoff is less than 1% (Kavazanjian et al. 2009). The experimental laboratory results show a promising potential of using biopolymers in soil erosion control. However, the in situ environmental condition results in different erosion behavior than laboratory test (Orts et al. 2000)

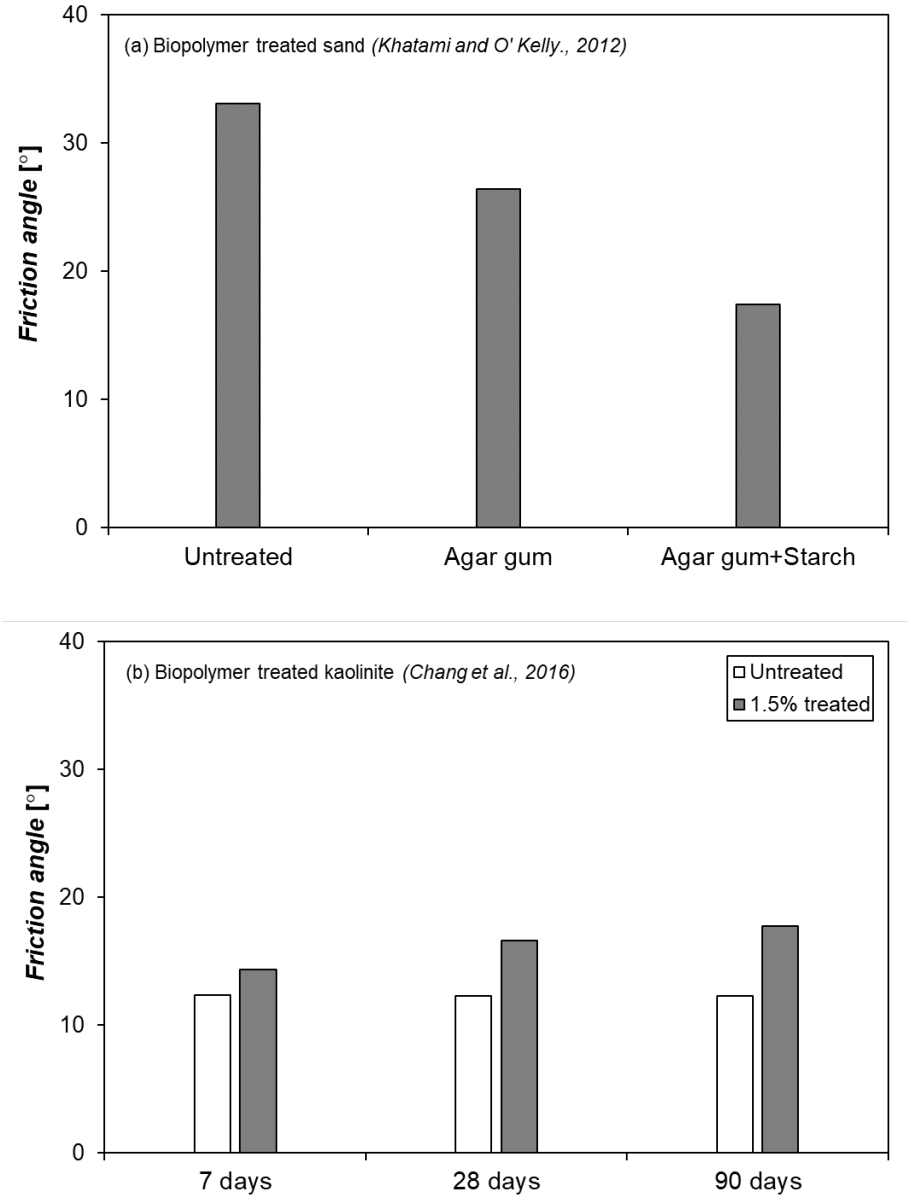

Figure 2.1 Shear strength parameters of biopolymer treated (a) sand and (b) kaolinite

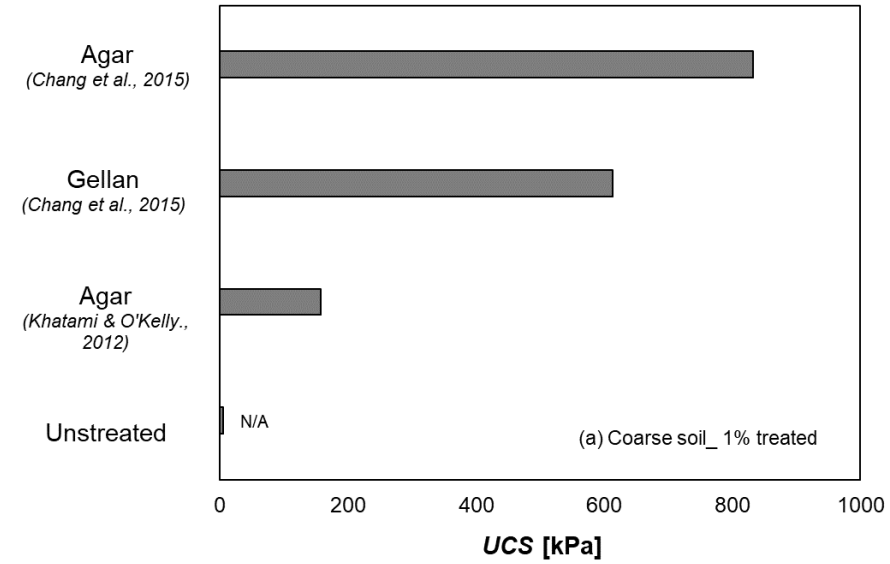

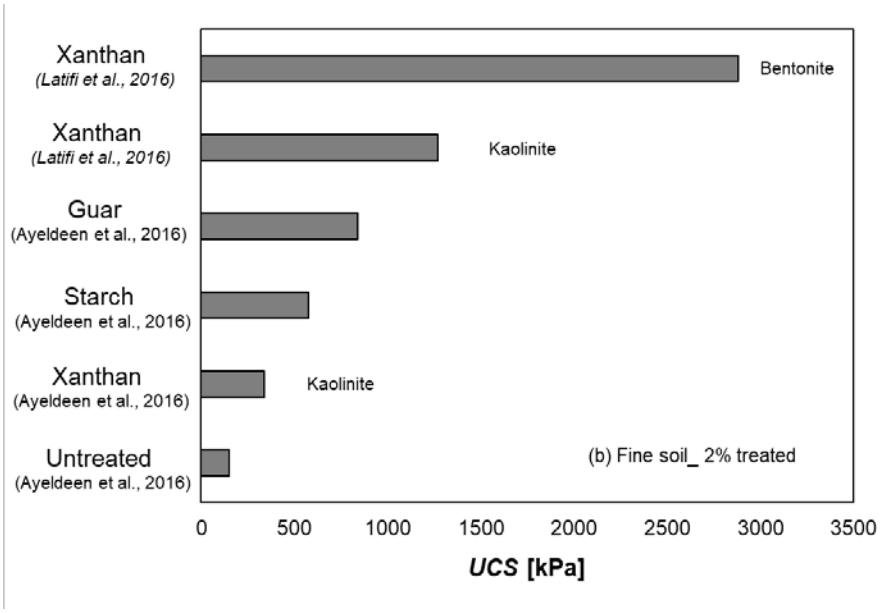

Figure 2.2 Effect of biopolymers on compressive strength of soils

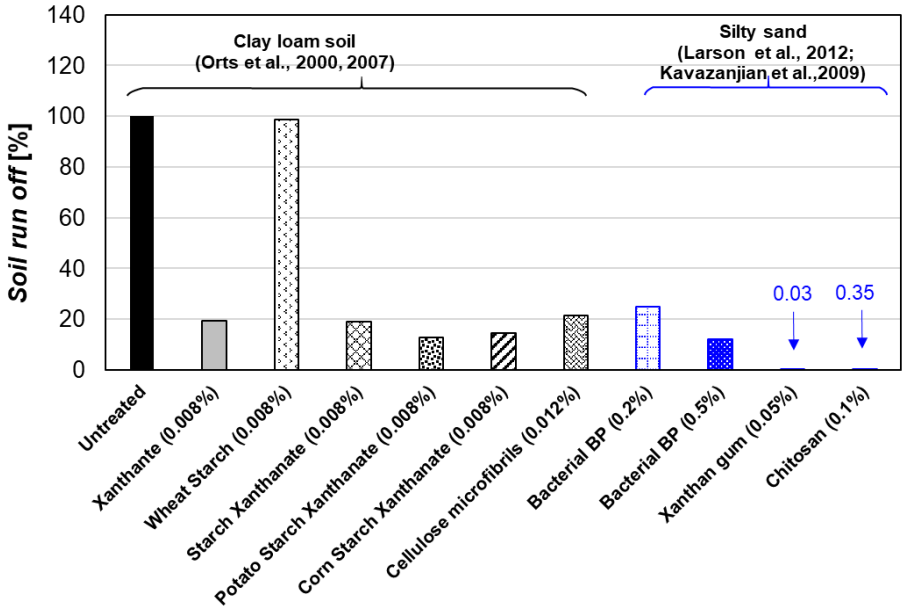

Figure 2.3. Effectiveness of the use of biopolymers on erosion control (referred to Orts et al., 2000, 2007; Larson et al., 2012, Kavazanjian et al., 2009)

2.1.2.3 Grouting purposes

For conventional underground grouting, biopolymers have been used to increase the viscosity of mixing water and enhance the stability of cement-based systems (Ghio et al. 1994; Khayat and Yahia 1997; Sonebi 2006). Biopolymer is highly effective at controlling bleeding because the long-chain molecules of biopolymers adhere to the periphery of water molecules (Khayat and Yahia 1998).

Previous studies show the addition of biopolymer gums in cement paste can increase the viscosity of the system. However, the effectiveness of biopolymer on viscosity increase is more significant at low shear rates than at higher shear rate (Ghio et al. 1994; Sonebi 2006). The increase in apparent viscosity is caused by the adsorption of water molecules via biopolymer via hydrogen bonding (Khayat 1998). For low shear rates the pseudoplasticity of the admixture, produced by the entanglement of the long chain polymers, has a higher influence on the apparent viscosity than for higher shear rate (Ghio et al. 1994). Due to the partial realignment of the polymer chains in the direction of flow and dislodge of the intertwined chains, the apparent viscosity is reduced, and the fluidity enhances at a higher shear rate (Ghio et al. 1994; Sonebi 2006).

2.1.2.4 Flow control purposes

The presence of biopolymer hydrogels can affect the hydraulic conductivity of soil via inducing soil pore-clogging (DeJong et al. 2013; Mitchell and Santamarina 2005). When the hydrogel treated soils are subjected to water, the interaction with water and accompanying swelling of hydrophilic gels can

minimize the pore spaces (Chang et al. 2016), and in turn, reduce the hydraulic conductivity of soil (Al-Darby 1996b; Bouazza et al. 2009; Chang et al. 2016; Khachatoorian et al. 2003b).

Figure 2.4 shows hydraulic conductivity behaviors of sand where the pore-clogging is induced by a continuous biopolymer solution flow (Khachatoorian et al. 2003b). Parts of biopolymers from the solution were retained on the sand surface, therefore blocking sand pores. For instance, over 11 days the circulation of biopolymer solution decreases the hydraulic conductivity of sand down to $10^1 \sim 10^3$ times depending on biopolymer type. Figure 2.5 shows the hydraulic conductivity of directly mixed biopolymer – sand (Bouazza et al. 2009; Chang et al. 2016). The pore-clogging is induced by the swelling of biopolymer when the water flow runs through the soil system. There should be a concern about the weakening and flushing out of hydrogel under high hydraulic pressure condition.

2.1.2.5 Water retention purposes

Biopolymers that can adsorb an extreme amount of water to their weight will alter the soil-water characteristic by rendering higher water retention (Al-Darby 1996b; Chenu 1989; Chenu 1993). Biopolymers hold water in the soil under high pressure due to the strong bonding of biopolymer with water molecules (Chang et al. 2010; Narjary et al. 2012).

However, the water retention behavior of soils depends on biopolymer types and concentrations. It is found that higher biopolymer concentration renders higher water content under a given pressure (Fig. 2.6) (Al-Darby 1996b). Different biopolymers show different water retention of the soil. For example, water retention of 1% biopolymer-treated sands in the order of xanthan gum > scleroglucan > dextran (Fig. 2.7) (Chenu 1993).

2.1.2.6 Vegetation growth purposes

Generally, plants require a small amount of water for their metabolic purposes; however, most of the water supplied to plants is lost through transpiration. Low water holding capacity of sandy soils result in the lack of water for the germination and root growth in drought condition (Crous 2017; Fan et al. 2005).

Due to the high water retention of biopolymer treated soil, the biopolymer can act as an additional water reservoir within the soil (Chang et al. 2015d; Yvin et al. 2002). The biopolymer can show high water retention behavior even under loose soil, which provides a proper environment for the seed germination and the root penetration in the soils (Chang et al. 2015d).

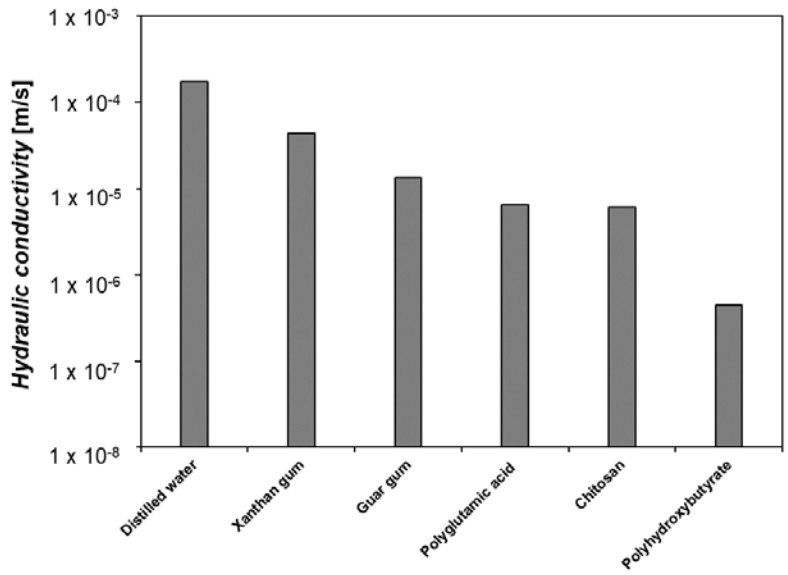

Figure 2.4. The pore-clogging effect of biopolymer flood on sand column (referred to Khachatoorian et al., 2003)

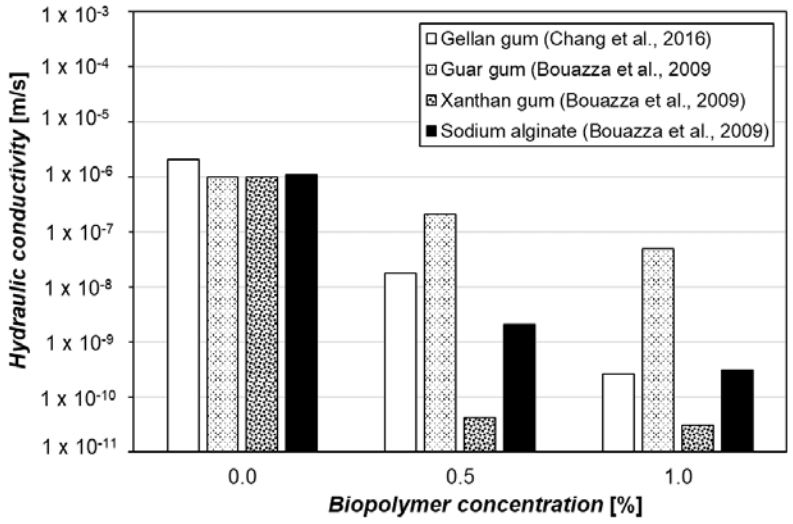

Figure 2.5. Effect biopolymer types on hydraulic conductivity of sand

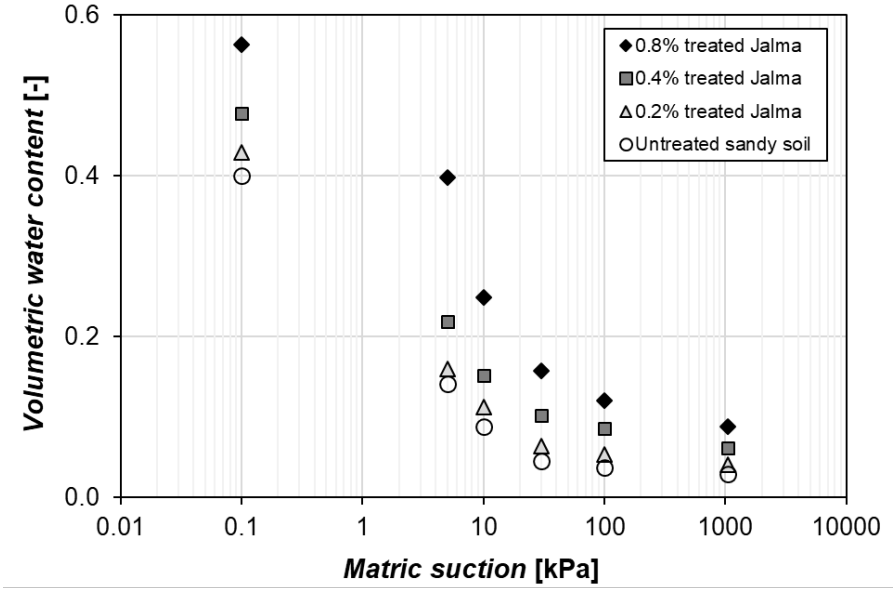

Figure 2.6. Improvement in water retention of sol using Jalma hydrogel with different content (referred to Al-Darby 1996)

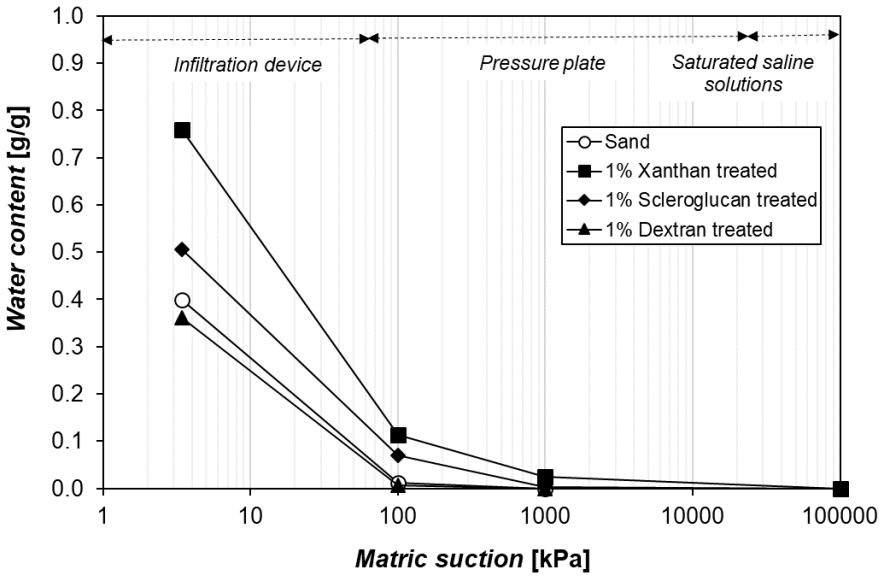

Figure 2.7 Effect of different types of biopolymers on water retention improvement for sand (referred to Chenu, 1993)

2.2 Hydrogel structure, hydrophilic rheology of hydrogels and its effect on soil behaviors

2.2.1 Hydrogel structure

Hydrogels are three-dimensional networks of hydrophilic polymers, which is able to absorb and retain large amounts of water or biological fluids while maintaining their dimensional stability (Guilherme et al. 2015; Kazanskii and Dubrovskii 1992). Hydrogel can be made from virtually any water-soluble polymer, including a wide range of chemical compositions and bulk physical properties (Hoare and Kohane 2008).

Based on the types of crosslinking within the hydrogel network, hydrogels can be classified into two types: physically crosslinked gels and chemically crosslinked gels. Hydrogels are called physical crosslinked gels when the network is held together by molecular entanglement, and secondary forces including ionic, H-bonding or hydrophobic force (Hoffman 2002). Meanwhile, hydrogels are called chemically crosslinked gels when they are covalently-crosslinked networks. The chemical hydrogel may also be generated by crosslinking of water-soluble polymers, or by conversion of hydrophobic polymers to hydrophilic polymers plus crosslinking to form a network (Gun'ko et al. 2017; Hoffman 2002). Both physical and chemical hydrogels are not homogeneous due to the formation of clusters where ionically-associated domains in physical gels or high crosslink density in chemical gels can be seen (Hoffman 2002).

The hydrogel hydrophilicity is owed to a number of water–solubilizing groups (i.e., functional group): -OH, -COOH, $-COO^{-}$, >C=O, $>CHNH_2$, $-CONH_2$, $-SO_3H$, etc., in the polymer network (Gun'ko et al. 2017), which relates to the amount of water absorbed.

2.2.2 Water in hydrogels

The available water content within hydrogel plays an important role in determining biological properties of hydrogels through interfacial free energy (Hu and Tsai 1996; Jhon and Andrade 1973) in biomedical application. The arrangement of water molecules inside hydrogel structures can be considered a critical point in understanding their rheological behavior (Pasqui et al. 2012). The amount of water within hydrogels may also reflect the water absorption ability of the hydrogel.

Figure 2.8 shows the different states of water in hydrogel: strongly bound water, weakly bound water and free water (Gun'ko et al. 2017). When a dry hydrogel begins to absorb water, the first water molecules entering the matrix will hydrate the polar, hydrophilic groups, forming the strongly bound water. As the polar groups are hydrated, the network swells and exposes hydrophobic group, which

also interact with water molecules, leading to the secondary bound water (i.e., weakly bound water). After that, the network will imbibe additional water, due to the osmotic driving force of the network chain towards infinite dilution resisted by the physical or chemical cross-links. The additional water is called free water (Hoffman 2002).

The bound water is directly attached to the polymer chain through hydration of functional groups or ions. The bound water remains as an integral part of the hydrogel structure and can only be separated at very high temperatures or high pressures/suction. Although other layers of water can be accommodated into the hydrogel structure, these have much weaker interactions with functional groups and ions as they are farther away from the functional cores. The free water can potentially be removed from the hydrogels by centrifugation and mechanical compression (Ottenbrite et al. 2010).

2.2.3 Hydrophilic rheology of hydrogels

Most of the hydrogels show the pseudoplastic or shear-thinning behavior where the more shear is applied; the fluid becomes less viscous (Agi et al. 2018; Huang et al. 2007; Marcotte et al. 2001; Miyoshi and Nishinari 1999). It has been recognized that pseudoplasticity represents an irreversible structural breakdown and the decrease in viscosity occurs as a result of molecular alignment that takes place within such a substance (Glicksman 1969). There are several models has been used to describe the flow behavior of hydrogels, for example, linear (Newtonian or Bingham), power law, and power law with yield stress (Fig. 2.9) (Agi et al. 2018; Marcotte et al. 2001). However, the rheology of the hydrogel can depend upon the combination of temperature (Marcotte et al. 2001; Miyoshi and Nishinari 1999), hydrogel types (Marcotte et al. 2001; Yaseen et al. 2005), concentration (Miyoshi and Nishinari 1999), and molecular weight (Amundarain et al. 2009; Tirtaatmadja et al. 2001).

Previous studies show that the presence of hydrogel in the soil will affect the colloidal properties of clay in suspension such as viscosity and flow behavior (Heller and Keren 2002). For instance, hydrogel adsorption by clay leads to an increase in viscosity and a change in yield stress of suspensions (Chang et al. 1992; Heath and Tadros 1983; Lagaly 1989; Wang et al. 2016), which depends on concentration, types and molecular weight of hydrogels (Heller and Keren 2002). The yield stress and the flow behavior of clay suspensions are sensitive indicators of clay particle interactions concerning the particle−particle association strength (Heller and Keren 2002; Lagaly 1989). Furthermore, the improvement in physical conditions of the soil stems from the linking of clay particles, or coating sand particles by hydrogel to yield soil aggregation stabilization (Barclay and Lewin 1985; Chang et al. 2015d; Marten and Frankenberger 1992). Additionally, hydrogel shows the effect on blocking the channels of losing water from the soil layer, i.e., the hydraulic conductivity

responsible for the gravitational flow or the physical evaporation. Therefore, hydrogels can provide an increase in the water content of the soil and, consequently, improve the water supply of plants (Kazanskii and Dubrovskii 1992).

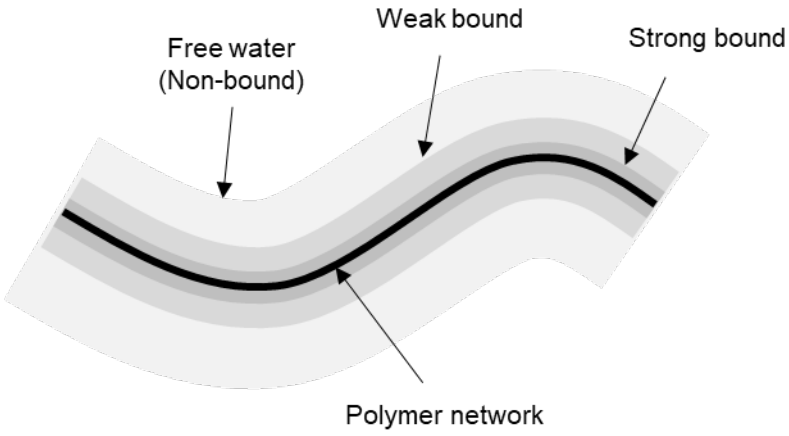

Figure 2.8 Type of water in hydrogels (referred to Ottenbrite et al. 2010; Gun'ko et al. 2017)

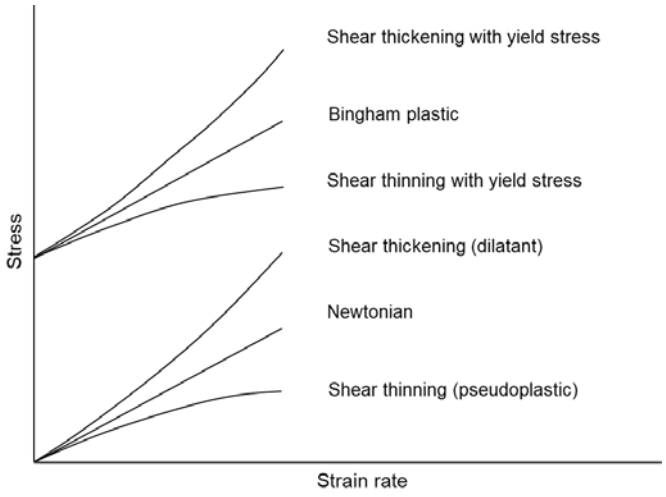

Figure 2.9 Rheology behavior of hydrogels (Agi et al. 2018)

2.2.4 Ion interaction

Hydrogels with physically well-defined three-dimensional porous structures and have chemically responsive functional groups can readily capture metal ions and dyes from wastewater and release the toxic pollutants upon changes in aqueous solution conditions. Hydrogel swells up to several times of their original volume in aqueous media which results in interaction and sorption of dyes and metal

ions on to polymer chain.

Adsorption of the metal ions by hydrogels takes place by the attraction mechanism, depending on the difference in charge between the positively charged metal cations and the negative charged active sites distributed everywhere along with the hydrogel structure and these active sites govern the whole uptake of the metal cations by the hydrogels. Besides the adsorption mechanism, there is a contribution of the ion exchange mechanism, which depends on types of functional groups. Different hydrogels have different functional groups that mainly contribute to the ion adsorption mechanism such as –SO2OH and COOH for poly[2-(acrylamino)-2-methyl-1-propanesulfonic acid-co-itaconic acid] hydrogel (Çavuş and Gürdağ 2008); –CO2H and –C=O or –OH groups for polycarboxulated starch-based hydrogels (Chauhan et al. 2010), –COOH groups for Xylan rich hemicellulose-g-AA gels (Peng et al. 2012), –NH2, –OH and –COOH for chitosan (Wang et al. 2009) and so on. Furthermore, the cation-exchange mechanism is the minor contribution of the metal ion adsorption of hydrogels (Kawahara et al. 1996; Kolla et al. 1987).

The charged hydrogel also interacts with clayey particles, which have electric charges, via hydrogen bonding and ionic bonding, which in turn improves geotechnical engineering properties of soils (Chang et al. 2016b; Chang et al. 2015a). The effect of hydrogels on soil properties was detailed mentioned in section 2.3.3

2.3 Unsaturated soil mechanics

Terzaghi (1943) had a meaningful contribution toward our understanding of unsaturated soil behavior via emphasizing the importance of unsaturated portion of the soil profile concerning “capillary forces” and “mechanics of drainage”, which provides insight into the fundamental nature and importance of the air-water interface (Terzaghi 1943). Later, unsaturated soil mechanics have been developed and is largely taught as an extension of the concepts fundamental to saturated soil mechanics. Unsaturated soil mechanics involved the engineering description of a multi-phase system that has soil, water and air. The air-water interface is also suggested as the fourth phase of the unsaturated soil (Fredlund and Morgenstern 1977). The description of unsaturated soil behavior needed to embrace a wide range of degrees of saturation. The degree of saturation of the soil ranged from saturation in the capillary zone to a discontinuous water phase in the dry soil zone (Fredlund 2017).

The unsaturated zone is defined as the earth’s terrestrial subsurface that extends from the surface to the regional groundwater water, which is an important definition to retain because of the manner in which the soil-water characteristic curve (SWCC) is measured in the laboratory and used in engineering practice (Fredlund 2017). The SWCC is used to describe the nonlinear relationship

between matric suction and water content of unsaturated soil, and water distribution within the body of unsaturated soil (Tao et al. 2017; Williams 1982). The SWCC has played an important role in extending saturated soil mechanics to embrace unsaturated soil behavior.

There are three water types in soil: adsorption water (Karube 1988), meniscus water and free water (Karube and Kawai 2001). Adsorbed water has tightly bound the surface of the soil particles via the static electric attraction on the surface of sand (Mitchell 1993; Wu et al. 2008). The meniscus water induces meniscus stress with suction, which works at the contact points between soil particles. The meniscus stress works internally and produces a pseudo-cohesive force in unsaturated soil media (Lourenco et al. 2012; Wu et al. 2008) to stiffen the soil skeleton. Free water is easily removed from the soil by a suction smaller than -0.3 bars. Meanwhile, a suction of (-31 ~ - 0.3) bars is needed to remove capillary water out from the soil (Plaster 2013). The adhesion force is the most potent force in the soil media, the adsorbed water; therefore, can be separated from soil surface under suction in the range of (- 10000 ~ -31) bars (Plaster 2013).

Therefore, the SWCC has three stages that describe the process of desaturation of soil as shown in Fig. 2.10 (Fredlund et al. 2012; Fredlund 2000), which reflects different properties of water in soil. The capillary saturation zone (or boundary zone) is where the pore-water is in tension, but the soil remains saturated. This stage ends at the air entry value, where the applied suction overcomes the capillary water forces in the largest pore in the soil. The transition zone (desaturation zone) is where water is displaced by air within the pores. This stage ends at the residual water content, where the pore water becomes discontinuous, and the coefficient of permeability is greatly reduced. The residual saturation zone is where the water is tightly adsorbed onto the soil particles, and flow occurs in the form of vapor. This stage is terminated at oven dryness (Fredlund 2000).

The SWCC is known as the central relationship in describing the behavior of unsaturated soils, which can be used as a significant value for the estimation of unsaturated soil property functions such as permeability, shear strength and volume change (Fredlund 2000). There are many researchers have described the nonlinear SWCC via empirical models or equations (Brooks and Corey 1964; Brutsaert 1967; Burdine 1953; Campbell 1974; Fredlund and Xing 1994; Gardner 1956; Laliberte 1969; McKee and Bumb 1987; Mualem 1976a; Pham et al. 2005; van Genuchten 1980). In which, the van Genuchten equation and the Fredlund and Xing equation are the best SWCC model for a variety of soils (Leong and Rahardjo 1997).

The van Genuchten equation is typical of proposed sigmoidal equation (van Genuchten 1980). The volumetric water content (θw) of soil is expressed as (Eq. 1):

$$\theta_w = \theta_r + \frac{(\theta_s - \theta_r)}{\left[1+(\psi/\alpha)^n\right]^m} \tag{2.1}$$

where θ_w is the volumetric water content; θ_s is the saturated volumetric water content; θr is the residual volumetric water content; ψ is the soil suction (kPa); α is a soil parameter related to the air entry value (AEV); *n* is a soil parameter associated with the rate of water extraction from the soil; and m is a soil parameter related to θ_r and *m*, which is calculated by $m = 1 - (1/n)$ (Mualem 1976a, 1976b; van Genuchten and Nielsen 1985).

The Fredlund and Xing (1994) equation can be written as follows

$$\theta_w = \theta_s \left[1 - \frac{\ln\left(1+\psi/\psi_r\right)}{\ln\left(1+10^6/\psi_r\right)}\right] \left[\frac{1}{\left\{\ln\left[e+(\psi/a)^n\right]\right\}^m}\right] \tag{2.2}$$

where θ_w, θ_s, θ_r, ψ have same meanings as in Eq. 2.1; a is the soil parameter related to the *AEV* of the soil (kPa); n is the soil parameter related to the slope at the inflection point (near the *AEV*) on the SWCC; *m* is the soil parameter related to the residual water content portion of the curve; e is the natural number 2.718; ψ_r is the residual suction (kPa) corresponding on the residual water.

The SWCC parameters obtained are used to calculate permeability, effective saturation, matric suction which are used to estimate the strength of unsaturated soil. The drying and wetting SWCCs are significantly different, and in many cases, it becomes necessary to differentiate the soil properties associated with the wetting curve. The geotechnical engineer must take a decision regarding the process that is to be simulated and the use the appropriate estimated unsaturated soil property function (Tami et al. 2004).

Effective stress is the term used to describe the general stress state that can subsequently be used to describe the physical behavior of saturated soils. The effective stress has been expressed in the form of an equation

$$\sigma' = \sigma - u_w \tag{2.3}$$

where σ’ is the effective stress, σ is the total stress and u_w is the pore water pressure.

It was recognized that there needed to be a separation between the effects of total stress changes and pore-water pressure changes when attempting to describe unsaturated soil constitutive behavior (Biot 1941). The oldest and most-often-used effective stress relationship is that proposed by Bishop (1959). The equation is commonly referred to as Bishop’s effective stress equation for unsaturated soil (Bishop 1959)

$$\sigma' = (\sigma - u_a) + \chi(u_a - u_w) \tag{2.4}$$

Where χ is a soil parameter with a value between zero and unity depending on soil type and the degree of saturation assuming that the pore water does not occupy the total pore volume (Cai and Ugai 2004), and u_a is the air pressure.

The value of parameter χ can roughly be replaced by the degree of saturation or the relative degree of saturation as (Vanapalli et al. 1996)

$$\chi = \frac{S_w - S_r}{1 - S_r} \tag{2.5}$$

Where S_w denotes the degree of water saturation, and S_r is the degree of residual saturation.

2.4 Hydraulic conductivity

The rate of water movement through soil is of considerable importance in many aspects of agricultural and urban life. An important soil property involved in the behavior of soil water flow systems is the conductivity of the soil to water. Hydraulic conductivity is the ability of the soil to transmit water (Klute 1965). The definition of the hydraulic conductivity *k* follows from Darcy's Law. In the saturated flow conditions, the velocity of water flow ν (m/s) in the soils is directly proportional to the hydraulic gradient i. The coefficient of this direct proportionality which is a constant with units of velocity is named as hydraulic conductivity. The relationship can be generally expressed by equation

$$\nu = k.i \tag{2.6}$$

In the saturated flow conditions and according to the Darcy's Law, the flow velocity ν can be expressed

$$\nu = k.\frac{\partial h}{\partial x} \tag{2.7}$$

where x (m) is the distance in the direction of groundwater flow, h (m) is the hydraulic head.

The hydraulic conductivity of soil is important in geotechnical projects related to the determination of seepage, stability analyses, and settlement prediction (Chung et al. 2018). Many researchers have found that hydraulic conductivity of soil is affected by many factors such as density (Sällfors and Öberg-Högsta 2002), water content (Sällfors and Öberg-Högsta 2002), void ratio (Sivapullaiah et al. 2000), grain size distribution (Hauser 1978), and soil types (Ebina et al. 2004; Ritzema 2006). Furthermore, in sandy soils, the k value is the same in all direction, but usually, the *k* values vary with the flow direction. Soil layers vertical permeability is very often different from horizontal permeability because of vertical differences in the structure, texture, and porosity.

At the flow goes through an unsaturated zone, the hydraulic conductivity decreases. It is because part of the pores in unsaturated soil is filled with air, which reduces the area available for flow and soil-water content. Therefore the unsaturated hydraulic conductivity is lower than the saturated conductivity. Many laboratory and field methods have been developed to measure the unsaturated hydraulic conductivity. Indirect methods, which predict the hydraulic properties from more easily measured data (e.g. soil-water retention and particle-size distribution), can provide reasonable estimates of hydraulic soil properties with considerably less effort and expense. The SWCC parameters can be used to have a predictive estimation on the unsaturated soil. For instance, the set of closed-form equations formulated by van Genuchten (1980), based on the Mualem capillary model (Mualem 1976a, 1976b; van Genuchten and Nielsen 1985), is used to represent the hydraulic characteristics of unsaturated soil as follows

$$\mathrm{K}(\theta) = k_s S_e^{1/2}\left[1-\left(1-S_e^{1/m}\right)^m\right]^2 \tag{2.8}$$

where S_e denotes the effective saturation (i.e., χ), m is SWCC parameters

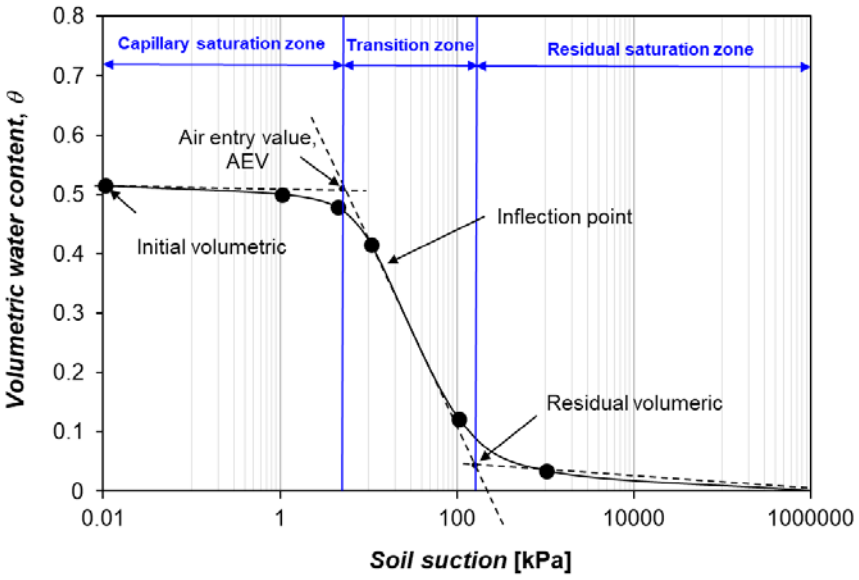

Figure 2.10 Soil-water characteristic curve illustrating the components (referred to Frendlund et al. 2012; Fredlund 2000)

2.5 Soil materials: Mineralogy and basic properties

2.5.1 Sand

Sand particles are made of mostly quartz and feldspar (Das and Sobhan 2013) which falls into a group of minerals called the silicates. The silicates are dominated by the invariance of the SiO4 pyramid unit (Greaves et al. 1981) (Fig. 2.11a).

In our study, Jumunjin sand which is a standard sand material in Korea is used in this study. Jumunjin sand has a specific gravity (Gs) of 2.65 (Chang and Cho 2019), and is classified as a poorly graded sand with D_{50} = 0.43mm. Its uniformity coefficient (Cu) and coefficient of gradation (Cc) are 1.39 and 0.76, respectively.

2.5.2 Clays

Clay Kaolinite consists of repeating layers of elemental silica-gibbsite sheets in a 1:1 lattice (Fig. 11b). Montmorillonite has one gibbsite sheet sandwiched between two silicate sheets (Fig.11c). The layers are held together by hydrogen bonding (Das and Sobhan 2013).

The charges on the clay surfaces are always negative regardless of pH (Bolland et al. 1976), but the magnitude is pH-dependent (Zhou and Gunter 1992). The charge on the edges is due to the protonation/deprotonation of surface hydroxyl groups and therefore depends on the solution pH (Zhou and Gunter 1992). At low and intermediate pH values, the charges of the edge faces are positive and turn to negative values at high pH (Preocanin et al. 2016).

In dry clay, the negative charged is balanced by exchangeable cation like Ca(II), Mg(II), Na(I) and K(I) surrounding the particles being held by electrostatic attraction. When clay interacts with water molecules between clay layers, water can create an interlayer ionic solution that causes swelling phenomena related to electrical double layer properties (Bolan et al. 1999; Karaborni et al. 1996b)
Kaolinite has a lower cation exchange capacity (CEC) than montmorillonite, on average (Arnott 1965; Mitchell and Soga 2005). In general, kaolinite is regarded as a less-swelling clay mineral (Osacky et al. 2015), whereas montmorillonite has been widely applied for drilling purposes owing to its high swelling tendency (Karaborni et al. 1996a). Because of the difference in the CECs, kaolinite, and montmorillonite are expected to interact with biopolymers differently.

This study used Bintang kaolinite (Belitung Island, Indonesia) and a pure montmorillonite material (CAS: 1302–78–9; Sigma Aldrich) for clays. Table 2.2 summarizes the basic properties of the clays

Table 2.3 summarizes materials used in each chapter of this study

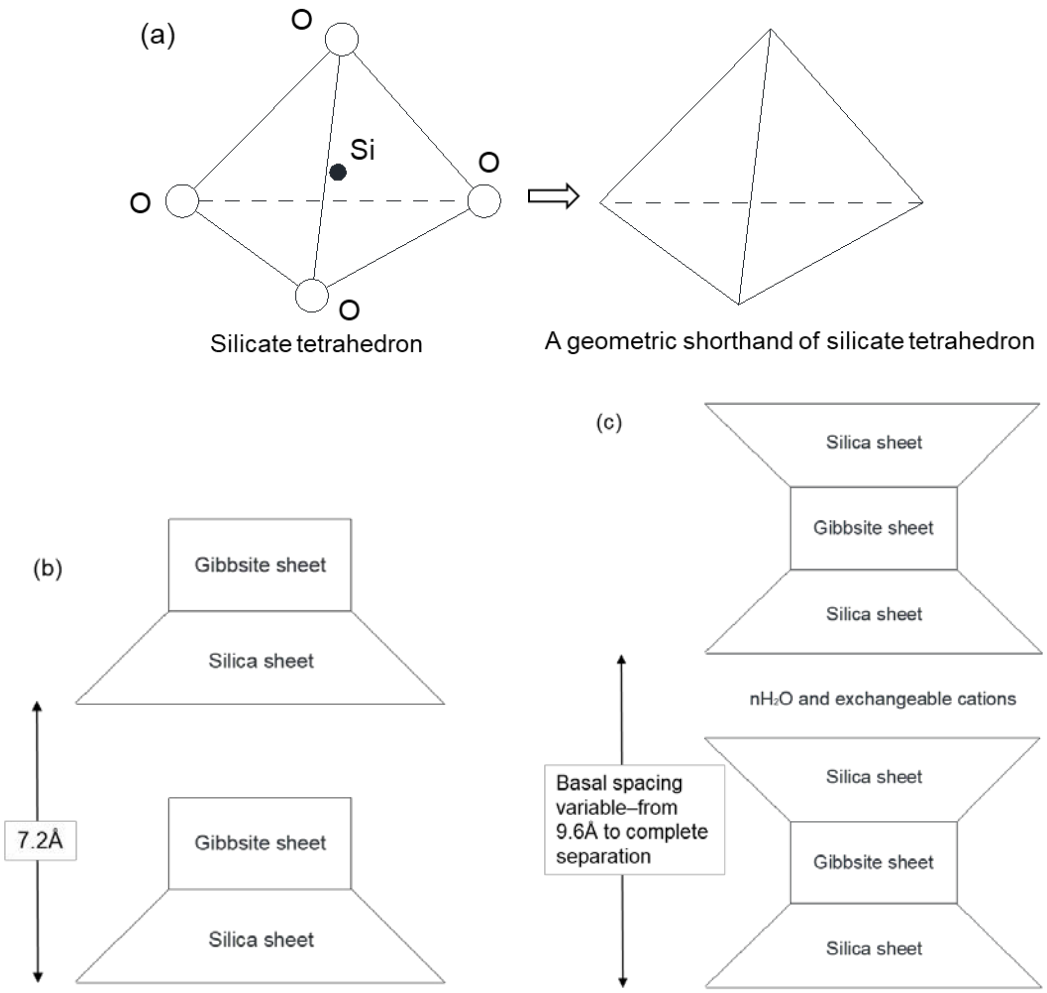

Figure 2.11 Diagram of structures of (a) sand; (b) kaolinite and (c) montmorillonite (referred to Das and Sobhan, 2013)

Table 2.2. Basic properties of clays

Clay	G_s	Liquid limit [%]	Plastic limit [%]	D_{50} [μm]	Specific surface area [m^2/g]
Kaolinite	2.65	59	25	44	22
Montmorillonite	2.70	295	42	0.07	220

Table 2.3. Materials used in this thesis

Materials		Reasons	Experiments
Soils	Jumunjin sand	Standard sand used in Korea	All tests
	Kaolinite	Used as an admixture in biopolymer-sand mixture for soil strengthening (Chang and Cho 2019)	Wetting biopolymer-soil water characteristics (Chapter 3) Pressurized hydraulic conductivity (Chapter 4)
	Montmorillonite	Widely used for hydraulic barrier materials	
Biopolymers	Xanthan gum	Show a good performance in water retention (Fig. 2.7) (Chenu 1993), hydraulic reduction (Bouazza et al. 2009)	Soil water characteristic (Chapter 3) Pressurized hydraulic conductivity (Chapter 4) Vegetation growth (Chapter 6)
	Gellan gum	Soil strengthening (Chang and Cho 2019) Thermo gelatin (Fig. 2.12) (Chang et al. 2015c)	Pressurized hydraulic conductivity (Chapter 4) Heavy metal ion control (Chapter 5)

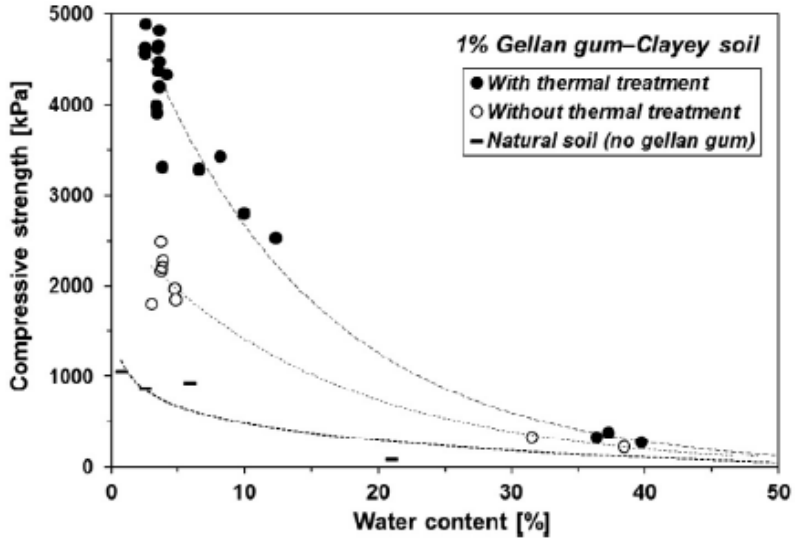

Fig. 2.12 Increase in strength performance of gellan gum-treated soil via heating process (referred to Chang et al. 2015c)

Chapter 3 Soil-water characteristic of biopolymer-treated soils

3.1 Introduction

3.1.1 Biopolymer–Soil–Water Characteristic Curve (B-SWCC) – Definition and concept

As mentioned in section 2.3 the SWCC is used to describe the relationship between matric suction and water content of unsaturated soil, and the water distribution with the body of unsaturated soil. When the sand is treated by biopolymer, the water absorption of biopolymer controls the amount of water held in the unsaturated soil. Different from original SWCC where expresses the effect of air pressure on water held by surface tension in the sand, biopolymer provides an artificial absorption layer for sand. Similarly, water held in clay is based on the water absorption of clay via double layer, however, in biopolymer-treated clayey, the water adsorption is induced by the biopolymer-clay matrix. Therefore, in this study, we define the curve that shows water distribution in the body of biopolymer-treated soil as biopolymer-soil-water characteristic curve (B-SWCC)

3.1.2 Water retention of hydrogel treated soils

Few studies are conducting on the effects of hydrogels on the SWCC of soils (Al-Darby 1996a; Bhardwaj et al. 2007; Chenu 1993; Narjary et al. 2012). The studies prove that hydrogel can increase the amount of retaining water in the soil under high suction compared to the untreated soil. However, the effect of hydrogel on the SWCCs depends on hydrogel types and concentration. It is because the presence of hydrogel can affect the soil structure (Chang and Cho 2014; Chang et al. 2015a; Neethu et al. 2018), and in turn, tends to change the SWCC shape for the materials involved significantly.

3.1.3 The role of the B-SWCC in engineering practice

Besides giving information on water distribution in soil, providing parameters for the numerical modeling methods which are used for the estimation of unsaturation soil property function is the main role of the SWCC. The B-SWCC could do the same role for biopolymer-treated soil, especially at where the biopolymer-soil treatment is used for surface treatment.

Therefore, evaluating the effect of biopolymer on water distribution within soils and obtaining B-SWCC parameters for numerical modeling are the main purpose of this chapter.

3.2 Experimental program for B-SWCC

3.2.1. Drying test

3.2.1.1 Specimen preparation: xanthan-soil mixtures

Xanthan gum solutions were prepared by dissolving xanthan gum powder into deionized water at room temperature (20°C) at different xanthan gum content (xanthan gum to water ratio in mass) according to the controlled xanthan gum content of 0.5; 1.0; 2.0 and 3.0 % to the mass of the sand. Each xanthan gum solution was mixed with dry soil at an initial water content equivalent to 10% of the mass of the soil.

3.2.1.2 Experimental procedure

Drying SWCCs of xanthan–treated sand were determined via Fredlund-type SWCC device (GCTS SWC-150). Xanthan gum-sand mixtures are molded into a specimen ring (diameter of 42 mm and height of 20 mm; 27.69×10^3 mm^3). The dry density of untreated and xanthan gum-treated soils was controlled at 1.54 ± 0.1 g/cm^3 to avoid the effect of dry density on the SWCC's results (Gallage and Uchimura 2010). Then, the specimens were saturated in deionized water for 24 hours to ensure that the soil samples can absorb water as much as they can.

After saturation, the specimen was carefully placed into the Fredlund SWCC cell right above the ceramic disk (75 mm in diameter). Pneumatic pressure was applied in steps as, 5 kPa, 10 kPa, 20 kPa, 50 kPa, 100 kPa, 200 kPa, 400 kPa, and 800 kPa, where each pressure was constantly applied for 24 hours. Water released from the specimen was measured via two volume tubes on the pressure panel during the test. The matric suction in soil is regarded to be identical to applied air pressure when after the volumetric water content (θ_w) in soil becomes stable (i.e., no more water release), where θ_w is defined as V_w (water volume in soil) / V_t (total volume of soil; 27.69 x 10^3 mm^3).

3.2.2 Wetting test

3.2.2.1 Specimen preparation: Xanthan gum–soil mixtures

Four types of soils were reconstructed: pure sand (100%; S10), sand 90%–kaolinite 10% (S9K1), sand 80%–kaolinite 20% (S8K2), and sand 90%–montmorillonite 10% (S9M1) specimens, where the clay and sand percentages are represented by mass composition. Xanthan gum solutions were prepared by dissolving pure xanthan gum in deionized water at room temperature (20 °C) at different xanthan gum concentrations (xanthan gum to water ratio, in mass), as summarized in Table 3.1. Each xanthan gum solution was mixed with dry soil at an initial water content equivalent to 10% of the

mass of the soil. Thoroughly mixed xanthan gum–soil mixtures were dried in an oven at 30 °C for 30 days before conducting laboratory wetting tests.

Table 3.1. Target xanthan gum content for wetting SWCC test (Tran et al. 2019b)

Xanthan gum	Biopolymer content [%] (xanthan gum to soil ratio in mass; m_b/m_s)	0.0	0.1	0.25	0.5	1.0
	Biopolymer solution concentration [%] (xanthan gum to water ratio in mass; m_b/m_w)	0.0	1.0		5.0	10
	Xanthan gum solution densities [g/cm^3]	0.99	0.99	1.00	1.01	1.02
	Average xanthan gum solution density [g/cm^3]	1.0				
Wetting test	H500 capillary tube (diameter 100-mm; height 500-mm)	○	-	-	○	○
	H100 capillary tube (diameter 35-mm; height 100-mm)	○	○	○	○	○

3.2.2.2 Experimental procedure

Two different capillary rise tubes were employed to obtain the wetting SWCCs of the xanthan gum–soil mixtures. First, a capillary rise tube with a 100–mm diameter and a 500–mm height (H500) (Yang et al. 2004) was used (Fig. 3.1a) (Tran et al., 2019). The dried xanthan gum–soil mixtures were compacted into the tube at a target dry density of 1.52 ± 0.03 (g/cm^3) and placed in a tray. In order to prevent evaporation from the soil surface, the top of the tube was sealed with parafilm to avoid evaporation from the soil surface. The tray was then filled by water up to a height of 10 mm and maintained during the test. The water in the tray started to move into the soil column. When the capillary water in the tube reached equilibrium, the 500–mm–height soil column was divided into several segments to determine the variation in the gravimetric water content along the soil column.

The matric suction (u_a–u_w) inside the soil tube was calculated as: ρ_f (the density of fluid) × g (the acceleration due to gravity: 9.81 m/s^2) × H (the height of the water inside the soil column, regarded as the negative pore water pressure head in soil, in m). A fluid density of 1.0 g/cm^3 was used in this study (Table 3.1). The capillary conductivity (i.e. flow velocity in unsaturated soil) was calculated as H / t (the time for the water inside the soil column to reach the H)

Xanthan gum–treated soils are known to exhibit pore–clogging behavior because of the hydrophilic water absorption and the corresponding hydrogel swelling of xanthan gum (Cabalar et al. 2017; Chang et al. 2016b), which is expected to interrupt the capillary rise of water in the soil.

However, the H500 tubes showed significant pore clogging at the bottom, which restrict the movement of water in soil column (Fig. 3.1a). Thus, additional tests using scale–reduced minitubes (with a diameter of 35 mm and a height of 100 mm) (H100; Fig. 3.1b) (Tran et al., 2019) were performed simultaneously to reveal the capillary behavior of the xanthan gum–soil mixtures more effectively. The water level in the tray was maintained at 5 mm. The capillary conductivity, which reflects the ability of water to infiltrate into the soil, was obtained by tracking the change in the water level within the soil column over time.

3.2.3 Analysis methods: van Genucten's equation

In this study, we use the van Genuchten's equation (Eq.2.1), the wetting SWCC parameters of the biopolymer–treated soils was obtained using a nonlinear fitting program (Seki 2007).

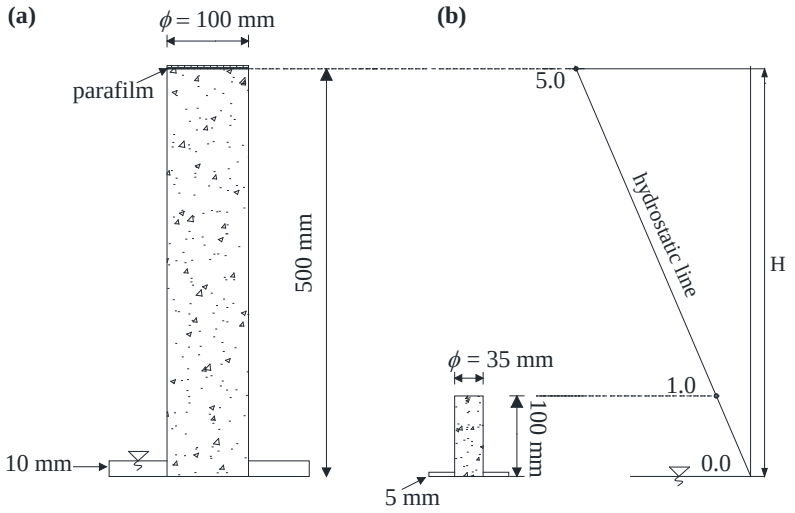

Figure 3.1 Schematic diagram of capillary rise tubes (a) H500 (500-mm-height, 100-mm-diameter) tube, (b) H100 tube (100-mm-height, 35-mm-diameter) (Tran et al. 2019b)

3.3 Results

3.3.1 Drying behavior of B-SWCC

3.3.1.1 Improvement of water holding capacity

Figure 3.2 shows the θ_w of the drying SWCCs of the xanthan gum-treated sand with different xanthan gum contents. The SWCC test data for each specimen was best-fitted using the van Genuchten (1980). The SWCC parameters are summarized in Table 3.2.

Xanthan gum -treated sand shows a higher initial θ_w (i.e. θ_s) than that of untreated sand due to the high water absorbing and holding capacity of xanthan gum, which instantly formed hydrogels

during the saturation process. As pneumatic pressure was applied for drying, the θ_w of the untreated sand significantly dropped by 84% at the suction of 800 kPa. Meanwhile, xanthan gum-treated sand showed a gradual reduction of θ_w which slightly decreased correspondingly to the xanthan gum contents. The water content decreased by 46.5%, 31.9%, 29.3% and 26.2% as the sand was treated by 0.5%, 1.0%, 2.0% and 3.0%, respectively.

The water content in the treated sand decreased and turned to a level off at xanthan gum content of 1%. The θ_s and θ_r values show an exponential relationship with xanthan gum content with $R^2 > 0.9$ (Fig. 3.3), which is expressed as follows:

$$\theta_s = \theta_0 + 0.054\left(1 - e^{-3.239XG}\right) \tag{3.1}$$

$$\theta_r = \theta_0 + 0.392\left(1 - e^{-2.461XG}\right) \tag{3.2}$$

where, θ_0 is volumetric water content at 0% xanthan gum content, XG is the xanthan gum content, and e is the exponential constant value (i.e., 2.718).

3.3.1.2 Relationship of xanthan gum content and drying B-SWCC's parameters

Figure 3.4 shows the change of AEVs with xanthan gum content. The experimental results show that the AEVs were almost similar (4.1 kPa) as the sand treated 0.0 % and 0.5%, then slightly increased to 4.6 kPa for 1.0% treatment. The AEVs then increased two folds for xanthan gum contents of 2.0% and 3.0% treatment. The relationship between AEV and xanthan gum content can be expressed using the four parameters logistic curve with $R^2 = 0.99$ (Fig. 3.4)

$$AEV_i = AEV_{i\max} + \frac{AEV_{i\min} - AEV_{i\max}}{1 + \left(\frac{XG}{1.6}\right)^{55.521}} \tag{3.3}$$

where AEV_i is the air entry value at i % xanthan gum content; i max is the maximum xanthan gum content; i min is the minimum xanthan gum content.

The presence of xanthan gum shows a strong effect on the n parameter. The n parameter significant decreased from untreated sand to 1% treated (Fig. 3.5). After this point, the increase of xanthan gum content did not show a decrease in the slope of the SWCCs. The decline in n parameter with xanthan gum content reflects the shallower of slope due to the lower rate of water change during the drying process. The n parameter which expresses the slope of the SWCCs shows an exponential decay relationship with $R^2 > 0.9$ as follows:

For the van Genuchten (1980) equation

$$n_V = 3.036 + 1.968\left(1 - e^{-3.239\,XG}\right) \tag{3.4}$$

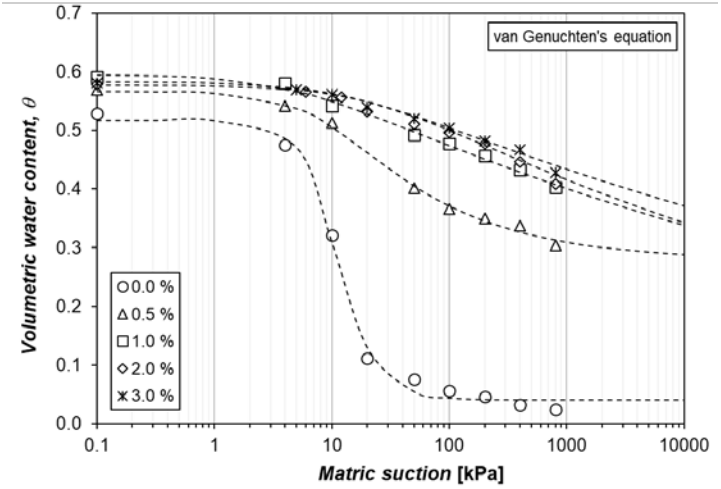

Figure 3.2 Drying soil-water characteristics of xanthan gum-treated sand

Table 3.2 van Genuchten B-SWCC parameters

Equation	Parameters	Xanthan gum content [%]				
		0.0	0.5	1.0	2.0	3.0
van Genuchten (1980)	θs	0.517	0.566	0.595	0.578	0.583
	θr	0.040	0.278	0.000	0.000	0.000
	a	0.110	0.107	0.209	0.046	0.077
	n	3.036	1.472	1.074	1.085	1.068
	m	0.671	0.321	0.069	0.078	0.064

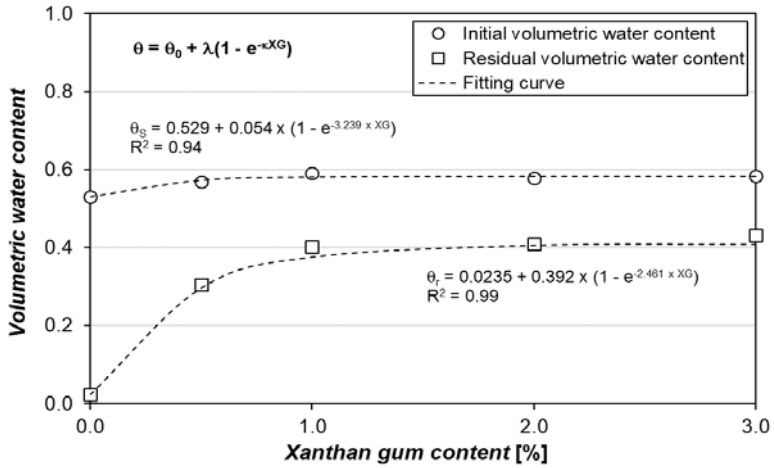

Figure 3.3 Volumetric water content and xanthan gum content relationship

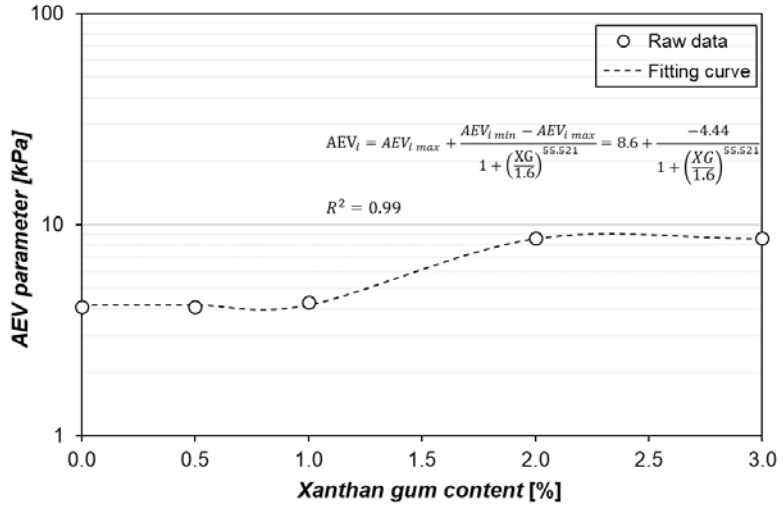

Figure 3.4 Increase in air entry value with xanthan gum content

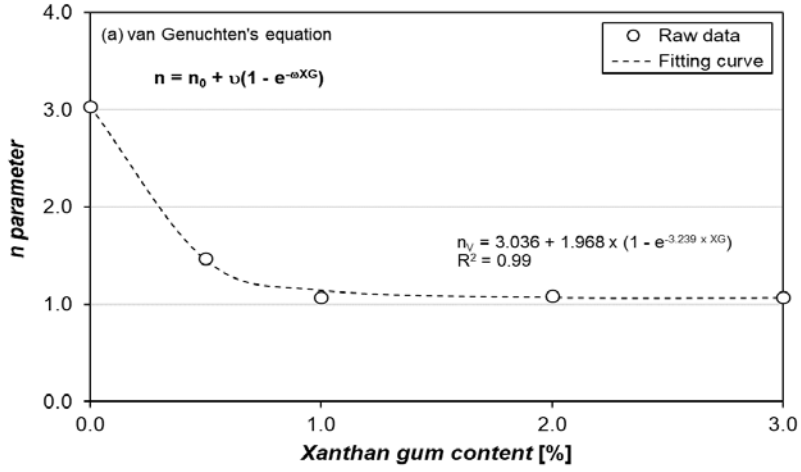

Figure 3.5 Decrease in n parameter with xanthan gum content

3.3.2 Wetting behavior of B-SWCC

3.3.2.1 Effect of biopolymer on capillary conductivity of soils

The effects of the xanthan gum biopolymer on the upward movement of water within the H500 and H100 tubes, are respectively shown in Fig. 3.6 and 3.7 (Tran et al. 2019b). For the untreated S10, water rose upward because of the surface tension force, whereas the xanthan gum treatment reduced the capillary conductivity of S10 with the increase in the xanthan gum content (Figs. 3.6a and 3.7a).

Compared to untreated case, the capillary conductivity of the sand–kaolinite mixtures, slightly increased at low xanthan gum contents (0.1% and 0.25%) and then became lower than the capillary conductivity when xanthan gum ≥ 0.5% (Figs. 3.6b-c and 3.7b-c). Meanwhile, the xanthan gum–treated S9M1 soil showed capillary conductivity reduction with the increase in the xanthan gum content (Figs. 3.6d and 3.7d).

The capillary conductivity of the different types of soil within the H100 tubes under the same xanthan gum treatment condition is showed in Fig. 3.8 (Tran et al. 2019b). For the untreated cases (Fig. 3.8a), the capillary conductivity decreased at higher clay contents, and the sand-montmorillonite mixtures showed a lower capillary conductivity than the sand-kaolinite mixtures. In general, the presence of clay tended to delay the movement of water in the soil via the double layer absorption and pore filling, which are enhanced at higher clay contents (Lu and Likos 2004).

Under the xanthan gum–treated condition, pure sand showed the lowest capillary conductivity, regardless of xanthan gum content (Figs. 3.8b–d). As the soils were treated by 0.1%, the sand–kaolinite mixtures started to show a higher capillary conductivity than the sand–montmorillonite mixtures (Fig. 3.8b) and 0.5% (Fig. 3.8c). Meanwhile, the variation in the capillary conductivity between the clay types and clay contents reduced at xanthan gum content of 1.0% (Fig. 3.8d). Overall, the capillary conductivity results (Figs. 3.6, 3.7, and 3.8) showed different xanthan gum–soil interactions with respect to the type of soil, and xanthan gum content.

Table 3.3 summarizes the maximal water level and related time in soil columns

3.3.2.2 Role of kaolinite in the wetting behavior of sand-clay mixtures

The variations in the capillary conductivity of the xanthan gum –treated S9K1 soil and S8K2 soil in the H100 tube at a matric suction of 0.3 kPa is shown in Fig. 3.9 (Tran et al. 2019b). As the soils were treated by xanthan gum contents lower than 0.25%, the capillary conductivity seemed to promote water transfer through the soil. Meanwhile, pore–clogging and water flow interruption mainly governed by the behavior at high xanthan gum contents (≥ 0.5%) (Fig. 3.9). Figure 3.10 (Tran et al. 2019b) showed the variations in the capillary conductivity of the different soil types treated by the

same xanthan gum content and matric suction. When xanthan gum = 0.5% and higher, the capillary conductivity of the S9K1 soil becomes lower than that of S8K2 (Fig. 3.10) which implied the role of a gel–type biopolymer–clay matrix formation in pore clogging and in the following capillary conductivity reduction (Chang and Cho 2019). In details, the xanthan gum–kaolinite matrix of S9K1 soil showed higher xanthan-to-kaolinite ratio than that of S8K2 soil for same xanthan gum content to the dry mass of soil (e.g., for 1% xanthan gum to soil content, xanthan gum to clay content becomes 10% and 5% for S9K1 and S8K2 soils, respectively). Thus, the S8K2 soil had more unbonded kaolinite particles than S9K1 soil, resulting in a higher capillary conductivity compared S9K1 at high xanthan gum-to-soil content (0.5%) higher capillary conductivity than S9K1 soil at high xanthan gum-to-soil contents (≥ 0.5%). Therefore, the S9K1 soil requires more time than the S8K2 soil to reach matric suction equilibrium, as shown in Fig. 3.11.

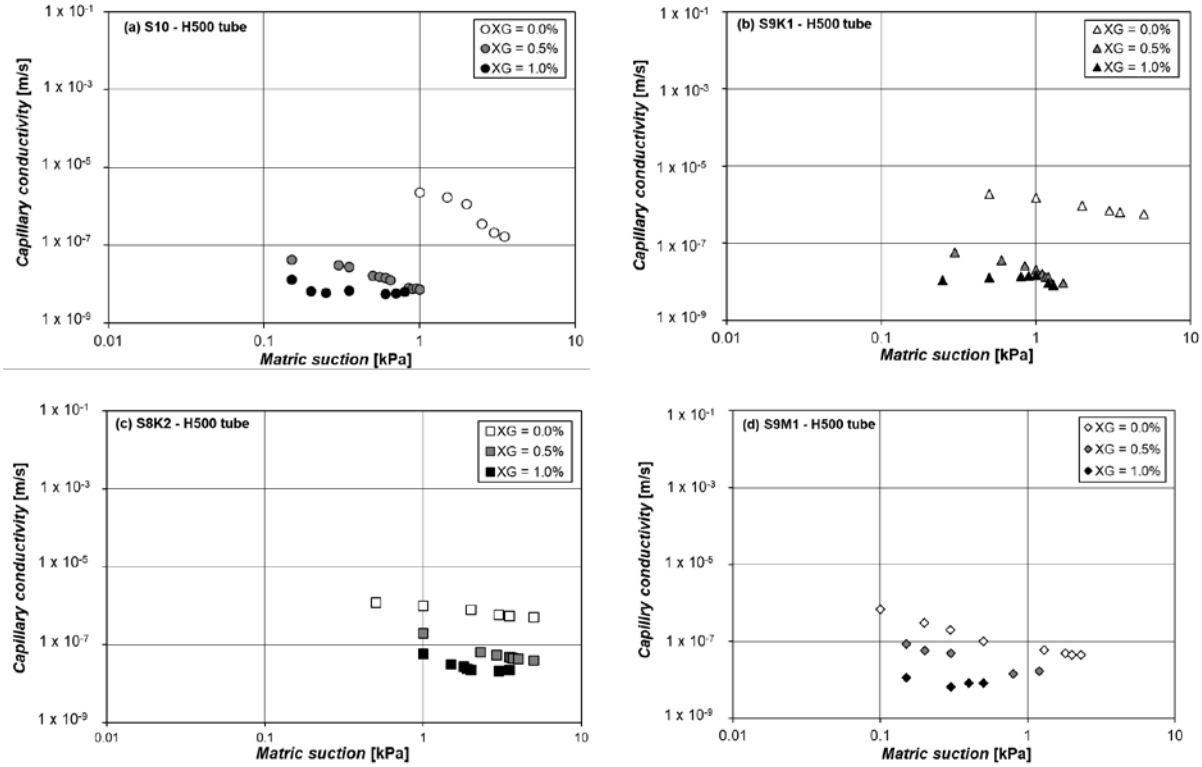

Figure 3.6. Capillary conductivity of xanthan gum–treated soils in H500 tube. (a) S10; (b) S9K1; (c) S8K2; (d) S9M1 soils (Tran et al. 2019b)

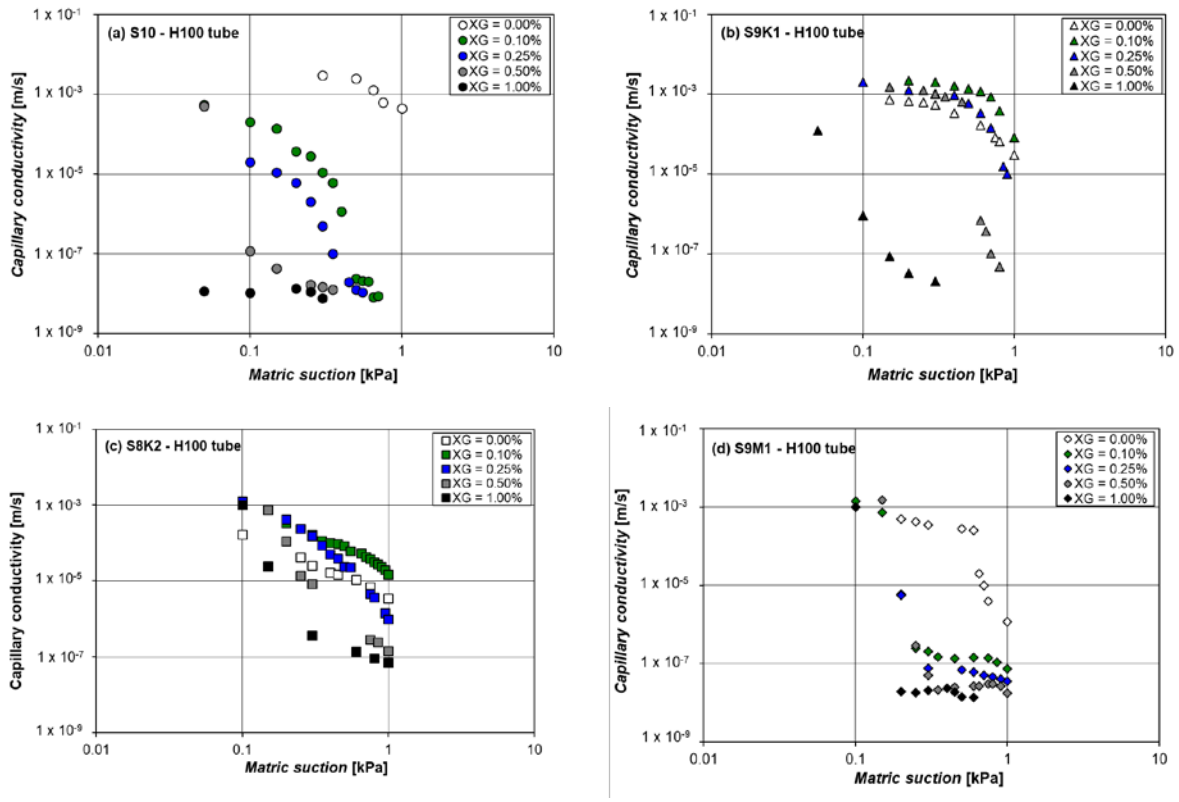

Figure 3.7 Effect of biopolymer content on capillary conductivity of soils in H100 tube. (a) S10; (b) S9K1; (c) S8K2; (d) S9M1 soils (Tran et al. 2019b)

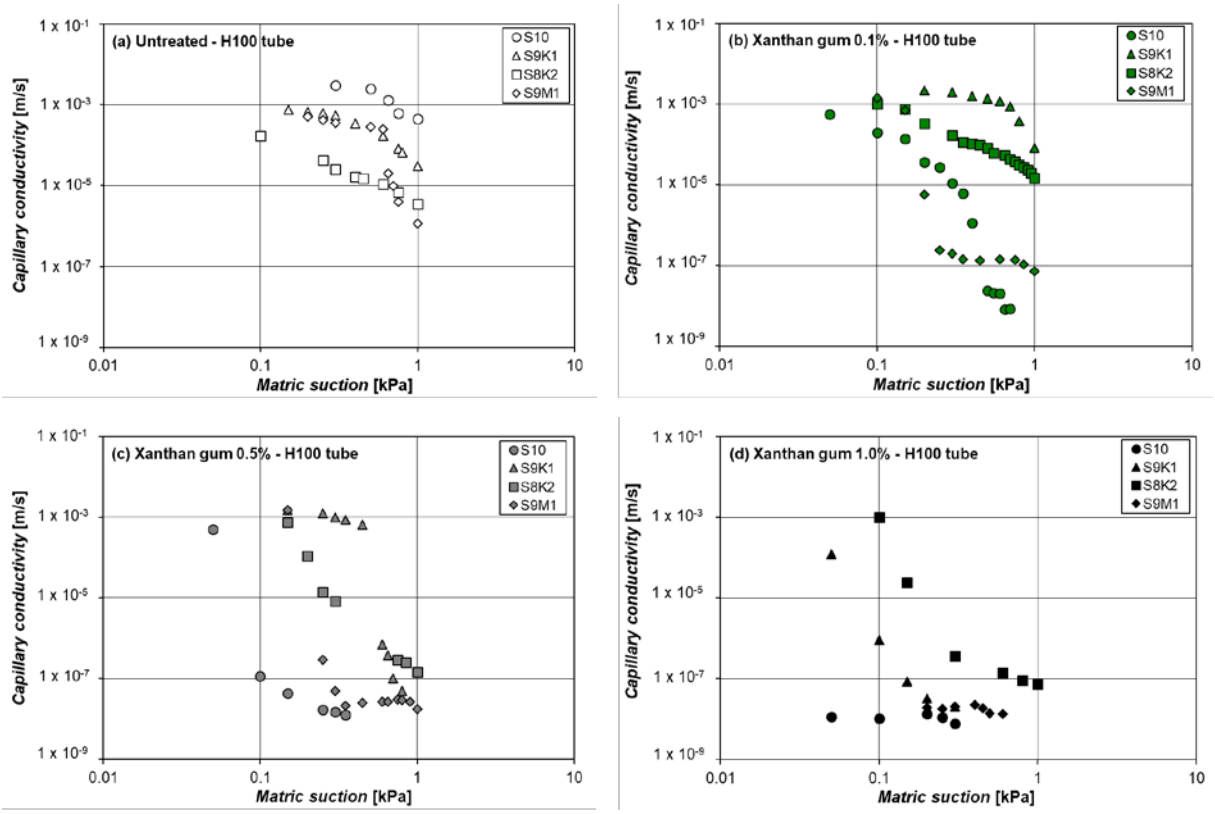

Figure 3.8 Capillary conductivity of xanthan gum–treated soils in H100 tube. (a) Untreated (0.0%). Xanthan gum–treated with (b) 0.1%, (c) 0.5%, and (d) 1.0% xanthan gum to soil content in mass (Tran et al. 2019b)

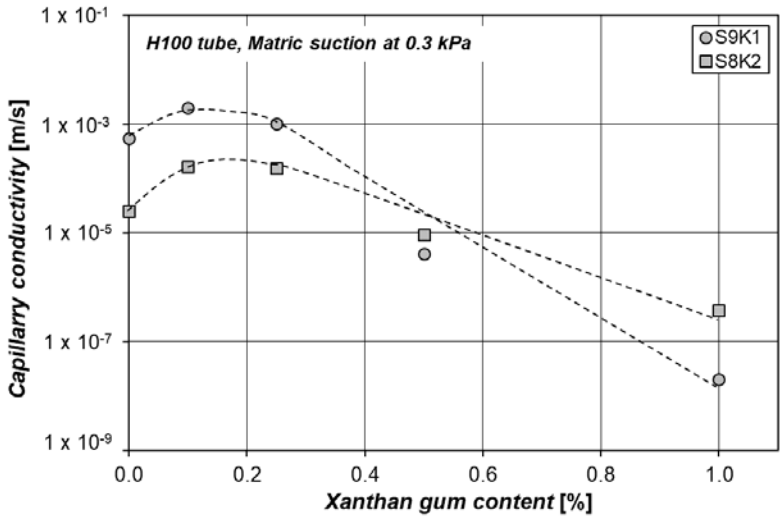

Figure 3.9. Capillary conductivity of sand–kaolinite mixtures with xanthan gum content variation (Tran et al. 2019b)

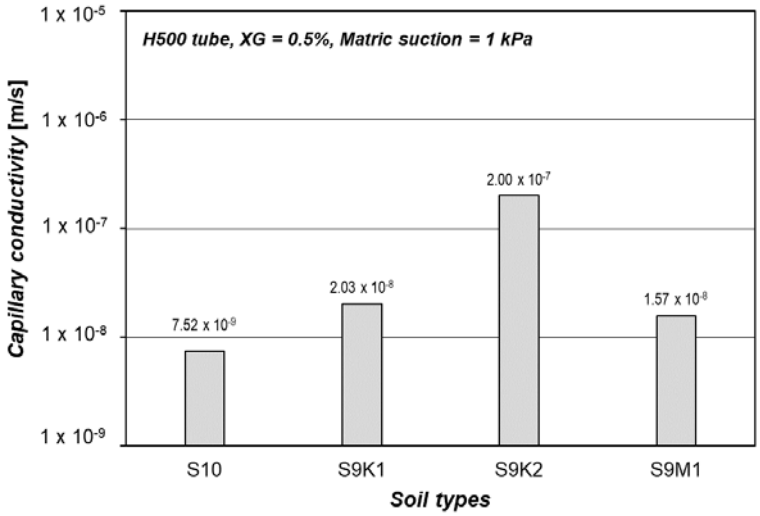

Figure 3.10. Capillary conductivity comparison of 0.5% xanthan gum–treated soils (Tran et al. 2019b)

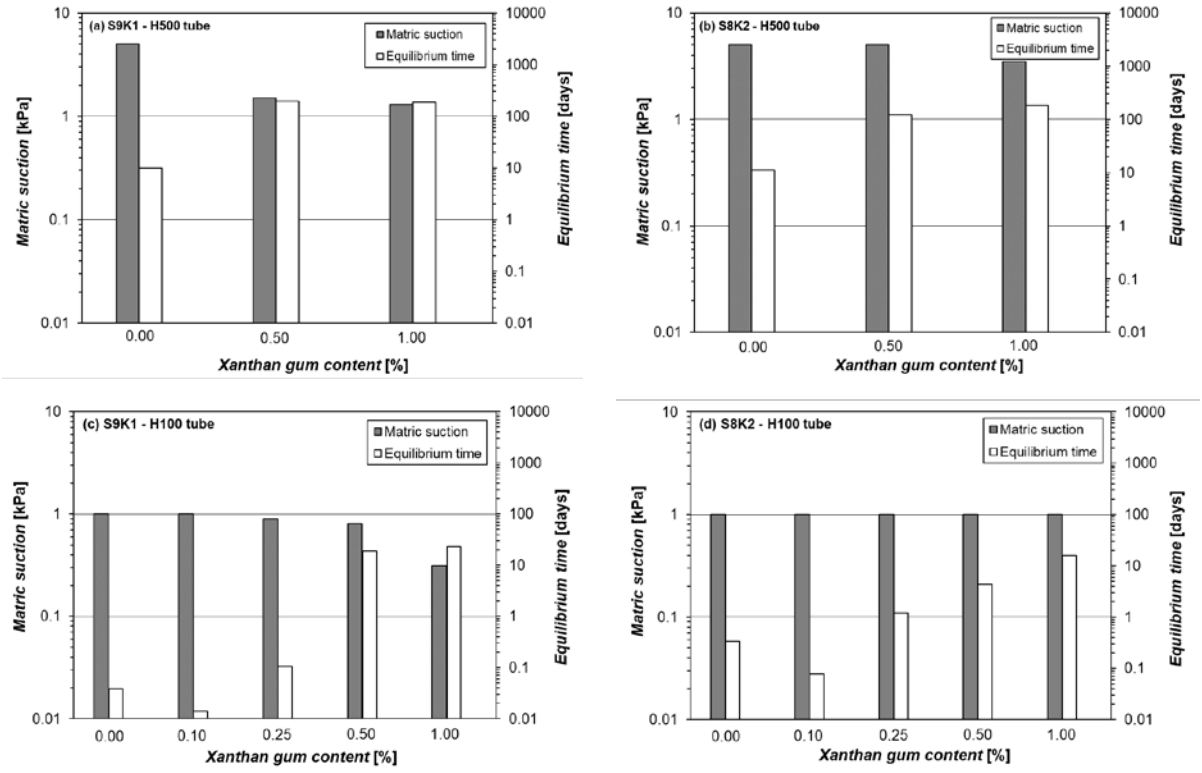

Figure 3.11 Matric suction and corresponding equilibrium time of xanthan gum–treated sand–kaolinite mixtures. (a) S9K1in H500 tube. (b) S8K2 in H500 tube. (c) S9K1 in H100 tube. (d) S8K2 in H100 tube (Tran et al. 2019b)

Table 3.3 Maximal water level and related time of the soils in H500 tube

Specimens		**Water level in soil column [kPa]**	**Time [days]**
Soil types	**Biopolymer content [%]**		
Sand	0	3.75	**23**
	0.5	1.00	**150**
	1.0	0.80	**151**
	2.0	0.55	**142**
10% kaolinite – sand	0	5.00	**10**
	0.5	1.50	**185**
	1.0	1.30	**186**
20% kaolinite – sand	0	5.00	**11**
	0.5	5.00	**122**
	1.0	3.50	**183**
10% montmorillonite – sand	0	2.30	**98**
	0.5	1.20	**81**
	1.0	0.50	**69**

3.3.2.3 Effects of xanthan gum on wetting SWCC curve

The wetting SWCCs and relevant parameters of untreated and 0.5% xanthan gum-treated S8K2 soils are presented in Fig. 3.12 and Table 3.4 (Tran et al. 2019b). The saturated volumetric water content (θs) of the treated soil (θs = 0.4) was higher than that of the untreated soil (θ_s = 0.28) because of the high water–holding capacity of the xanthan gum hydrogels (Bhardwaj et al. 2007; Hatakeyama and Hatakeyama 1998; Zhang et al. 2016). At a certain suction level, the effects of xanthan gum on the increases in pore clogging and surface tension were exhibited which alter significant reduction of the water suction, which in turn significantly reduced the water suction. The difference became inconsiderable when the matric suction is ≥ 5 kPa. The volumetric water content (θ_w) values at 5 kPa were 0.122 and 0.136 for treated and untreated S8K2, respectively. Thus, the *n* value of the xanthan gum–treated soil (2.27) is significantly higher than that of the untreated soil (1.81), whereas the difference in the *m* values was less. The results demonstrate the significant effect of xanthan gum on the water retention of the soil (i.e., θ_s or θ_w) at suction levels lower than 5 kPa.

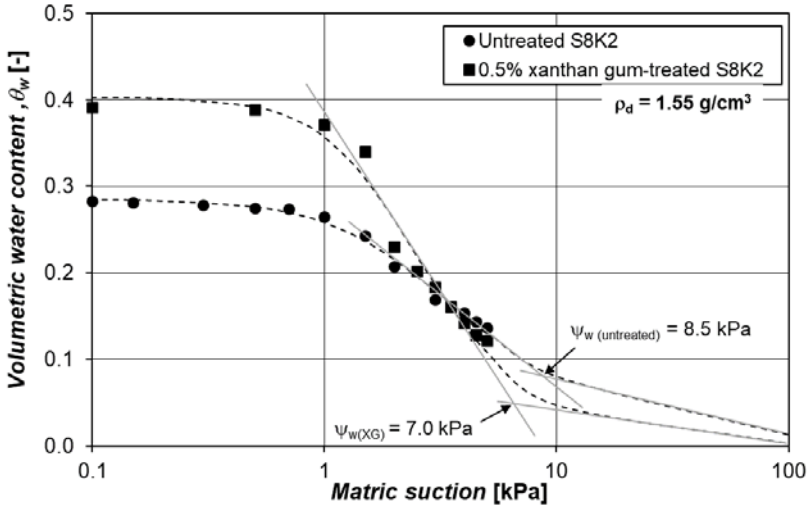

Figure 3.12. Wetting soil–water characteristic curves of the untreated and 0.5% xanthan gum–treated S8K2 soil (Tran et al. 2019b)

Table 3.4 SWCC parameters of untreated S8K2 and 0.5% treated S8K2 (Tran et al. 2019b)

Van Genuchten parameters		20% kaolinite-sand	
		Untreated	Treated
θ_s		0.28	0.40
θ_r		0	0
α	[kPa $^{-1}$]	0.46	0.54
n		1.81	2.27
m		0.45	0.55
WEV	[kPa]	8.50	7.00

3.4 Discussions and summary

3.4.1 Discussions

3.4.1.1 Drying B-SWCC

3.4.1.1.1 Water-related behavior of xanthan gum–treated soils during drying process

Figure 3.13 shows a schematic model of the drying behavior of untreated and xanthan gum –treated sands. At the saturation stage of the drying test, xanthan gum -treated sand contains more water than untreated sand (Fig. 3.13a and b). It is because the saturation of untreated sand is governed by a capillary force which is always affected by gravity force. The sand itself has very low water holding

capacity (Mustafa et al. 1989). Therefore, the surface of the untreated sand specimen is not fully covered by water. Meanwhile, the water absorption of xanthan gum is essential to saturate the treated soil system. The xanthan gum absorbs and swells until the pore spaces are fully filled. The role of hydrogel on improvement the saturated volumetric water content of the sand obtained seem to coincide with that of many previous studies (Al-Darby 1996a; Bhardwaj et al. 2007; Chenu 1993).

As the soil specimen is subjected to higher suction, for the untreated sand, together with the soil skeleton the free water can stand a suction which is lower than air entry value. When the suction reaches to the air entry value, the free water is replaced by air immediately (Karube and Kawai 2001). After that, the increase of suction reaches a value at which the meniscus water is removed from the untreated sand. The water keeps moving out quickly from the sand with higher suctions (Fig. 3.13c).

The amount of bound water in hydrogel decides the strength of xanthan gum hydrogel matrix. The higher the xanthan gum content, the stronger the xanthan gum hydrogel. Therefore, the treated sand can bear higher air pressure, and control the penetration of air into the sand system. As a result, the *AEV*s and the amount of remaining water at higher suctions are higher in the case of the treated sand compared to the untreated sand (Fig. 3.13d).

Furthermore, the inconsiderable of volumetric water content for cases of 1%, 2%, and 3% is due to the constant pore size of the specimen (Chang et al. 2016). At 1% xanthan gum treatment, the sand pores are mostly filled with bound water. From this point, the excess amount of xanthan gum shows less effects on the water absorption of specimens.

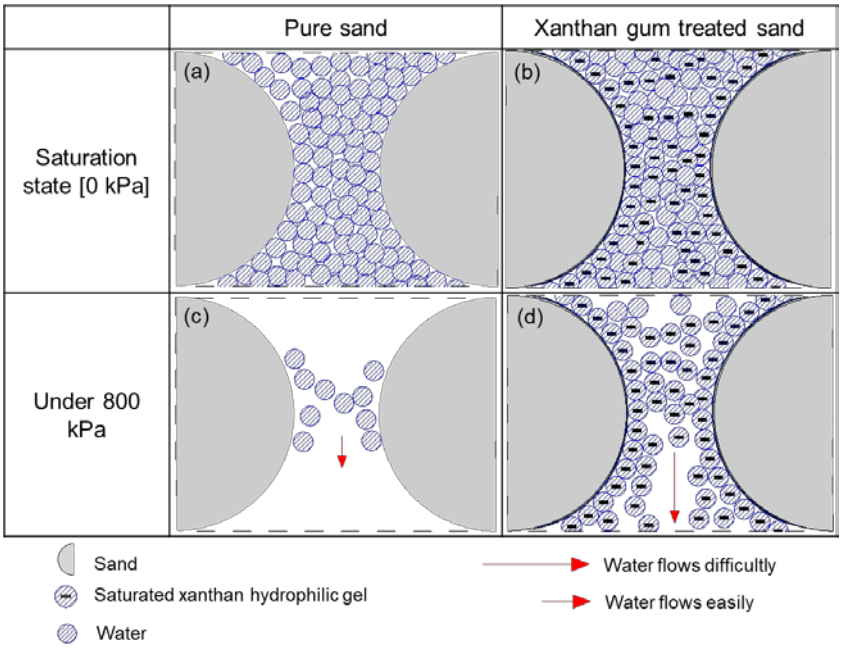

Figure 3.13 Schematic model of the drying of untreated and xanthan gum -treated sands

3.4.1.1.2 The rate of change in water storage

On the SWCC, the slope of the line joining the *AEV* and the residual point provides a measure of the rate at which water is removed from the soil as suction is increased past the *AEV*. The slope of the SWCC indicates the rate of change in water storage in the soil concerning soil suction. The *n* parameters of fitting curves reflect the slope of the SWCC. Since the specimens have similar dry density, the presence of xanthan gum hydrogel solution is the main affecting factor on the change of the SWCC for jumunjin sand.

The *n* parameter decreases as the xanthan gum content increases. It is because the water absorption of xanthan gum play a leading role in holding water and controlling the decreases in pore size. As a result, the higher xanthan gum content used, the shallower the slope of the SWCCs and the lower n parameters. However, as the xanthan gum content is beyond 1%, the effect of fixed pore size on the amount of water absorbed causes the less impact of xanthan gum on the *n*.

3.4.1.2 Wetting B-SWCC

3.4.1.2.1 Water-related behavior of xanthan gum–treated soils during wetting process

Figure 14 shows a schematic of the wetting behavior of the xanthan gum–treated soils. For the S10 soils, the dried xanthan gum instantly absorbs water due to hydrophilicity, then clog the inter–granular pore spaces, restricting the upward flow of water (Fig. 3.13a) (Bueno et al. 2013; Lehrsch et al. 2011). Water within a soil column is known to rise until the total surface of the capillary system is balanced by the weight of the water that is lifted (Free 1911). As the sand contains xanthan gum, xanthan gum absorbs an abundant amount of water owing to its hydrophilicity, thus significantly increasing the soil water content from the wetting datum. The amount of water in treated soil column have to carry a great effect of gravity. Moreover, as the funstional groups in xanthan gum completely interact with water, the xanthan gum hydrogels located at the bottom of the soil column may exhibit a hydrophobic wetting characteristic that results in a significant reduction in the capillary conductivity (Nagy and Deák 2013), as shown in Fig. 3.14a.

The untreated S9K1 and S8K2 soils show a steady upward water flow and reach higher water levels in the capillary tubes compared to the S10 soil. However, the water absorption of the kaolinite particles in the inter–granular pore spaces requires more time for sufficient wetting because of their high water absorption, compared to the untreated S10 sand (Fig. 3.8a). In treated soils, a xanthan gum –kaolinite matrix via hydrogen bonding is formed (Nugent et al. 2009), during the wetting process xanthan gum-kaolinite bridge get loosen due to the simultaneous water absorption of xanthan and

kaolinite (Fig. 3.14b). At low xanthan gum contents (0.1 and 0.25%), the xanthan gum –kaolinite matrix works well to spread the water rapidly. xanthan gum with its water absorbability reduces the frictional effects due to the water absorption of the kaolinite particles in the pore spaces. When the xanthan gum content ≥ 0.5%, xanthan gum seems to fully clog the pore spaces, accompanied by a significant capillary conductivity reduction (Figs. 3.7b and c).

Moreover, as montmorillonite has a specific surface area and CEC values higher than kaolinite (Kahr and Madsen 1995), the untreated S9M1 soil shows a lower capillary conductivity than the untreated S10 and S9K1 soils (Fig. 3.8a) via the pore clogging induced by high swelling ability of montmorillonite particles as it contacts with water (Fig. 3.14c). Xanthan gum treatment can improve the water absorption and the swelling ability of montmorillonite (Razakamanantsoa et al. 2014), which in turn shows a significant effect on the capillary conductivity of the sand–montmorillonite mixtures, as shown in Fig. 3.7d. Montmorillonite can adsorb more xanthan gum compared to kaolinite because montmorillonite have smaller particles and the thicker double layer (Du et al. 2010); therefore, under the same conditions of the xanthan gum treatment, the treated S9M1 soils exhibit a lower capillary conductivity than the treated sand–kaolinite mixtures (Figs. 3.8b–d).

3.4.1.2.2 Significance of the wetting B-SWCC of biopolymer-treated soil

As mentioned above, the xanthan gum–treated soils show a distinctive absorption behavior compared to the untreated soils. In particular, biopolymer-treated soils show promising potential for immediate infiltration prevention. An example of using the wetting behavior of the xanthan gum–treated soils for slope stability against heavy rainfall are provided. In fact, the water-entry suction value of the xanthan gum–treated soil ($\psi_{w(XG)}$ = 7.0 kPa) is lower than that of the untreated soil ($\psi_{w(untreated)}$ = 8.5 kPa) (Fig. 3.12, Table 3.4). If water entry is the only deciding factor for the slope stability, the xanthan gum treatment should be more vulnerable to slope stability. Although xanthan gum quickly absorb water, water holding and swelling of xanthan gum which cause the reduction in hydraulic conductivity becomes the dominant factors for the behavior of the entire soil area because of the significant reduction in the hydraulic conductivity (and infiltration) of the soil. Note that the trend in the wetting SWCC shown in this example is for the 0.5% xanthan gum-treated S8K2 soil. Different biopolymer types and contents will render different wetting behaviors, especially water-entry values. Therefore, the overturning trend in the biopolymer–treated soil to untreated soil may be different.

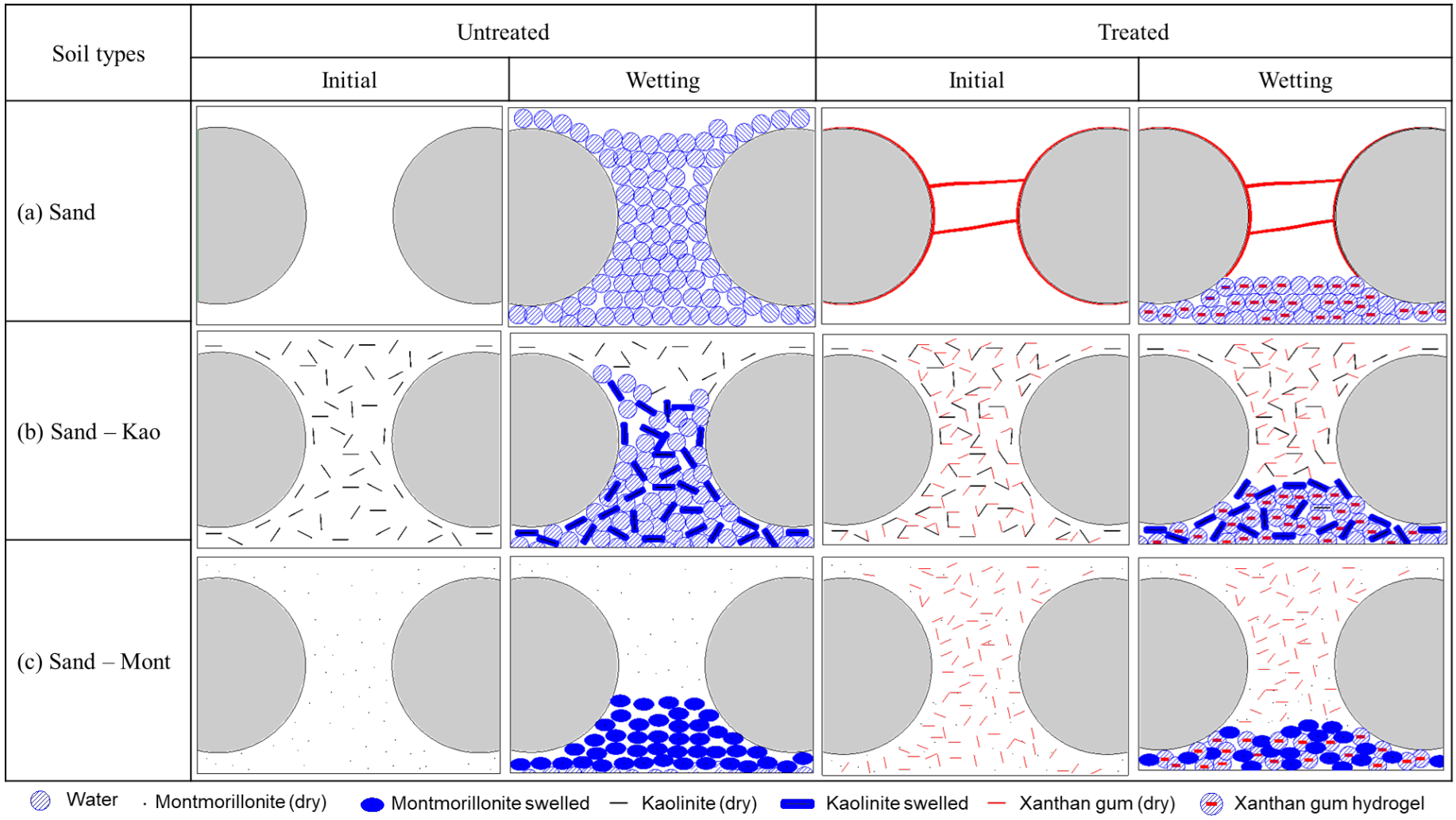

Figure 3.14. Schematic comparison of the wetting and water retention behaviors of untreated and xanthan gum biopolymer–treated soils (Tran et al. 2019b)

3.4.2 Summary

The drying and wetting soil-water characteristics was conducted to understand the effect of xanthan gum via water absorbing and holding capacity on water distribution in unsaturated soil. Fredlund SWCC device was used to conduct the drying test, while, column test was used to obtain the wetting behavior of xanthan gum-treated soils.

The drying-SWCC shows that xanthan gum enhance volumetric water content, and air entry values via high water-absorption and water-holding capacity as the soil subjected to high air pressure. Furthermore, the slope of the BSWCC of xanthan gum treated sand is less steep than that of untreated sand, which show the low rate of change in water storage. It is because xanthan gum hydrogel can decrease pore size of soil via water absorbing-swelling-water holding capacity. The fixed soil pore size is the main factor renders the exponential decay relationship between xanthan gum content and van Genuchten parameters n and θ. The volumetric water increases with xanthan gum content; however, at 1% and higher xanthan gum content treatment, there is no significant change in amount of water absorbed. This finding indicates that 1% xanthan gum hydrogel fully filled pores of soil with dry density of 1.55 g/cm^3. This finding can be useful for agriculture purpose where xanthan gum is used as anartificial water storage for plant. The 1% xanthan gum treatment can cause a bad aeration condition in soil.

The wetting-SWCC provides the role of water absorption and holding capacity of xanthan gum in capillary conductivity of soil. If the water risen in sand column is due to the surface tension, then water absorption and holding capacity of xanthan gum reduces the water movement in sand column. The presence of clay in sand render different wetting behaviors corresponding to type and amount of clay which affecting factors on number of kaolinite and xanthan gum interaction. At low xanthan gum treatment, xanthan gum can work as a water transferor since the water can quickly transfer within kaolinite-xanthan gum matrix. The uses of xanthan higher than 1% quickly blogs soil pores which causes the difficult in movement of water flow. Due to the pore-clogging effect of xanthan gum. This phenomenon happens only to kaolinite clay. Montmorillonite with smaller size particles, thicker double layer, higher charge and strong swelling capacity renders decrease in capillary conductivity with xanthan gum content. This finding of water movement in unsaturated xanthan-gum treated soil can

provide a quick understanding on unsaturated hydraulic conductivity of xanthan gum-treated soil as it is applied to geotechnical engineering.

Chapter 4 Hydraulic conductivity of biopolymer-treated soils with stress variations

4.1 Introduction

In order to investigate the water absorbing and holding capacity of biopolymer-treated soils subjected to stress variations, hydraulic conductivity was investigated.

The laboratory experimental methods to estimate the pore-clogging effect of hydrogels used in these studies can be divided into two groups. Groups 1 includes methods where water flow goes through hydrogel treated soil such as falling head permeabiliy test (Andry et al. 2009), constant head permeameter (Al-Darby 1996a; Narjary et al. 2012), and flexible wall permeameter (Bouazza et al. 2009; Chang et al. 2016). Group 2 are methods where hydrogel solution runs through untreated soil pack such as pressure pumping flow (Etemadi et al. 2003; Khachatoorian et al. 2003a). In this study, a pressured hydraulic conductivity apparatus, which can be classified in group 1, is introduced. The advantage of the equipment is to be able to investigate the effects of the effective stress and pore pressure on hydraulic permeability of soils, which has yet to be considered commonly.

Previous studies show that the gel-type biopolymers show better inter–particle interaction with clay particles via a direct ion or hydrogen bonding than that of sand (Chang et al. 2016; Chang et al. 2015b). And, the ratio in the mass of biopolymer to clay becomes the dominant parameter governing the strengthening behavior of the gellan gum–treated sand–clay mixtures (Chang and Cho 2019). However, a detailed understanding of the interactions of gellan gum and soils and their permeability reducing behaviors, especially for sand–clay mixture with different gellan gum content, has yet to be achieved.

Thus, the chapter seeks to address the following questions: 1) the effect of inter–particle interaction on the effectiveness of gellan gum on hydraulic conductivity reduction; 2) Hydraulic behavior of gellan gum–treated soil in consideration of external pressures. To reach the target of this study, a series of laboratory hydraulic conductivity tests using a pressurized hydraulic conductivity system was conducted on gellan-treated soils. Furthermore, a single case of xanthan gum treatment was conducted to have a comparison on the workability with gellan gum at initial condition (i.e. right after mixing).

4.2 Experimental program for hydraulic conductivity test

4.2.1 Sample preparation

The tests was conducted on xanthan gum and gellan gum treated sand. To prepare thermos–gelated gellan gum–treated soil mixtures, gellan gum powder was first dissolved and hydrated in deionized water heated at 100°C to obtain a gellan gum solution. After that, the dry soil and hot gellan gum solution were uniformly mixed. The heated gellan gum -treated soil slurry was molded into a cylindrical cell which is a part of the equipment. The soil specimen was cooled down at room temperature (i.e., 20°C) to form a solid state. The specimen conditions were summarized in Table 4.1.

To prepare xanthan gum-sand mixtures, the xanthan gum powder was first dissolved and hydrate in deionized water at room temperature. Xanthan gum content was 1.0% and initial water content was 35%.

4.2.2 Experimental design and process

The saturated permeability of soils was determined using a pressurized hydraulic conductivity system (Fig. 4.1). The soil mixtures were set into a cylindrical cell which is 9.3 cm in height and 8.0 cm in diameter. However, specimen height depends on soil type and biopolymer hydrogel viscosity, which was measured for every test. At the top and bottom of the specimen, filter papers were placed so that water can evenly distribute within specimen during the experiment process.

The confining stress was applied when the specimen was cooled down to room temperature. The confining pressure was applied to the soil under the drained condition using a pneumatic air compressor, which was set up at 100, 200 and 400 kPa (Table 4.1). The consolidation process lasted for 24 hours at where the vertical strain of soil reached constant (Fig. 4.2a-b). At the beginning of the consolidation process, water dropped out due to the movement of free water under high air pressure. The amount of water loss was lower than 6% of the initial water designed for the test. The water loss depended on the amount of gellan gum concentration. For instance, for the case of treated S9K1 soil, there were 6% and 1.3% water loss (in the mass of the initial water weight) for 0.25% and 2% gellan gum concentration, respectively. At the end of the consolidation process, there was no more water loss, and the confinement pressure worked as the effective stress σ' on the soil system. The dry density of soil after consolidation was tabulated in Table. 4.2.

For the case of xanthan gum treated sand, the volume of xanthan gum-sand specimen quickly changed (Fig. 4.3), and xanthan gum kept flushing out of xanthan gum hydrogel with time (Fig. 4.4). It is because the viscosity of xanthan gum hydrogel solution, which can be easily pressed out with air

flow. Meanwhile, gellan gum with its thermal-gelation properties did not show unstable state of hydrogel.

Curing was carried out for saturation purpose via supplying water pressure of 70 kPa into the specimen. To de-air the specimen, the outlet valve was open at the beginning of the saturation process. After that, the outlet valve was closed. The flow rate was tracked via a pump controller. As the flow rate dropped down to zero, the specimen was considered to be fully saturated.

When the specimen was fully saturated, the outlet was opened, and the permeability test was conducted. The water drained out was collected and weighted with time. The hydraulic conductivity was observed at varying water pressures. The inlet water pressure (hereafter, IWP) was applied for 24 hours to ensure that the specimen reached a stable hydraulic conductivity.

Table 4.1. Specimens and experimental conditions

Soil types	Gellan gum content [%]	Initial water content [%]	Effective stress [kPa]	Inlet water pressure, Δu [kPa]
Sand (S10)	0; 0.5	30	100; 200; 400	> 70
	1.0	36		
	2.0	44		
Sand−10% kaolinite (S9K1)	0; 0.25; 0.4; 0.5	30		
	0.75	35		
	1.0	36		
	1.5	38		
	2.0	44		

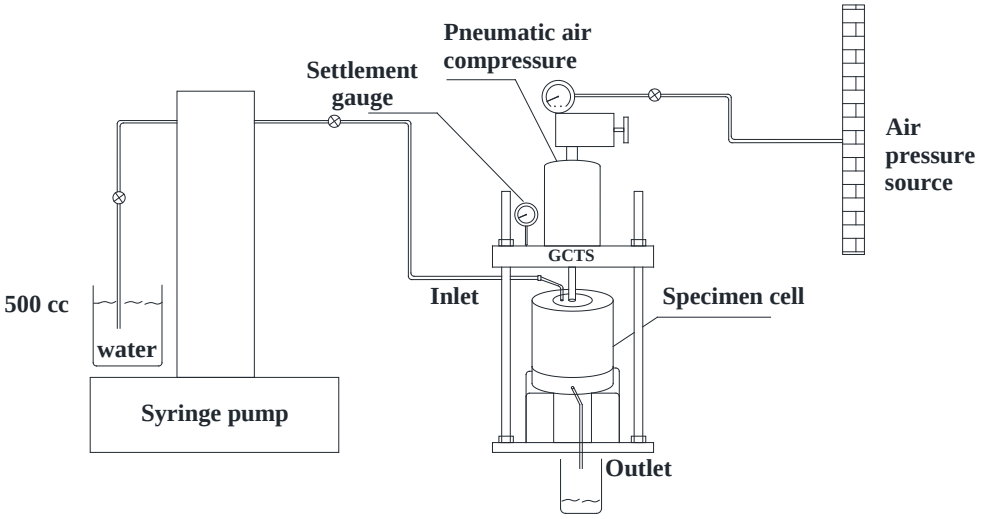

Figure 4.1. Schematic diagram of pressurized hydraulic conductivity

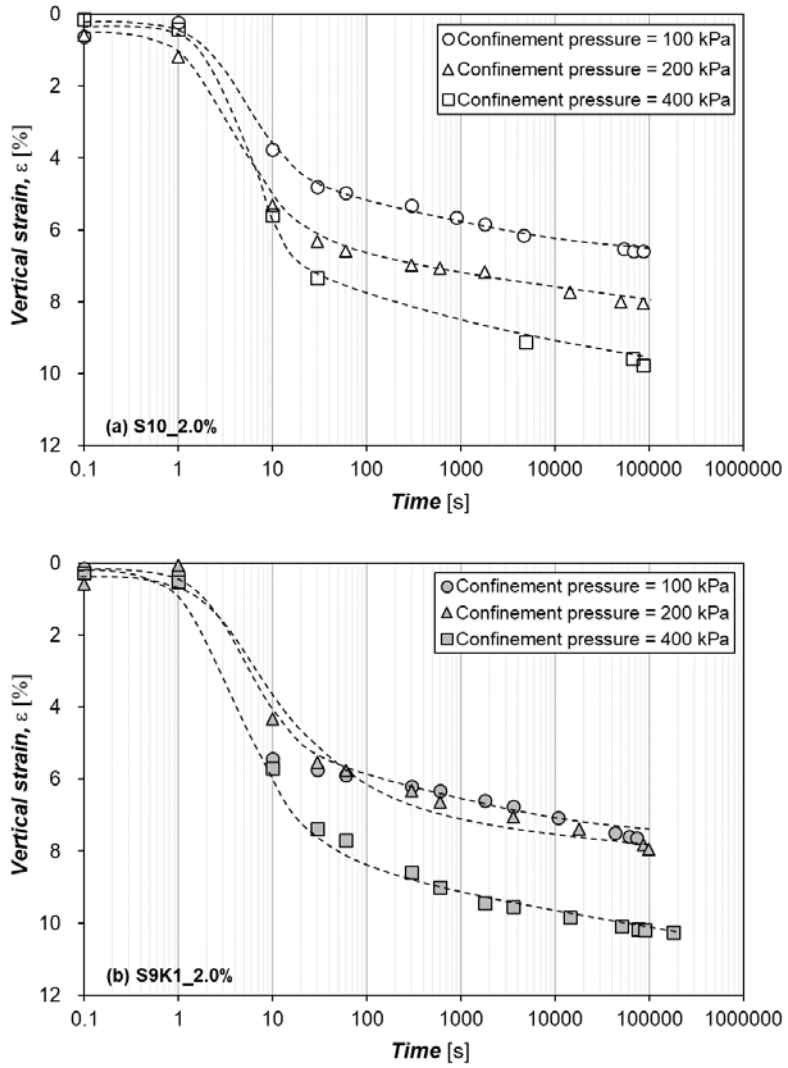

Figure 4.2. Vertical deformation of 2% gellan-treated (a) 100% sand (S10) and (b) sand–kaolinite mixture (S9K1) at different confinement pressures

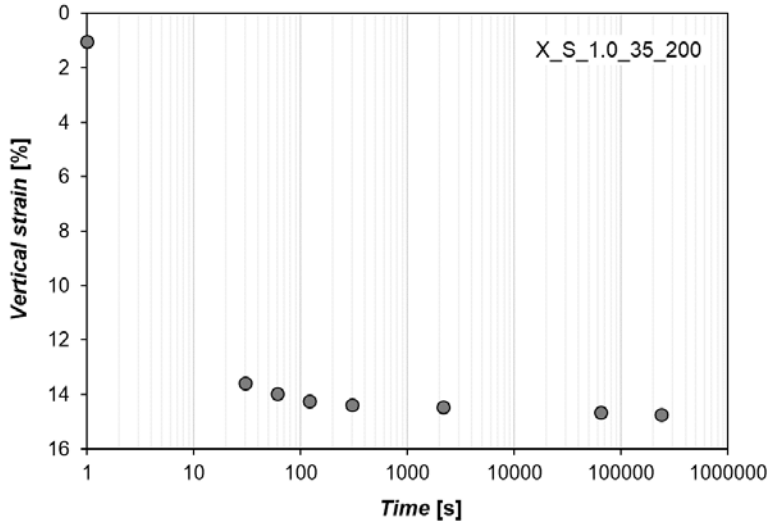

Figure 4.3. Vertical deformation of 1% xanthan gum treated sand under at confinement pressure of 200 kPa

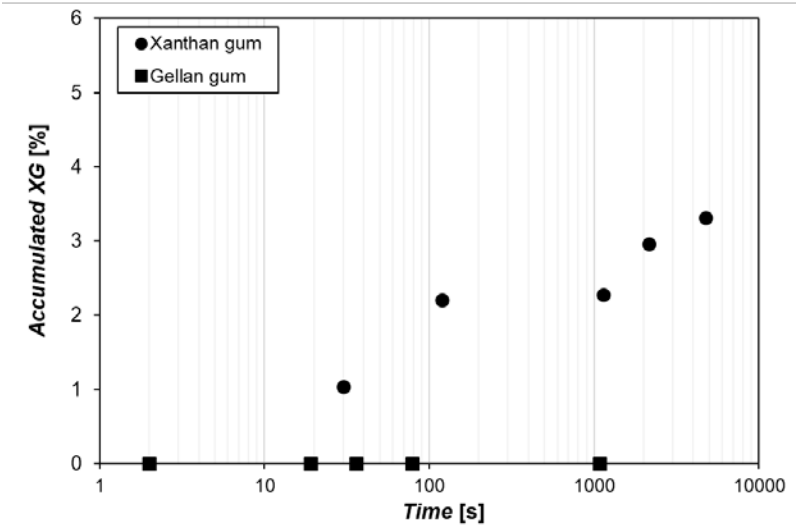

Figure 4.4 Flushing out of biopolymers with time under 200 kPa confinement pressure

Table 4.2. Dry density of soils with different effective stress

Gellan content [%]	Gellan gum to soil ratio in mass (m_b/m_s)	0	0.25	0.40	0.50	0.75	1.00	1.50	2.00
	Gellan gum to solution ration m_b/m_w	0	0.83	1.33	1.67	2.14	2.78	3.95	4.55
S10	ρ_d [g/cm^3]	1.48			1.65		1.48		1.50
S9K1	ρ_d [g/cm^3]	1.53	1.62	1.57	1.77	1.51	1.53	1.58	1.58

4.2.3 Analysis method

In order to know if the flow which runs through the soil system is turbulent or laminar flow, the Reynold number is calculated as follows

$$R_e = \frac{\rho.v.D}{\mu} \tag{4.1}$$

The Reynolds number values for some cases are provided in Table 4.3

Table 4.3 Reynolds number values

Gellan content [%]	Effective stress [kPa]	S10			S9K1		
		IWP			IWP		
		100	200	400	100	200	400
0	100	11.47	21.56	32.50	12.18	19.89	23.77
	400	10.70	14.70	25.70	11.08	18.02	24.12
0.5	100	0.74	0.53		0.01		
	400	0.27	0.52	1.75	0.01	0.00	0.06
1.0	100	0.01			0.00	0.02	
	400	0.01	0.03	0.15	0.00	0.00	0.01
2.0	100	0.02	0.06		0.00	0.02	
	400	0.00	0.01	0.08	0.00	0.00	0.01

When the Reynolds number is below 1-10, the flow pattern is considered to be laminar (Bear 2012, 2013); otherwise, the flow pattern is transitional and turbulent (Chen and Wagenet 1992).

Based on the Reynold number, the flow through untreated soil is non-laminar flow. Therefore, the flow velocity and hydraulic conductivity is nonlinear. The hydraulic conductivity (HC) is calculated as follows (Mulqueen 2005)

$$k = \frac{V}{A.t}.\left(\frac{L}{h}\right)^{0.5} \tag{4.2}$$

The flow through the treated soil is laminar flow. The HC for the gellan gum-treated soil is calculated following Darcy's law

$$k = \frac{V.L}{A.h.t} \tag{4.3}$$

where V is the collected volume of water, L is the height of soil specimen, A is the area of soil specimen, h is the head difference, and t is the time required to the V volume.

4.3 Results

4.3.1 Workability of biopolymers at initial state

Figure 4.5 the initial xanthan gum gum did not have any effect on hydraulic reduction, even the HC of xanthan gum treated sand was lower than untreated sand (Fig. 4.5) due to its unstable condition. Therefore, it is concluded that at initial state, xanthan gum hydrogel is not proper materials for hydraulic conductivity reduction of soil. Further testing will focus on gellan gum-treated soil

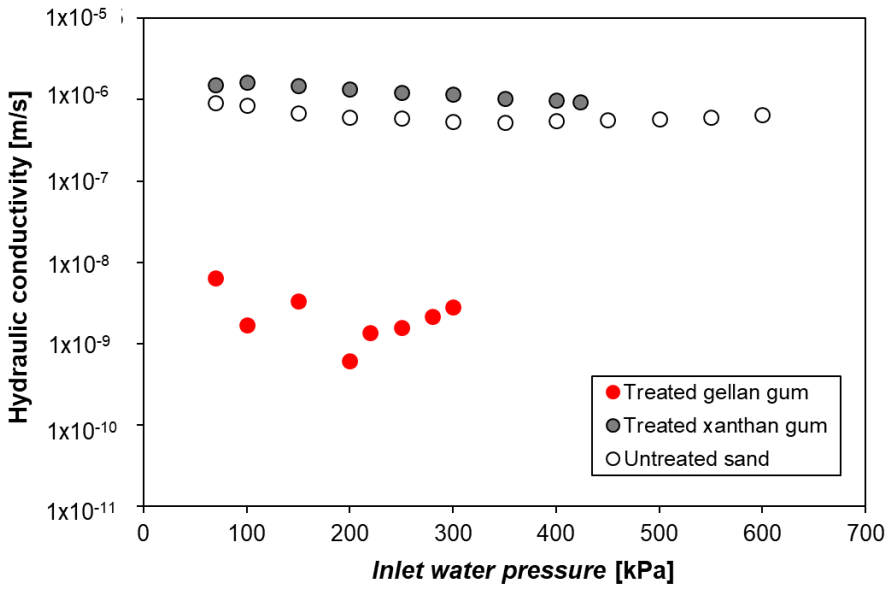

Figure 4.5 A comparison on effectiveness of xanthan gum and gellan gum at initial hydrogel state

4.3.2. Hydraulic conductivity of gellan gum-treated soils

Figure 4.6 shows the changes in the HC of gellan gum–sand (S10) with the increase in pore water pressure. The untreated sand (i.e. gellan gum = 0.0 %) obtained the HC values which were in a range of 5.29 ~ 6.70 x 10^{-7} m/s (Fig. 4.6a). The HCs seemed to have similar regardless of the σ′. Meanwhile, as the sand was treated by gellan gum, the starting value of HC at IWP of 70 kPa decreased significantly compared to the untreated sand, corresponding to the gellan gum content (Fig. 4.6b, c, d). For treated sand, the changes of HC with IWP formed upward concave curves. In the beginning, the HC gradually decreased to a minimum value, as the IWP reached a certain value, the HCs started increasing. The sand itself shows a low capacity of holding water (Mustafa et al. 1989), which allowed the pressurized water to run through the soil easily. The presence of gellan gum in the sand system improves the strength of soil and water holding capacity (Chang et al. 2016), which in turn enhanced the stability of the sand under high pore water pressure applied. Furthermore, gellan gum played a role in filling pore space within the sand specimen (Chang et al. 2016), and in turn, showed

more resistance on the water flow.

The relationships between HC and IWP of sand–kaolinite mixtures (S9K1) with different gellan gum content were shown in Fig.4.7. Similar to the S10, the upward concave curves which express the HC–IWP relationship for the gellan gum-treated S9K1 was achieved, which depended on the gellan gum concentration. The water interaction of gellan gum-kaolinite matrix was essential to water control in the S9K1 soil. A linear relationship was obtained as the sand–kaolinite mixtures were treated by 0.0% and 0.25% (Fig. 4.7a, b). For the untreated S9K1 soil, the HCs were in a range of 3.77 ~ 4.49 x 10^{-5} m/s, which were as same as the values of the untreated sand. The loss of kaolinite particles during the increase of IWP could be a reason for the results obtained (Fig. 4.8). The water pressure was so high that kaolinite particles could not hold water or keep themselves stable in the soil system. For the case of 0.25% gellan gum-treated S9K1 soil, even though its HCs were lower than that of the untreated soil, the HC showed a linear increase trend with IWP. At gellan gum = 0.5% and higher, the strength of the soil was improved because of the stronger gellan gum–kaolinite matrix (Chang and Cho 2019), which allowed the soil to be able to stand a higher water pressure and to perform the interaction with water.

Linear tangent lines of the upward concave curves allowed determining the minimal HC (k_min) and the relative IWP (P_{k_min}) of the soils (Fig.4.9). For further sections, the k_min was used to estimate the effect of gellan gum content and effective stress on the HC.

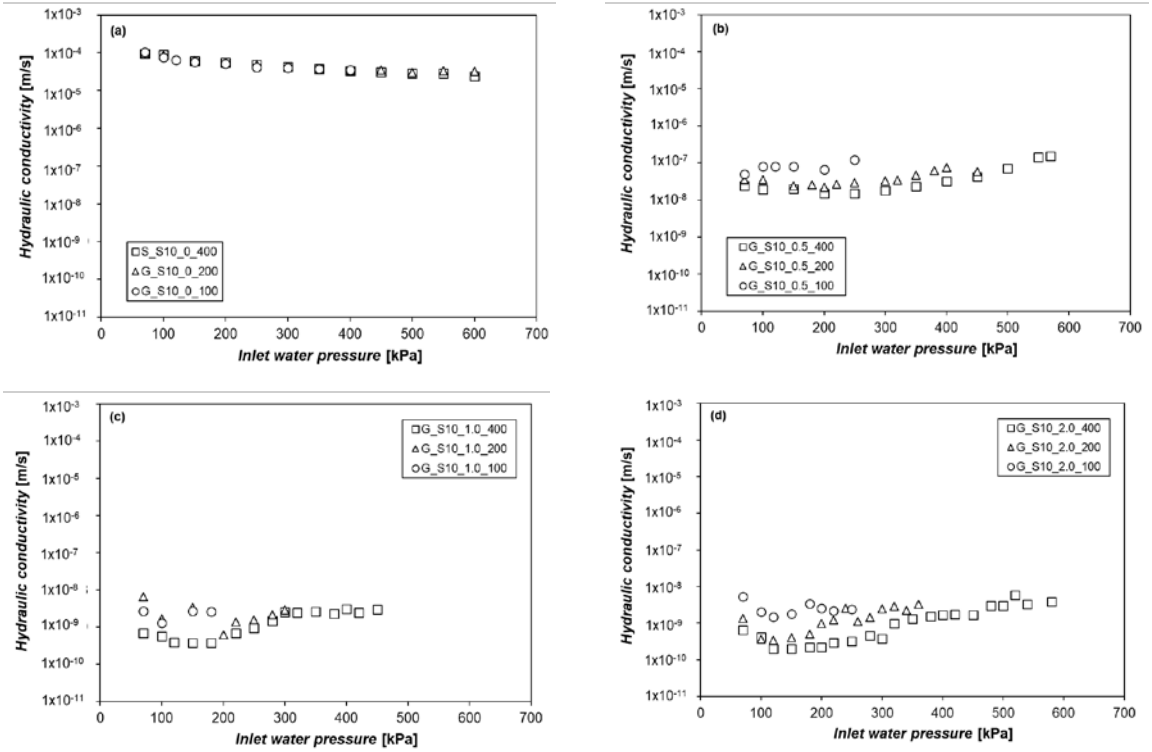

Figure 4.6. Hydraulic conductivity with pore water pressure of sand treated (a) 0.0%; (b) 0.5%; (c) 1.0 % and (d) 2.0% of gellan gum content

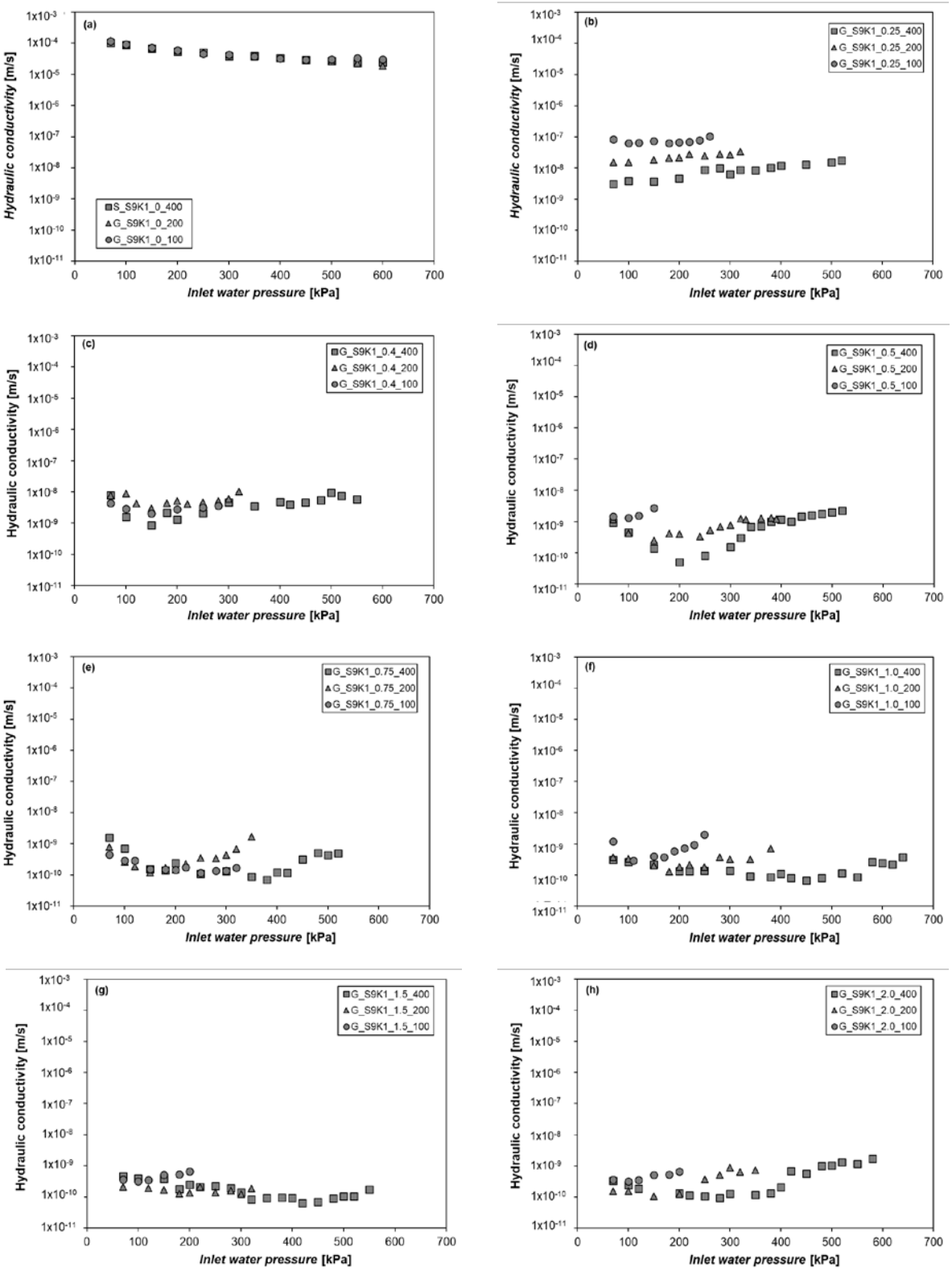

Figure 4.7. Hydraulic conductivity with pore water pressure of sand–kaolinite mixture treated (a) 0.0%; (b) 0.25%; (c) 0.4%; (d) 0.5%; (e) 0.75%; (f) 1.0%; (g) 1.5% and (h) 2.0% of gellan gum content

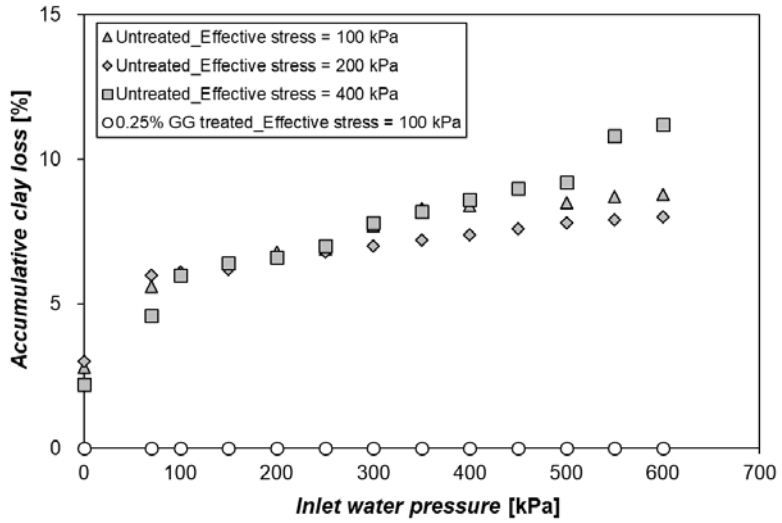

Figure 4.8. The loss of kaolinite with the increase of inlet water pressure

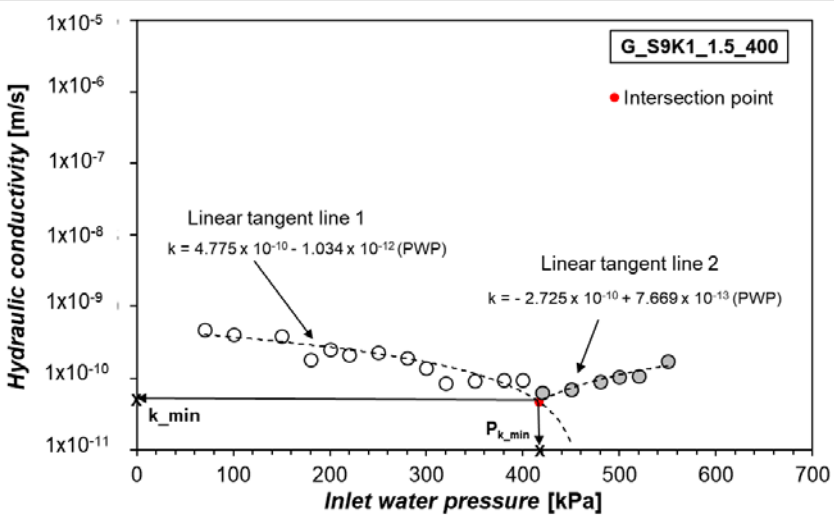

Figure 4.9. Minimum hydraulic conductivity and related inlet water pressure of gellan gum–treated soil

4.3.3 Effect of gellan gum content on the pressurized hydraulic conductivity behavior

The HC of gellan gum–treated soils in the initial state decreases exponentially (Fig.4.10). The HC of gellan gum–treated sand significantly reduced from an untreated condition to 1% gellan gum content. After that, above gellan gum content toward a stabilized HC was obtained (Fig.4.10a). The trend is in consistency with the results obtained by Chang et al. 2016 (Chang et al. 2016). The HC of the S9K1 also exhibited the exponential relationship with GG content (Fig.4.10b). For the S9K1 soil, the convergence started at the gellan gum approximately 0.75%. The effective stress did not show a significant effect on the shape of the trend. However, the HCs of the treated soils shifted down slightly with the higher effective stress.

The decrease of HC with gellan gum content was due to the increase in water holding capacity of GG. With higher gellan gum content, there were more strongly bound water molecules that were formed in the soil system, which rendered the reduction in HC for the S10 soil. The HC was converged at gellan gum of 1% was because within a fixed pore size, the gellan gum hydrogel was entirely filled the pore space with strongly bound water under saturation condition. From this point, the excess amount of gellan gum no longer had a significant effect on hydraulic conductivity reduction (Chang et al. 2016). Meanwhile, the gellan gum–treated S9K1 converged earlier state of gellan gum treatment (0.75%), which was because the higher water holding capacity of the soil was governed by gellan gum-kaolinite matrix. Thus, the pore spaces were quickly filled with water absorbed by gellan gum-kaolinite matrix.

Figure 4.8 shows the relationship between gellan gum content and the Pk_min. To avoid the effect of σ', the P_{k_min} was divided by the σ'. For the S10 soil, the P_{k_min} decreased slightly with gellan gum content regardless of σ' (Fig. 4.11a). The hydraulic behavior of the soil mainly depended on the rheological properties of gellan gum. Meanwhile, for the S9K1 as gellan gum content lower than 1% was used the P_{k_min} increased with gellan gum content. Above 1%, the P_{k_min} decreased with gellan gum content. Here, the hydraulic behaviors of the soil were based on the interaction mechanism of gellan gum and kaolinite in their matrix and their responses under water pressure.

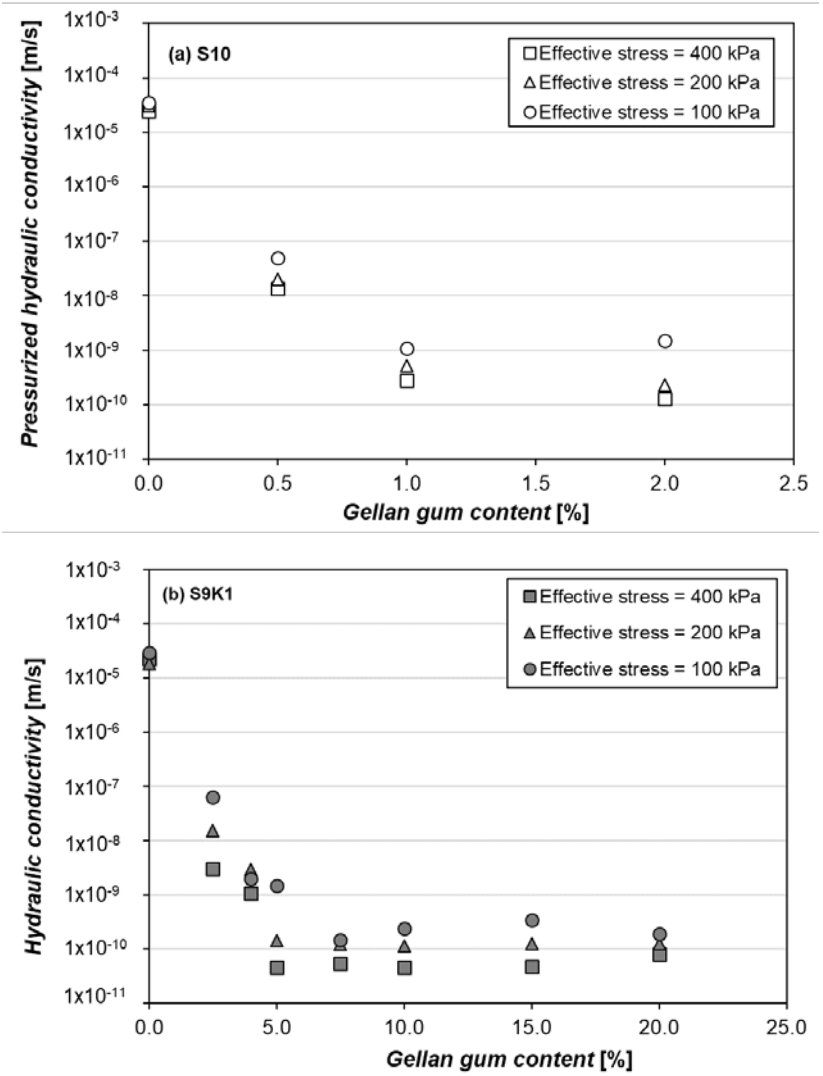

Figure 4.10. Reduction in hydraulic conductivity with gellan gum content of (a) 100% sand (S10) and (b) sand – kaolinite mixture S9K1

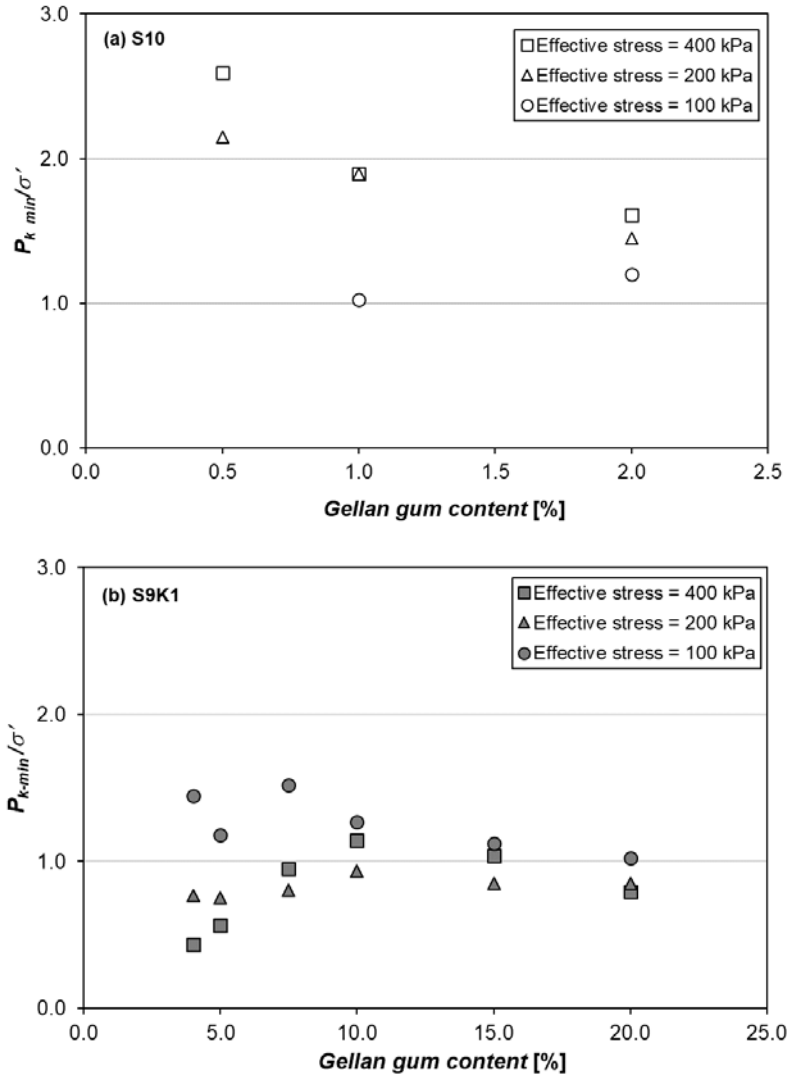

Figure 4.11. Effect of gellan gum content on P_{k_min} of (a) 100% sand (S10) and (b) sand – kaolinite mixture (S9K1)

4.3.4 Role of kaolinite particle on hydraulic conductivity behavior

Sand–kaolinite mixtures have advantages that result in higher strength due to the conglomeration effect between the gellan gum–kaolinite matrix and sand particles compared to pure sand (Chang et al. 2018). In this study, the gellan gum–kaolinite matrix not only suggested higher stability of the soil structure under the high water pressures but also introduced a higher water absorbability and holding capacity in the soil system. Thus, the HC values of the S9K1 soil were lower than that of the S10 soil regardless of effective stress. At 0% gellan content, the HCs of both soils were almost similar (5.0 ~ 6.8 x 10^{-7} m/s). As gellan gum and kaolinite interacted with water, the gap in HC of treated sand and treated sand–kaolinite mixture could be seen (Fig. 4.12)

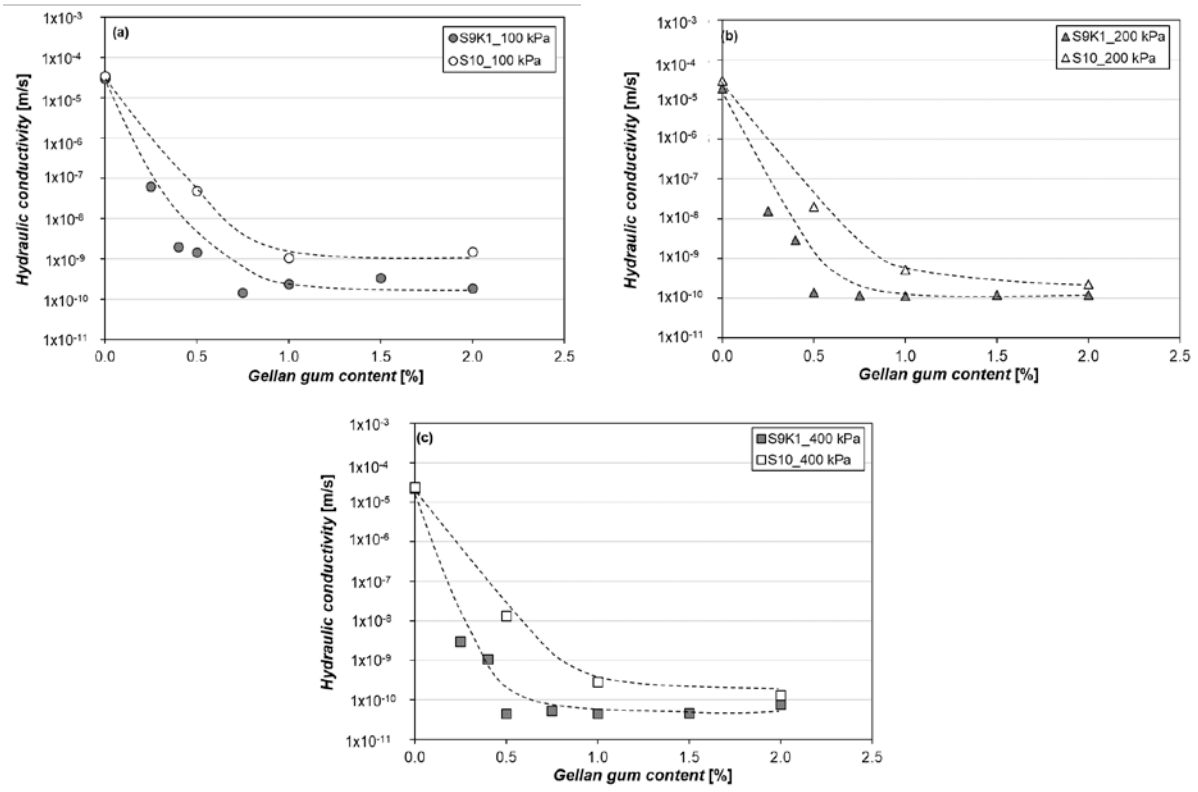

Figure 4.12. Effect of clay particles on hydraulic conductivity of gellan gum-treated soil

4.3.5 Effect of effective stress on hydraulic conductivity

At the beginning of the HC test, the applying confining pressure on the specimens suggested closer contacts of the particle–particle, gellan gum–particle, and gellan gum–gellan gum as the effective confining pressure reduced the pore space (i.e., porosity) in the soils. The soil system could increase the resistance to the water flow. The pore space of soil is an essential factor to control not only the amount of water contained in the pore space but also the water absorption and the swelling ability of gellan gum and kaolinite. The effective stress does not only limit the water absorption by the hydrogel, but it also extends the swelling time (Lejcuś et al. 2018). Thus, the HC obtained decreased with the σ' regardless of soil types, and gellan gum content (Fig. 4.13).

As the soils had the same gellan gum treatment condition, the lower amount of water penetrating to the gellan gum solution or gellan gum–kaolinite mixture system, the higher strength of hydrogels could be seen during water absorption process under higher water process because of the less effect on the rheological behavior of gellan gum. Therefore, the P_{k_min} value increased with the σ' with regardless of gellan gum content (Fig. 4.14).

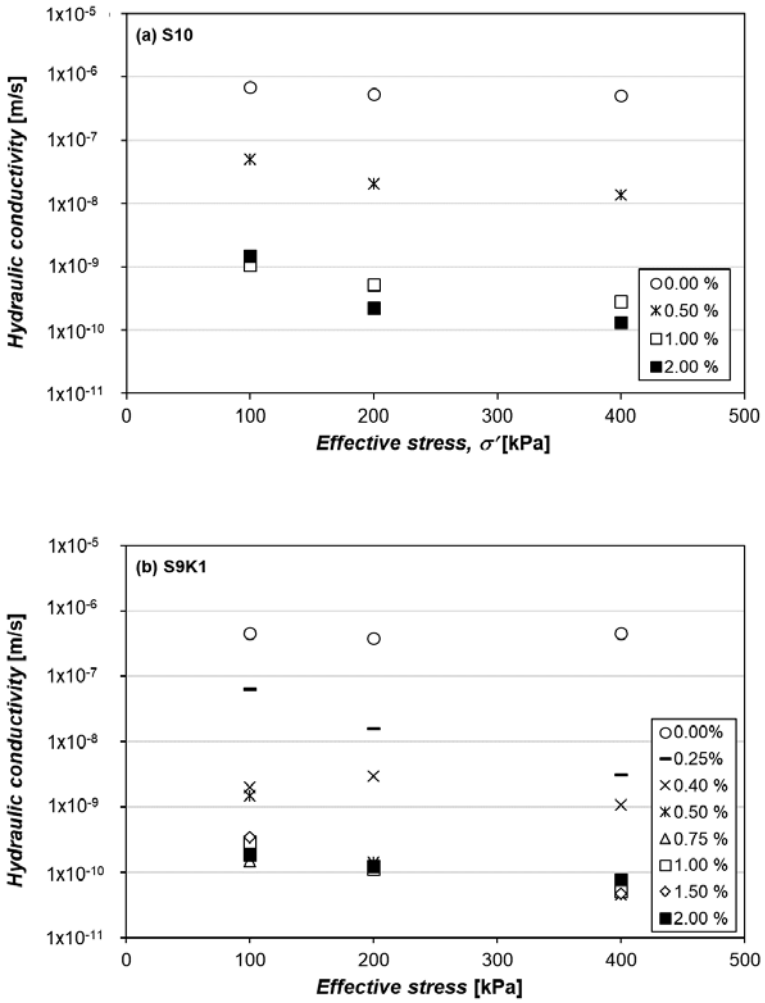

Figure 4.13 Effect of effective stress on hydraulic conductivity of (a) 100% sand and (b) sand – kaolinite mixture

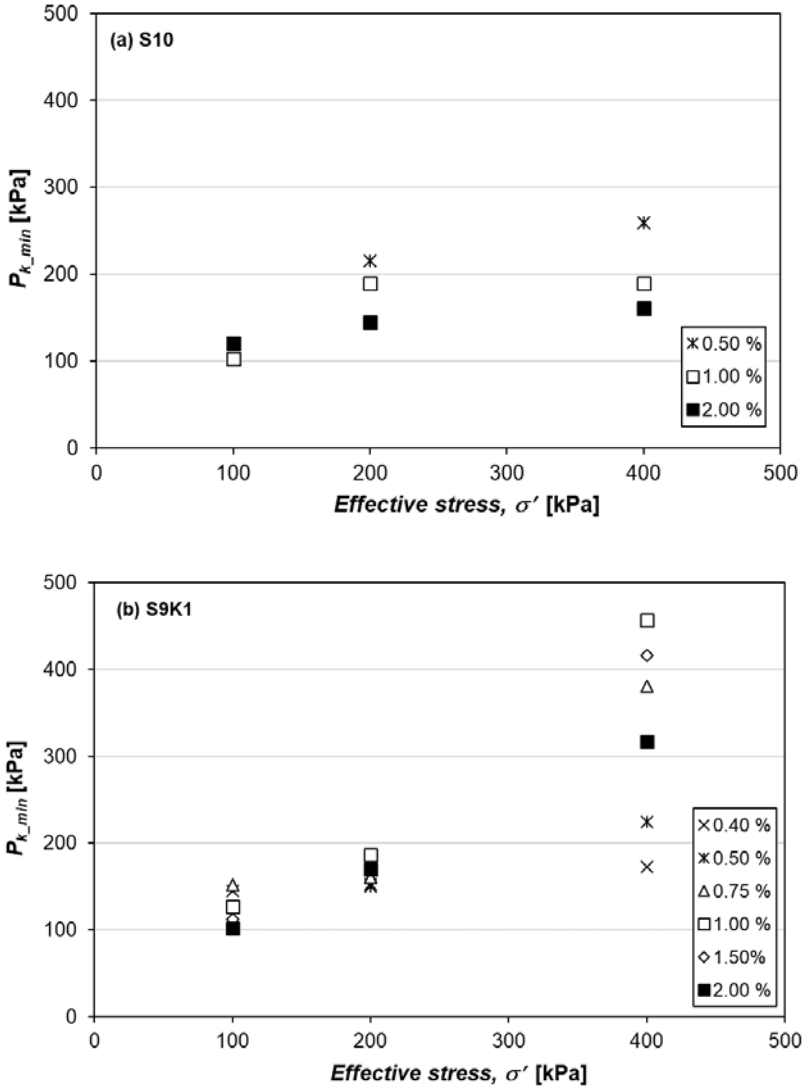

Figure 4.14 Effect of effective stress on P_{k_min} turning pressure of (a) 100% sand and (b) sand–kaolinite mixture

4.4 Discussions and summary

4.4.1 Discussions

4.4.1.1 Interaction mechanism of gellan gum with pressurized water

For the untreated S10, after water molecules fully fill soil pores, there are two types of water in the soil. Water molecules, which are close to the sand surface, can be held by surface tension. The others are free water. Under water pressure higher than 70kPa, free water can be flushed out easily without any interruption. The drained out water molecules are quickly replaced by new water molecules, which in turn cause an even water circulation in the soil system. Therefore, the HCs are almost constant with the pore water pressure (Fig.4.6a). For the untreated S9K1, the presence of kaolinite cannot support for the water holding which is expected to reduce the HC. It is because there is no interaction or bonding between sand and kaolinite; meanwhile, kaolinite itself cannot stand under the pressure applied. Therefore, a constant in HC with the pore water pressure is also obtained.

The water exists in the gellan gum–treated sand are strongly bound, weakly bound, and free water, which depends on gellan gum content. At the water pressure below the P_{k_min}, when the water flow contact to the soil surface, the speed of the water flow is reduced via pore–clogging effect of gellan gum. First, the extra water molecules are held by the gellan gum on the top of the specimen. Meanwhile, the pressure spreads through the specimen and pushes the free water or weakly bound water, located at the bottom, out of the specimen. The water that moved out gives more spaces for the movement of water from the upper parts. Free water and even weakly bound water that are trapped at the upper parts can move down. As the water holding process predominates over the water removing process, therefore, a decrease in HC can be seen (Fig. 4.6b~d). As the IWP gradually increased above the P_{k_min}, due to the reduction in viscosity and the strength of gellan gum and magnitude of pressure, the gel cannot hold water molecules as strongly as before. Thus, the water removing process predominates, and in turn, increases the HC (Fig. 4.6b~d).

For the S9K1 treated, a similar mechanism occurs at gellan gum content of 0.4% or higher. It is noted that the strength of gellan gum–kaolinite matrix plays a significant role in reducing water flowing into the specimen, and in holding water during the HC test. At gellan gum content of 0.25%, there are more free water and weakly bound water distributed in the gellan gum–kaolinite matrix, which smoothly moves out even under a minimum IWP of 70 kPa. The water holding process is taken over by the water removing process from the beginning of the HC test (Fig. 4.7b).

Chang and Cho 2018 recommended the mass ratio of gellan gum to kaolinite (m_b/m_c) of 4% for the maximum strength capacity (Chang and Cho 2019). In this study, the gellan gum–kaolinite matrix was subjected to a series of high pressure and was gradually weaken induced by the water absorption

process. Therefore, the ratio of higher than 0.75% is suggested as an optimal ratio for the minimum HC (Fig. 4.10).

4.4.1.2 The formation of P_{k_min}

P_{k_min} was obtained from two trends of the upward concave curve. For the S10, the lower value of P_{k_min} with gellan gum content indicated that the increasing trend come earlier at higher gellan gum content. At higher gellan gum treatment, the soil pores were fully filled by bound water. The water molecules penetrating to the gel can be due to the combination of osmosis driving force and compression force of water pressure. The osmosis driving force will have a direct effect on the strength of gel via decreasing the viscosity of the gel. Meanwhile, the water pressure gives a compression force that pushes water to move into the gel or soil system. The combined force can suddenly cause the formation of microcracks, micro water pathways, which can disturb the gel system and affect the water distribution within the soil system. Furthermore, low gellan gum content (< 0.5%), the gels are much more sensitive and have a quick response to the water pressure. Meanwhile, at high gellan gum content, the gel may be less sensitive to the water pressure; therefore, it performs sudden changes in hydraulic behaviors. As a result, the higher the gellan gum content, the lower P_{k_min} was obtained (Fig. 4.11a).

For the S9K1 soil, ratio m_b/m_c is essential to the P_{k_min}. The adsorption of anionic gellan gum occurs primarily onto the edge surface of kaolinite via hydrogen bonding (Chang and Cho 2019). (Nasser and James 2007). At low gellan gum concentration, gellan gum can facilitate inter–particle bridging forces between kaolinite and grains, which in turn increases the strength of the sand– gellan gum–kaolinite (Shaikh et al. 2017). The bridging system improves water absorption, distribution, and water holding in the soil system. Therefore, the soil can quickly response to the increase in water pressure, and the P_{k_min} is related to the IWP at where the strength of GG–kaolinite lose its strength and connection (Fig. 4.11b). This behavior can be seen as $0.75 \leq P_{k\_min} \leq 1.0$.

Gellan gum content increases suggested disruption of the kaolinite network structure. The adsorption of polymer molecules onto kaolinite and enhanced electrostatic repulsion through polymer anionic functional groups (Chang and Cho 2019; Lagaly 1989; Wang et al. 2016). The electrostatic repulsion between kaolinite particles and the anionic hydrogel allows limited polymer adsorption (Nasser and James 2007) (Fig. 4.15)

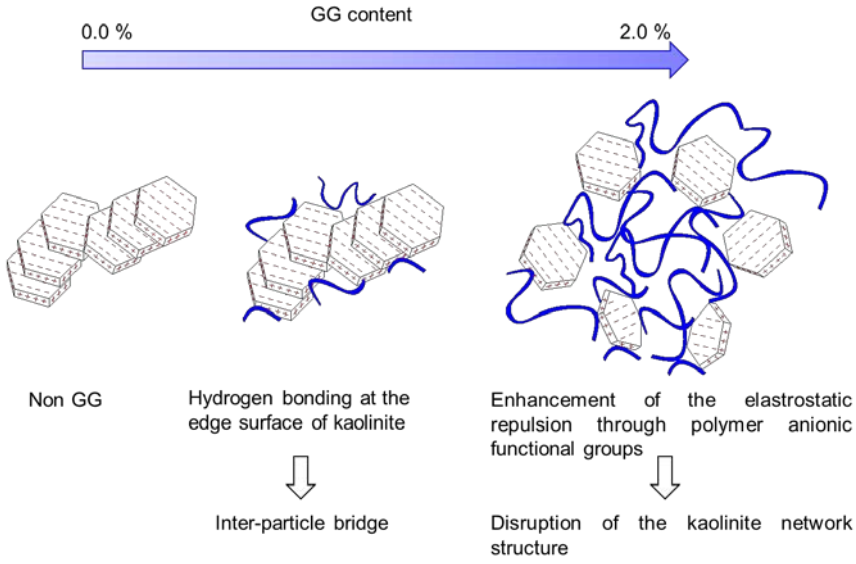

Figure 4.15. Gellan–clay matrix at pH = 6.5 ~ 7.0

4.4.1.3 Exponential decay of hydraulic conductivity

Most of the studies, which estimates the effects of hydrogels on the hydraulic conductivity of the soils, perform the relation between the additive concentration and the hydraulic conductivity via equations (Al-Darby 1996a; Ivanov and Stabnikov 2017). In this study, the hydraulic conductivity of treated soil depends on the content of gellan gum by the following equation

$$k = k_0 - \alpha\left(1 - e^{-|\beta|x}\right) \tag{4.2}$$

where k_0 is the HC at 0.0% of gellan gum; α is related to the difference between the maximum of HC (i.e., k0 of the untreated soil) and the lowest HC; $|\beta|$ is the decay parameter, which reflects the slope of the decreasing line; x is gellan gum content (%).

The relationship between HC and gellan gum content was found to be exponential decay with R^2 = 0.99 (Fig. 4.16, Table 3). The $|\beta|$ of the trendlines of S9K1 soil are much higher than that of S10 soil. At high effective stress, the difference in $|\beta|$ even reaches two times higher for S9K1 soil compared to the S10 soil. It is due to the S9K1 soil has a significant drop in hydraulic conductivity compared to the S10 soil as they are treated at the same GG content.

The decay parameter $|\beta|$ shows a logarithmic relationship with effective stress (σ') (Fig.4.17). Although the $|\beta|$ increases with the σ' for all soil cases, the effect of σ' on the increase in $|\beta|$ is much obvious for the case of the S9K1 soil. It indicates that the gellan gum-kaolinite matrix is much sensitive to the σ'concerning the arrangement of soil structure or pore space reduction which is one of controlling factors of the HC reduction in gellan gum-treated soils.

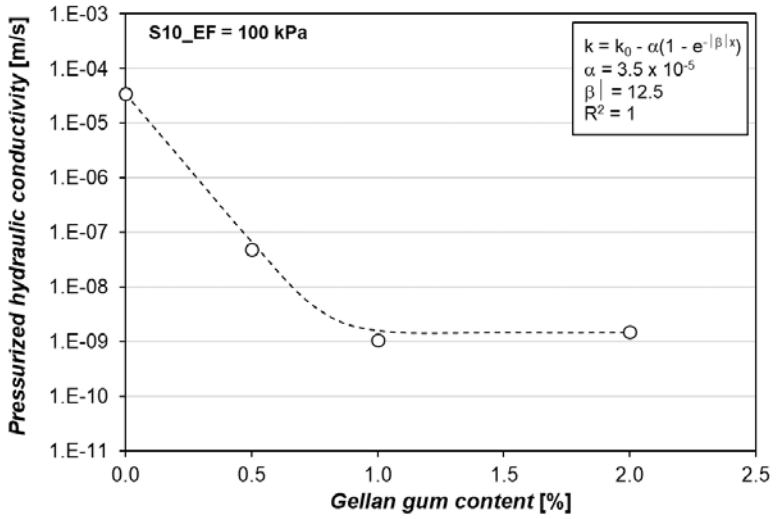

Figure 4.16 Trendline for hydraulic conductivity – gellan gum content for sand

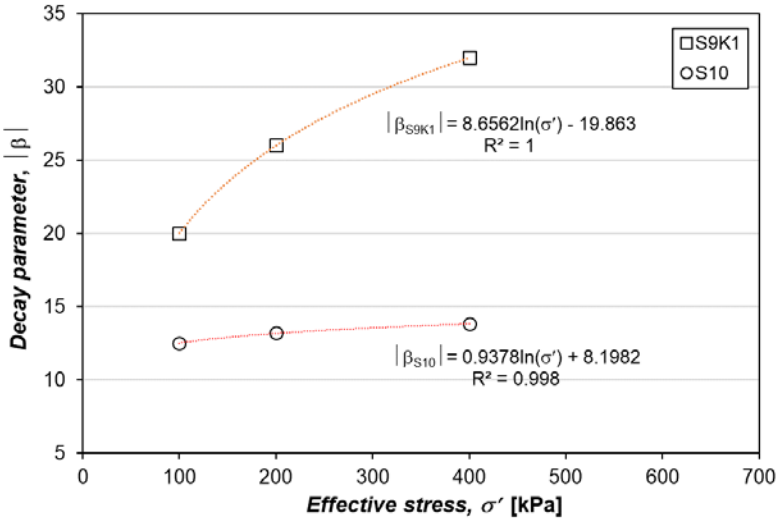

Figure 4.17 Relationship between decay parameter and effective stress

Table 4.4. Parameters for the exponential decay trendlines

Soil types	Effective stress	α	$\lvert\beta\rvert$	R_2
S10	100	3.50×10^{-5}	12.5	1.00
	200	3.02×10^{-5}	13.2	1.00
	400	2.43×10^{-5}	13.8	1.00
S9K1	100	4.48×10^{-7}	20.0	0.99
	200	3.77×10^{-7}	26.0	0.99
	400	4.49×10^{-7}	32.0	1.00

4.4.2 Summary

Water absorption ability of biopolymer can reduce the hydraulic conductivity, however, the thermo-galated biopolymers such as gellan gum which is used in this study allow biopolymer-treated soil can withstand higher pressures and reduce hydraulic conductivity. The hydraulic conductivity shows an exponential decay relationship with gellan content. The hydraulic conductivity decreases and keeps constant at gellan gum 1% and higher content due to the effect fixed soil pore.

Furthermore, hydraulic conductivity follows an “upward concave curve” trend with the inlet water pressure. The minimal hydraulic conductivity is result from multi processes such as water absorption of gellan gum, water pressure-induced compression on gellan gum, the water distribution in soil, as well as the formation of water pathways and micro cracks.

The presence of kaolinite admixture enhances the effectiveness of gellan gum in hydraulic conductivity reduction because kaolinite-gellan gum matrix at the same time absorption. It is also found that the gellan gum hydrogel can control the loss of kaolinite in the soil system.

It is concluded that the significant hydraulic behavior enhancement of gellan gum-treated soil for high effective stress and water pressure suggests the considerable potential of gellan gum application for geotechnical engineering such as grouting and hydraulic barrier materials which can control the water leakage, leachate, and pressure distributions. The relationship between HC and gellan gum can become a useful tool for engineers to have a general evaluation, prediction of the hydraulic conductivity of the gellan gum-soil treatment in the site application at where the effective stress or excess pore water pressure need to be considered

Chapter 5 Adsorption behavior of biopolymer-treated sand

5.1 Introduction

Nowadays, there is an increasing number of researches suggesting soft technologies (i.e., biosorption) to remove the contaminants (Bassi et al. 2000; Lázaro et al. 2003; Mogollon et al. 1998; Zhang 2016), and to reduce the hydraulic conductivity (Bouazza et al. 2009; Chang et al. 2016). The principal mechanism of ion adsorption involves the formation of complexes between a metal ion and functional groups (carboxyl, carbonyl, amino, amino, sulfonate, phosphate and so forth) presenting on the surface or inside the porous structure of the biological material (Fourest and Volesky 1997). Biopolymers with hydrophilicity, furthermore, interact with water molecules via hydrogen bonding (Mani et al. 2015), which leads to pore-clogging and controls the flow and transport properties of the porous media (Aal et al. 2010).

Nickel is one of toxic heavy metals. It is known that nickel is used in a wide variety of metallurgical processes such as electroplating, alloy production (Das et al. 2008) and batteries (Rydh and Karlström 2002). Contact with nickel compounds can cause a variety of adverse effects on human health, such as nickel allergy in the form of contact dermatics, lung fibrosis, cardiovascular and kidney diseases and cancer of the respiratory tract (Oller et al. 1997; Seilkop and Oller 2003). Therefore, nickel received a shameful name as the “Allergen of the Year” in 2008 (Brunk 2008).

Gellan gum has been shown the highest accumulation of Ni(II) compared to other biopolymers (Fig. 5.1) (Lázaro et al. 2003). This study aims to investigate the nickel removal ability of gellan gum-treated sand from a nickel-contaminated flow via an upward flow system.

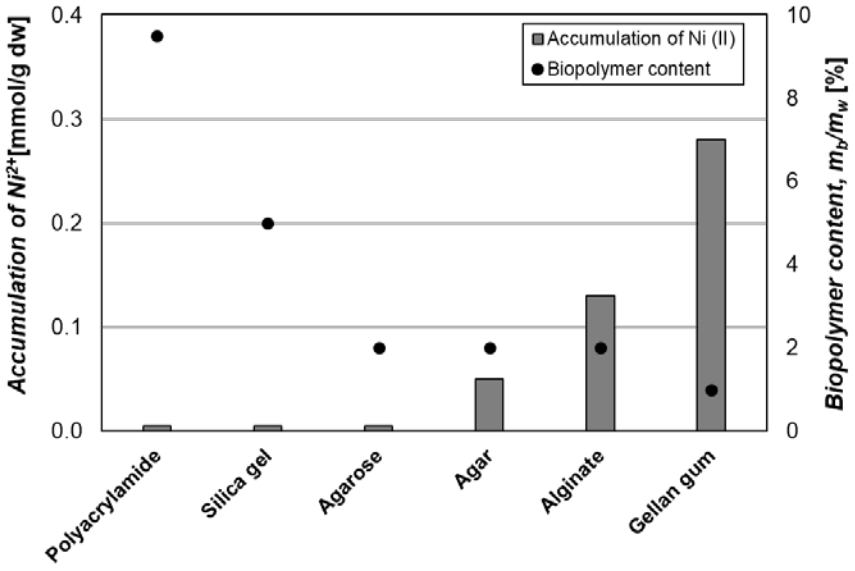

Figure 5.1 Nickel adsorption of different biopolymers

5.2 Experimental programs

5.2.1 Sample preparation

Gellan gum–soil mixtures were prepared with gellan gum contents (to the mass of soil) of 0.5; 1.0 and 2.0%. To allow thoroughly mixing, the initial water content has been set at 35%. gellan gum was first dissolved and hydrated into deionized water heated at 100°C to obtain a uniform gellan gum solution. Dry sand and heated gellan gum solution then were uniformly mixed. After that, gellan gum –sand specimens were formed in a mold of 3.5 cm in diameter and 10 cm in height. The samples were cooled down at the room temperature (i.e., 20°C), and dried in an oven at 100°C. The samples were trimmed to get the target height of 5 cm, which were defined as hydraulic barrier liners (hereafter, HBL) in this study. The specimens are referred to as 0.5HBL, 1.0HBL and 2.0HBL corresponding to the gellan gum content used to form HBL; 0.5, 1.0 and 2.0% respectively. The dry densities of specimens were summarized in Table 5.1.

Table 5.1 Information of soil column

HBL	GG content [%]	0.0	0.5	1.0	2.0
	Dry density [g/cm^3]	1.61	1.57	1.54	1.53
Sand column	Dry density [g/cm^3]	1.61			
Soil column Symbol		0.0HBL	0.5HBL	1.0HBL	2.0HBL

5.2.2 Pressurized upward flow system

The experimental flow system used consists of three main parts; a syringe pump, an acrylic cylinder (diameter of 3.5 cm; length of 12 cm) and pressure data logger (Fig. 5.2). A syringe pump, which allows supplying a constant flow rate, pumping $NiCl_2.6H_2O$ solution from a 60 ml syringe to the soil column in the acrylic cylinder via the inlet system. Dry jumunjin sand was compacted at in the acrylic column before setting the dry HBL on the top of the specimen. The heights of the sand column were 12 and 7 cm corresponding to the height of HBL; 0 and 5 cm, respectively. The bottom and top caps include inlet and outlet systems. The pressure data logger was used to track the change in pressure in the specimen column.

First the specimen was de-aired and wetted by $NiCl_2.6H_2O$ solution. After that, as the nickel solution keep supplied continuously, outlet solution was obtained with time. The solution was used to track the change in hydraulic conductivity of the soil column, and Ni(II) removability analysis.

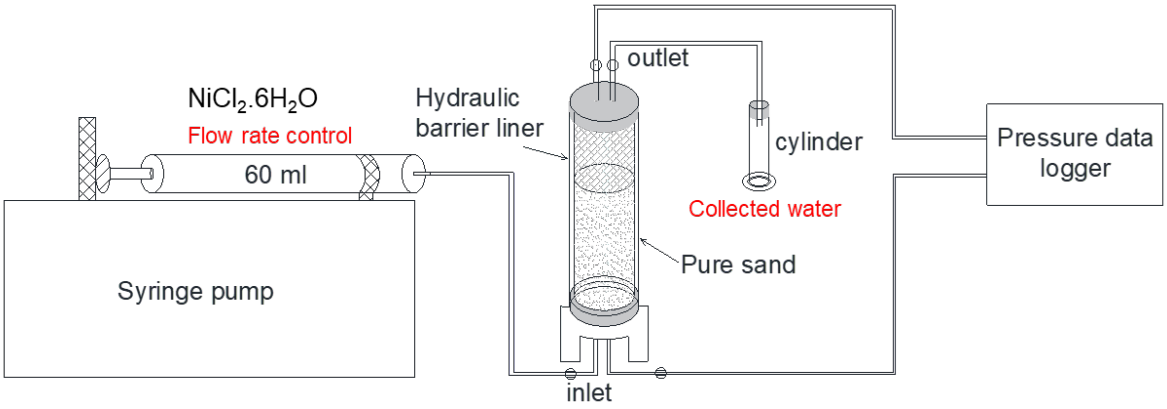

Figure 5.2 Schematic diagram of a pressurized upward flow system

5.2.3 Adsorbate preparation

Nickel concentration in groundwater and municipal tap water in polluted areas are in the range of 100 – 2500 mg/L; meanwhile over 1000mg/L is an extreme value found in water boiled in electric kettles (Rathor 2014). In this study, to assume the worse condition of environmental pollution, an initial concentration of $NiCl_2.6H_2O$ of 1000 mg/L was used. The concentration has been used in many studies (Krishnan et al. 2011; Panda et al. 2007).

5.2.4 Adsorption isotherm and kinetic study

To study the adsorption mechanism of gellan gum–treated sand mixture on nickel, equilibrium isotherm study was conducted. Different concentrations of nickel (10-1000mg/L) were experimented to check the equilibrium isotherm. 40mL of samples with designated nickel concentrations were mixed with 5g of gellan gum treated sand (0HBL, 0.5HBL, 1.0HBL, and 2.0HBL) in 50mL Falcon tubes. Samples were then shaken at 120rpm, 25℃ for 24 hours, and filtrated using 0.45μm nylon filter for further analysis.

The empirical equilibrium adsorption isotherm was modeled using Langmuir and Freundlich isotherm equation. The adsorption isotherm gives the insight into understand the interaction between the adsorbent and adsorbate. The Langmuir model is written as

$$q_e = \frac{q_{\max} k_L C_e}{1 + k_L C_e} \tag{5.1}$$

where q_e is the metal uptake per adsorbent (mg/g), q_{max} is the maximum adsorption, k_L is the Langmuir constant, and C_e is the equilibrium metal concentrations (mg/L). Langmuir isotherm fitting indicates a monoayer process where the k_L can be a criteria of adsorbate affinity to adsorbent. Higher the k_L,

stronger the interaction. In other words, Langmuir isotherm can be directly related to the homogenous surface with uniform adsorption energy.

The Freundlich equation is written as

$$q_e = k_F C_e^{1/n} \tag{5.2}$$

where k_F is the Freundlich constant, and n is the empirical constant. Freundlich isotherm empirically considers a multi-layer coverage on rough surfaces. Model fitting of the experimental data was checked with the correlation coefficient R^2.

To understand the kinetic uptake of nickel adsorption according to time, gellan gum treated sands with 25mg/L, 50mg/L, and 100mg/L nickel solution were tested and taken according to the desired time. Other experimental conditions were the same as those written above.

5.2.5 Analysis methods

5.2.5.1 Hydraulic conductivity analysis

The hydraulic conductivity (HC) is calculated following Darcy's law

$$k = \frac{V.L}{A.h.t} \tag{5.3}$$

where V is the collected volume of water, L is the height of HBL, A is the area of soil specimen, h is the head difference, and t is the time required to the V volume.

The L is the height of HBL because the presence in HBL is the main factor governing the reduction in hydraulic conductivity.

5.2.5.2 Heavy metal analysis

The concentration of nickel ions in the solution was measured using Inductively Coupled Plasma-Optical Emission Spectrometry (Agilent ICP-OES 5110, USA), calibrated by the standardized metal solution. Amount of nickel uptake (mg/g) was calculated using the following equation,

$$q_e = \frac{(C_i - C_t).V}{1000.W} \tag{5.4}$$

where C_i and C_t are the metal ion concentration at the initial and at t stage, respectively (mg/L), W is the amount of adsorbent (g), and V is the volume of solution (mL).

5.2.5.3 Surface morphology

Samples of gellan treated sand with nickel adsorption were taken for Scanning Electron Microscopy (SEM-SU5000, Hitachi, Japan). Morphologies of samples were taken along with the energy dispersive X-ray spectroscopy (EDS) for element characterization. SEM-EDS was carried out for at least 10 spots per sample to lessen deviations. Samples were coated with platinum prior to the analysis to enhance the electrical conductivity on the surface.

5.3 Results and analysis

5.3.1 Isotherm and kinetics of heavy metal adsorption mechanism

Figure 5.3 shows the adsorption of nickel solution on each of gellan gum-treated sand. The results show that gellan gum and sand had the ability in adsorbing nickel. All three conditions (Sand, 0.5HBL, 1.0HBL, 2.0HBL) show a logarithmic trend at equilibrium state. The equilibrium uptake of nickel adsorbate increased as the gellan gum concentration increased. Figs. 5.3a and b show the Langmuir and Freundlich isotherm models respectively. All three data were fitted more to Langmuir isotherm model, compared to the Freundlich isotherm model, with the R^2 value of 0.9881 to 0.9983 for Langmuir model (Fig. 5.3b) and 0.782 to 0.9197 for Freundlich model (Fig. 5.3c).

The Langumuir model is the best fitting model for the data set, therefore, the adsorption of Ni(II) on gellan gum and sand indicated monolayer coverage of the adsorbate on the surface of the adsorbent, which is coherent with the other studies on heavy metal adsorption on biopolymer (Huang et al. 1996; Panda et al. 2007; Stojakovic et al. 2011). The slopes of the Langumuir fittings (Fig. 5.3b) were converted into q_{max} for better understanding of the adsorption model. The q_{max} started from 0.19 mg/g for 0HBL (pure sand) to 0.29 mg/g for 0.5HBL, 0.40 mg/g for 1.0HBL and 0.60 mg/g for 2.0 HBL (Table 5.2).The results show that gellan gum had higher adsorbability compared to pure sand. The q_{max} increased with gellan gum, which indicated that the use of gellan gum in HBL could improve the nickel adsorption ability of the entire HBL, and can be the main adsorbent of the HBL system.

Kinetic study on nickel adsorption by gellan gum according to time shows a sudden increase in q_e and steady state after certain time (Fig. 5.4) (Panda et al. 2007; Panda et al. 2006). The adsorption can be illustrated by two stages, where the first stage goes through rapid removal regardless of the nickel concentration within first 1 min, and the latter stage reaching equilibrium around 40 minutes. Rapid removal in the initial stage may be attributed to ample sites for adsorption on the surface of gellan gum.

SEM EDS spectra, as shown in Fig. 5.5, shows peaks of gellan gum in its pure state and nickel-adsorbed state. The EDS data show a reduction of potassium peak and appearance of the nickel peak.

This can be considered as cation exchange mechanism of gellan gum with nickel ion, similar to the result of other adsorbents on nickel (Panda et al. 2007). The replacement of Ni(II) for potassium in gellan gum indicates that gellan gum used is a potassium-type gellan gum (Kawahara et al. 1996; Tsutsumi et al. 1993). Furthermore, the functional groups in gellan gum; carbonyl, methylol, and methyl are also responsible for chemical interaction with nickel ion (Kawahara et al. 1996). Meanwhile, the sand can adsorb nickel via the inner−sphere interaction where Ni(II) can interact with silanol groups at the sand surfaces (Awan et al. 2003; Takahashi and Kuroda 2011).

5.3.2 Nickel adsorption behavior of sand column

For the cases of 0.0HBL, 0.5HBL, and 1.0 HBL specimens, as nickel solution was continuously supplied to the specimen, nickel adsorption behavior followed a similar trend. At first, nickel ions were quickly adsorbed due to the high amount of free exchangeable ions of absorbents. Then, the adsorption reached its equilibrium as the free sites for nickel became less value to the constant adsorption.

In general, the pure sand column had the lowest total amount of cumulative nickel adsorbed. The presence of gellan gum in HBL improved the amount of nickel removed from the nickel-contaminated solution. The higher gellan gum content, the more considerable amount of nickel ion could be adsorbed because there were more functional groups and potassium cation exchange in the specimens provided by gellan gum. Based on the nickel adsorption trends obtained from Fig. 5.6, Fig. 5.7 shows the potential maximal nickel adsorption ability of specimens with different gellan gum-treated sand at different flow rates. Total nickel adsorption varies proportionally with gellan gum content.

Flow rate is essential to control contact time between Ni(II) and adsorbent materials, which is crucial for determining the amount of nickel adsorbed. Therefore, there was a gap in the total amount of adsorbed nickel, which was obtained from the low and high flow rates. For instance, under the low flowrate (i.e., 0.04 ml/min), the 0.0HBL specimen could adsorb 40 mg of nickel ion as 200 ml of nickel solution ran through the specimen (Fig. 5.6a and Fig. 5.7). Meanwhile, 29.98 mg of nickel was removed from 200ml nickel solution supplied via high flowrate (0.2 ml/min) (Fig. 5.6b and Fig. 5.7). This phenomenon also happened to gellan gum-treated sand. The 2.0HBL adsorbed 86.89 mg and 109 mg nickel as 600ml nickel solution was provided at flowrate of 0.2 ml/min and 0.04 ml/min, respectively (Figs 5.6 and 5.7).

5.3.3 Effect of gellan gum content on hydraulic conductivity control

The change in HC with time is shown in Fig. 5.8. The HC values of 0.0HBL specimens were approximately 1 x 10^{-5} m/s as the flowrate ran through the specimens. HC of pure sand column kept constant with time.

As HBLs were installed into the soil column, the initial HC (1 x 10^{-6} m/s) became lower compared to the HC of pure sand column. It is due to the water absorption of gellan gum. Furthermore, the HC decreased with time due to the pore clogging effect of gellan gum as gellan gum interacted with water.

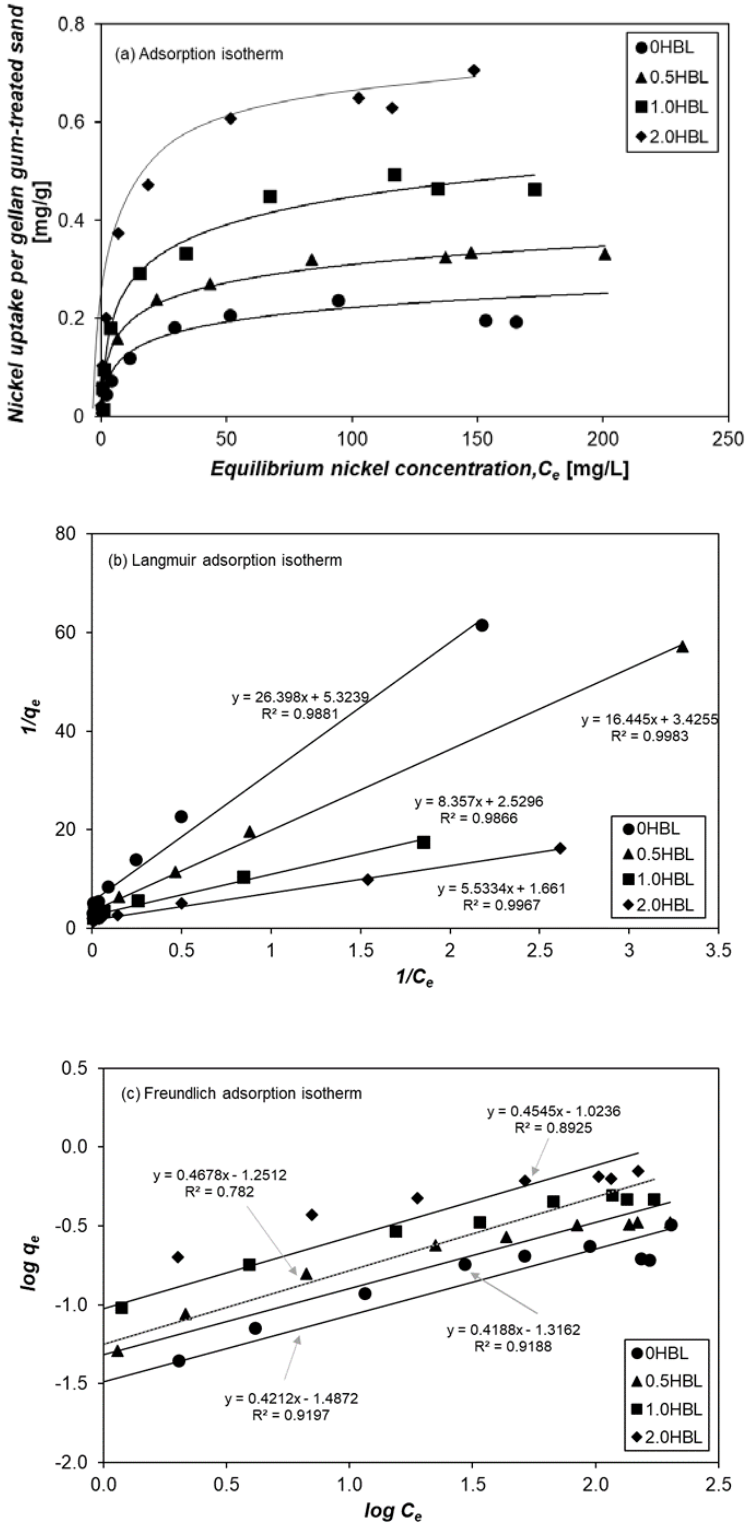

Figure 5.3 Adsorption isotherm at various initial nickel concentrations (10–1000 mg/L) on gellan treated sand (a), Langmuir adsorption isotherm (b), and Freundlich adsorption isotherm of nickel on sample (c)

Table 5.2 Parameters of Langmuir fitting model

Soil column symbol		0.0HBL	0.5HBL	1.0HBL	2.0HBL
Parameters	q_{max} [mg]	0.19	0.29	0.40	0.60
	R^2	0.9881	0.9983	0.9866	0.9967

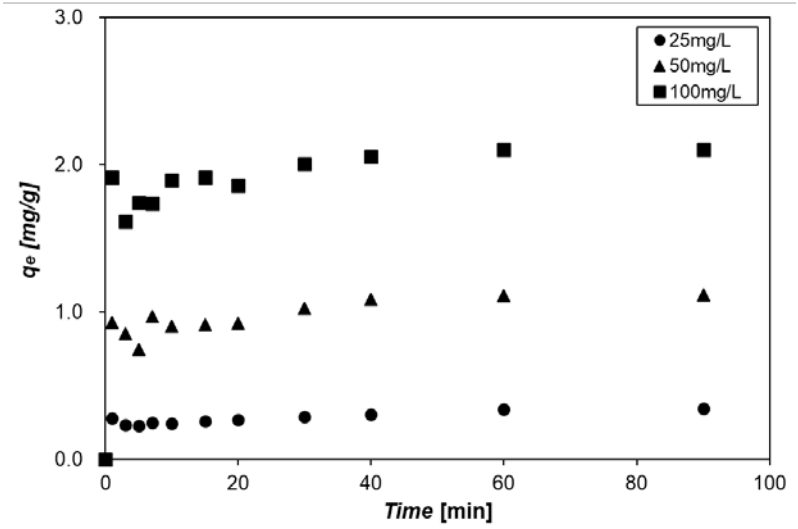

Figure 5.4 Kinetics of Ni binding to the gellan gum at different initial nickel ion concentrations of 25mg/l, 50mg/l, and 100mg/l

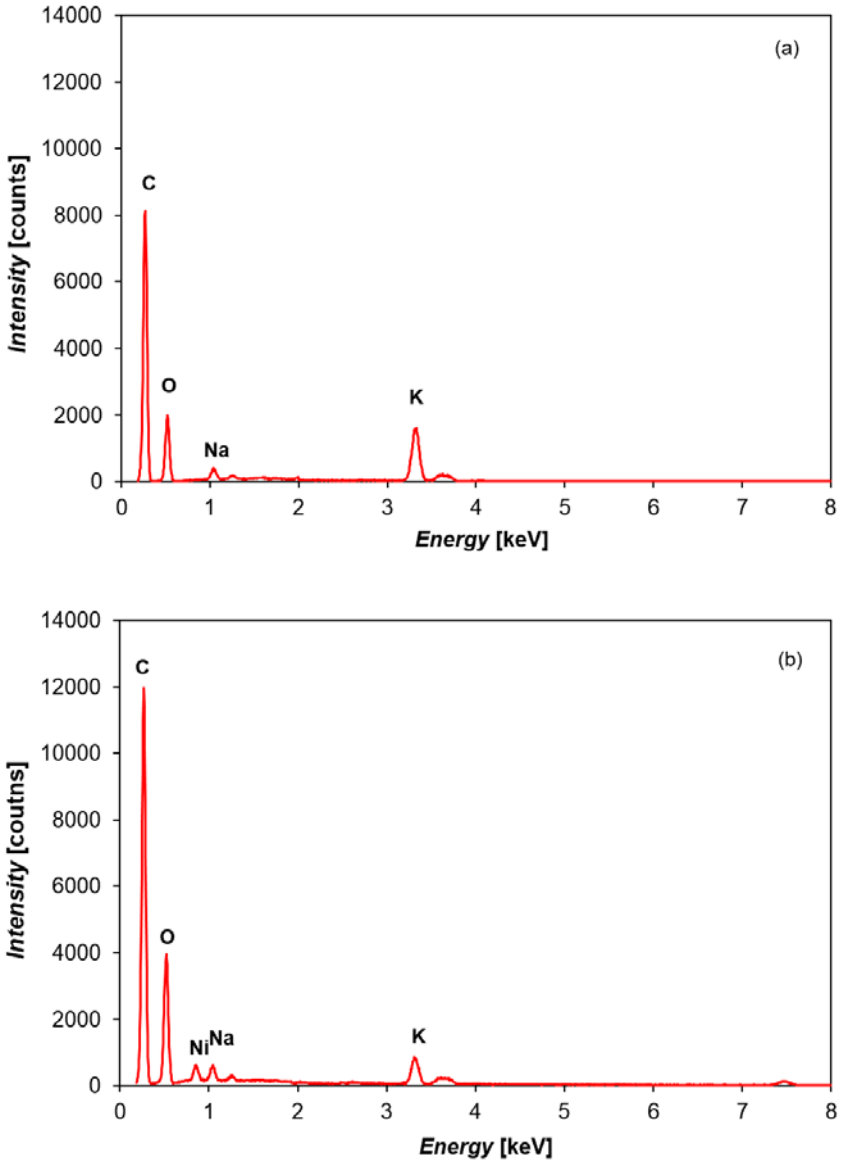

Figure 5.5 SEM-EDX spectra of (a) pure gellan and (b) nickel adsorbed gellan

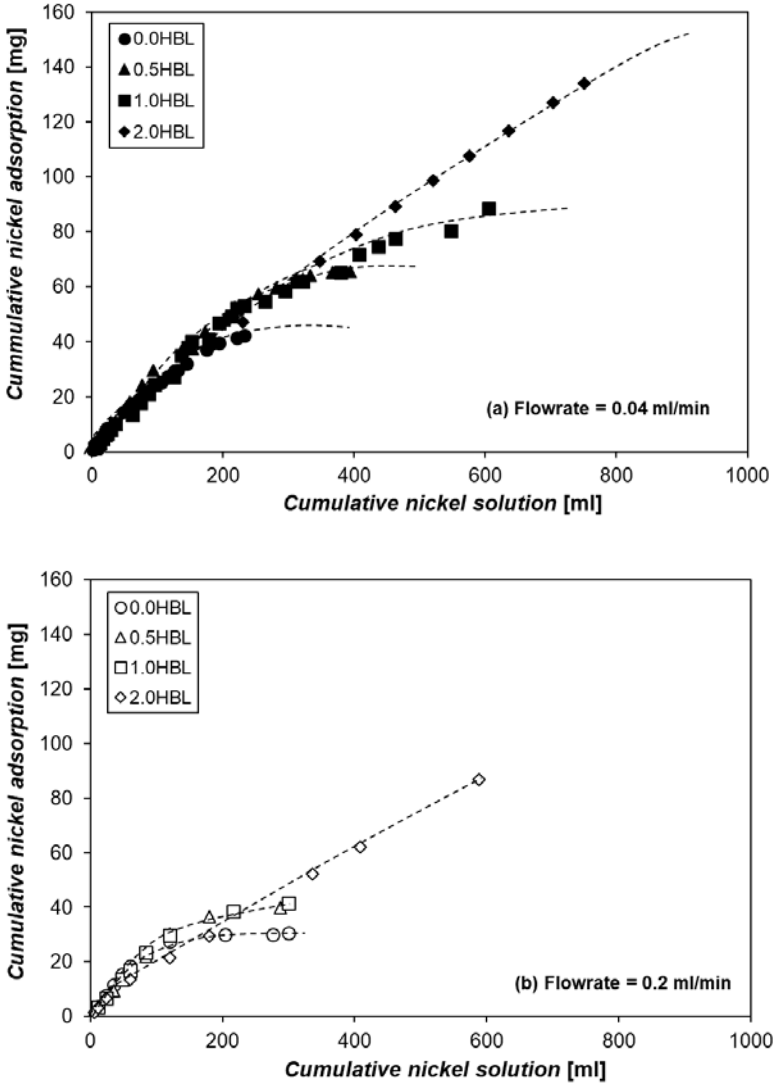

Fig. 5.6 Cumulative nickel adsorption at flowrate of (a) 0.04ml/min and (b) 0.2ml/min

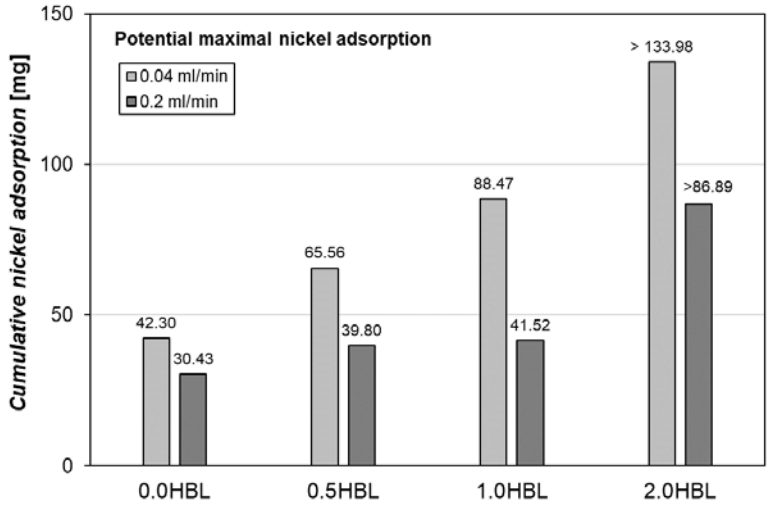

Fig.5.7 Potential maximal nickel adsorbability of specimens

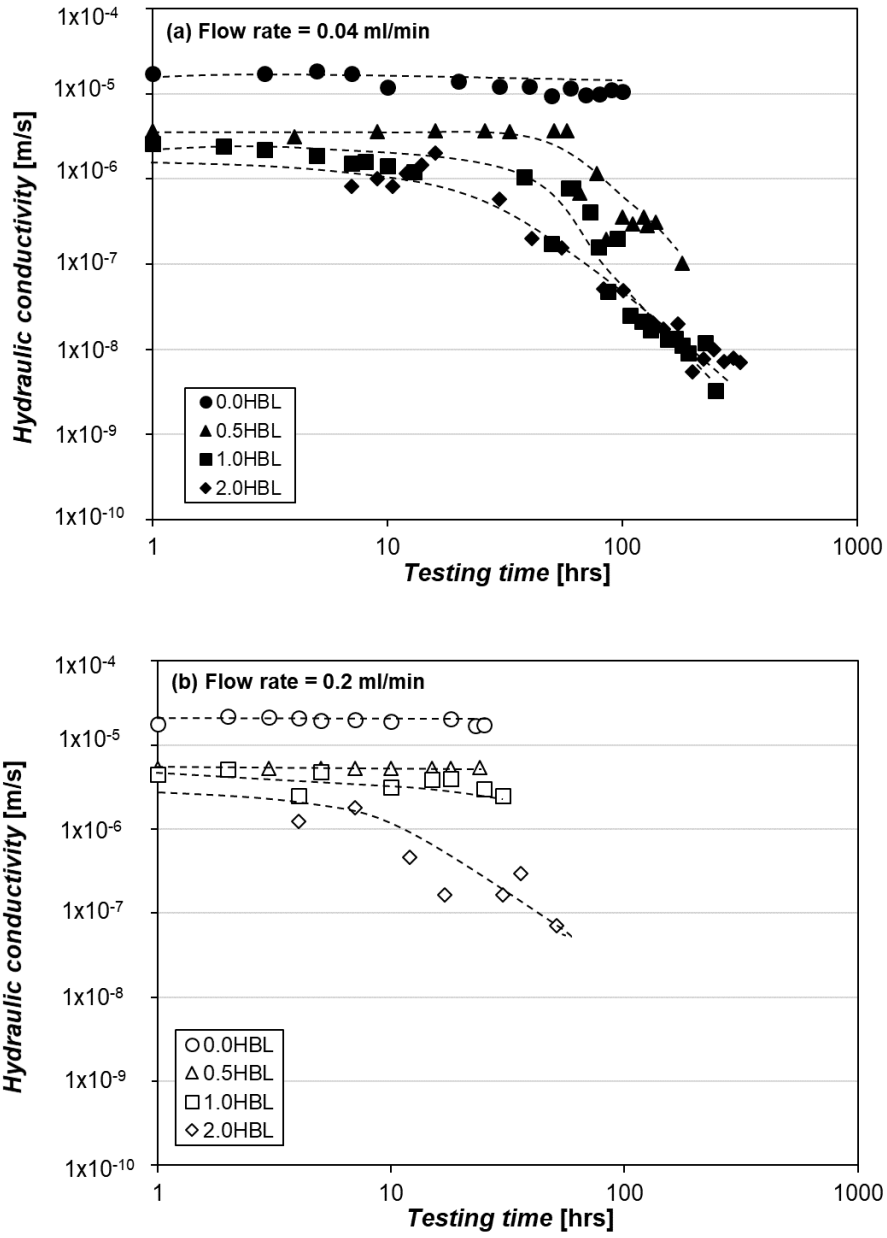

Figure 5.8 Change in hydraulic conductivity of soil column

at flow rate of (a) 0.04ml/min and (b) 0.2 ml/min

5.4 Discussion and summary

5.4.1 Discussion

The difference in the amount of adsorbed nickel was rendered by gellan gum content. This study shows the improvement in nickel adsorption using gellan gum-treated sand. Based on the result obtained, the potential nickel adsorbability of $1m^3$ is suggested (Fig. 5.9).

The effect of hydraulic reducing with gellan content is shown to decrease nonlinearly and level off at gellan gum content of 1.0%, which is provided in Chapter 4. However, if gellan gum-treated sand is suggested for nickel treatment, 2% gellan gum can show much significant effectiveness on nickel removal (Fig. 5.7). To form 1m3 of 2% gellan gum-sand mixture, 26.5 kg gellan gum needs to be dissolved in 463-liter heating water before mixing with 1.3 tons sand. If the gellan gum-sand mixture is used to treat a 1g/L Ni(II) contaminated flow with flowrate of 0.04 ml/min, 1906 kg of nickel can be trapped by gellan gum.

The experiment was conducted in a given time; therefore, 2% gellan gum could not reach its equilibrium. The amount of adsorbed nickel by $1m^3$ gellan gum-treated sand was calculated based on the experimental data; therefore, in the field application, the real nickel adsorbed may be much higher.

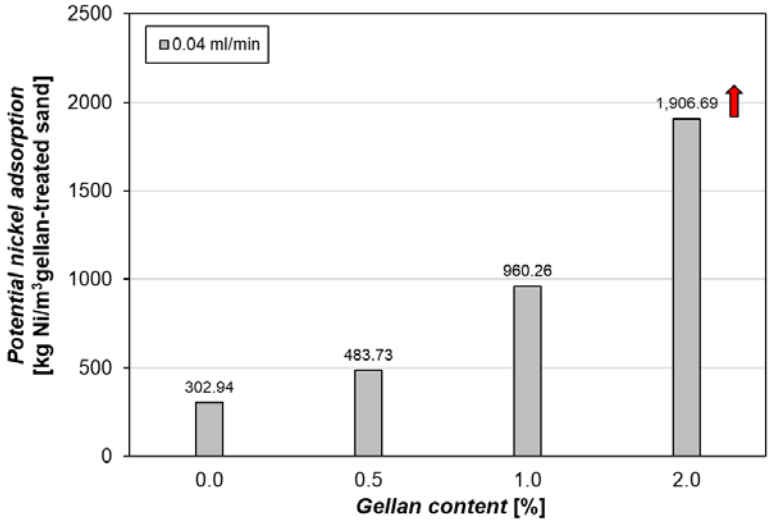

Figure 5.9 Potential nickel adsorption by $1m^3$ gellan gum-treated sand

5.4.2 Summary

To investigate the applicability of bio-soil treatment on heavy metal removal, a series of nickel adsorption test was conducted on gellan gum-treated jumunjin sand using the pressurized upward flow system. Furthermore, to have a better understanding of the insight of nickel adsorption mechanism, the adsorption isotherm and kinetic studies were carried out.

Jumunjin sand can absorb nickel via silanol functional groups and a tiny amount of fine particles that may contain in sand. As gellan gum is treated with jumunjin sand, gellan gum enhances nickel adsorption of sand via adding functional groups such as carbonyl, methylol, and methyl for ion exchange mechanism, and potassium cation exchange. Therefore, the installation of gellan gum-treated sand in the sand column promotes higher nickel removal rate. It is noted that the potassium cation exchange of gellan gum that was found in this study may only correct for the Ni(II) adsorption. Other heavy metal ions may show different mechanisms, which depends on valence and ionic radii of heavy metal ion. Furthermore, due to the pore-clogging effect induced by gellan gum, the hydraulic conductivity of soil decreased with gellan gum content.

In general, based on the ability of heavy metal adsorption and flow control of gellan gum, gellan gum-treated sand can be used as a filter and a membrane as well.

Chapter 6 Feasibility assessments for practical applications of biopolymer-based hydrogels in geotechnical engineering

6.1 Vegetation growth behavior of biopolymer-treated soils

6.1.1 Background

Vegetation cover plays a number of roles in controlling soil erosion, such as mitigating surface runoff and severe soil losses in most climate zones (Chang et al. 2015d). The stability of a slope, which is often comprised of well-drained and low-cohesive soil, depends on the mechanical reinforcement provided by the plant roots in the soils and on the soil-water suction characteristics (Chirico et al. 2013; Roering et al. 2003). Vegetation dynamics is one of the key indicators of an ecosystem's response to climate change. Climate change alters numerous site factors and the biochemical processes of vegetation communities, which affect nutrient and water availability and, in turn, affect the root distribution (Hufnagel and Garamvölgyi 2014). Therefore, soil erosion control will likely continue to present problems.

Global average temperatures have increased over the past 100 years due to the increase of greenhouse gases. The global warming phenomenon becomes more severe in arid and semi-arid regions (Huang et al. 2012; Ji et al. 2014). Arid and semi-arid areas are classified due to low, erratic rainfall, long periodic droughts, and high evaporation levels (Maghchiche et al. 2010). Generally, soils in these areas easily erode because they contain a low amount of organic acids and natural substances that can provide shear resistance against erosion (Marinari et al. 2000). Furthermore, a temperature increase reduces the water storage capacity of the soil and may exceed the drought tolerance of vegetation, which is known to be a limiting factor for seedling survival (Cao 2008; Chang et al. 2015d).

Thus, to reduce the effect of increasing temperatures on the survival of seedling in drylands, the use of gel conditioners for irrigation water retention becomes an important issue in which hydrophilic hydrogels are expected to maximize the efficiency of vegetation water uptake (Koupai et al. 2008).

Chapter 3 proved the effect of xanthan gum on water retention of jumunjin sand. It is suggested that lower than 1.0% xanthan gum should be used for vegetation purpose in order to avoid the negative aeration condition due to waterlogging. Therefore, in this chapter 0.5% of xanthan gum-treated sand was used to investigate the effect of xanthan gum on the germination and growth of ryegrass

6.1.2 Experimental programs

6.1.2.1 Vegetation types

Perennial ryegrass *(Lolium perenne L.)* is one of the common cool-season turfgrasses that have been utilized to improve the environment for humans for more than 30 centuries. Moreover, the turfgrass used in this study is known to have functional benefits, such as soil erosion control, flood control, and dust stabilization (Beard and Green 1994).

6.1.2.2 Vegetation growth in the environmental control chamber

The soil specimens were distributed in a vegetation tray that consisted of 12 circular sections. Each section had dimension as 60-mm in diameter and 30-mm in height (Fig 6.1). Specimens were cultured in an environmental control chamber at a temperature of 25°C, a humidity of 85%, and daylight of 12 hours/day (Table 6.2). During the first 30 days, each specimen was watered by 7mL for seed germination and sprout growth, while a drought condition with a daily water supply of 0 mL/day/specimen was simulated after 30 days. The temperature was increased to 33°C while the chamber humidity was decreased to 57% in order to model the drought condition (Table 6.1).

The germination rate is used to estimate the viability of a population of seeds. The equation to calculate the cumulative germination rate is given as follows:

(number of germinated seeds/ total seeds) × 100.

When the turf grasses are subjected to water stress, they merely run out of the available water and wilt. As the green grasses start turning yellow, they are named wilted sprouts in this study. The wilting rate is calculated as follows:

(number of wilted grasses/total grasses) × 100.

The height of the grass is the height above the surface (Chen et al. 2013b) (i.e., the length from the top of the main tiller to the crown). The root length was the length from the crown to the end of the main root. The means and standard deviations were calculated.

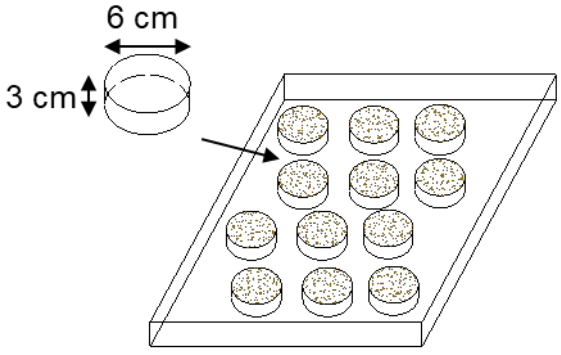

Figure 6.1 Vegetation tray

Table 6.1. Experimental conditions

Temperature [°C]	Humidity [%]	CO_2 [ppm]	Lighting [h/day]	Watering [mL/day]
Normal: 25	80	915	12	7
Drought: 33	57			0

6.1.2.3 Softness of soil – Unconfined compressive strength

Cubic samples (3.5 cm × 3.5 cm × 3.5 cm) of the biopolymer treated sands were prepared to a dry density of 1.58 ± 0.02 g/cm^3. Unconfined uniaxial compressive testing was performed with a Humboldt digital master loader (HM-5030.3F). The axial strain rate was controlled at a rate of 1% strain/min, according to ASTM D2166 (ASTM 2016). The test was conducted on specimens dried at 30°C in an oven. The maximum unconfined compressive strength was obtained by averaging three different measurements for each single soil condition.

6.1.3 Results

6.1.3.1 Effect of xanthan gum on softness of soil

The high viscosity of biopolymers could improve the inter-cohesion between the sand particles, which in turn significantly increased the compressive strength of the sand. Fig. 6.2 (Tran et al. 2019a) showed the compressive strength values of sand treated xanthan gum. UCS data from the untreated sand could not be obtained due to the particles being unbound as the sand was dried. Meanwhile, xanthan gum showed the best performance in strength improvement for sand due to its high viscosity providing a strong binding with the sand particles. The softness of the soil could be reflected by the strength data, which possibly affected the germination of seeds or root penetration (e.g., root size and length) into the soil.

In general, biopolymers affect the soil structure and in turn change the aeration, water uptake condition of the soil environment, and root-soil contact. Thereby, biopolymer concentrations and types influence the growth mechanism of vegetation. Their effects were described in the next section.

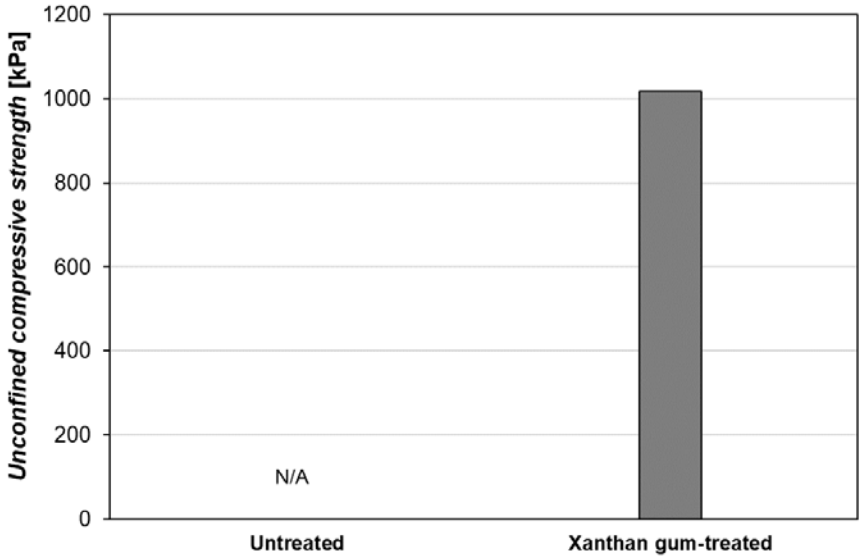

Figure 6.2 Unconfined compressive strength of xanthan gum treated sand (referred to Tran et al., 2019a)

6.1.3.2 Effects of biopolymer on seed germination

Figure 6.3 (Tran et al. 2019a) show the cumulative germination rate of ryegrass seeds cultured in untreated and treated sand. Untreated sand showed the best germination rates because of good aeration conditions formed within the soils. The pores contained a proper ratio of air and water for seed germination. As the amount of xanthan gum increased, a significant change in the amount of water within the soil may lead to unbalanced air–water circulation or waterlogging, which in turn could delay the germination of ryegrass seeds.

The germination behavior also differs with soil type, where the aeration condition of the soil seems to be the primary factor. The grass height of 9 cm has been observed in the untreated sand medium (Fig. 6.4a) (Tran et al. 2019a) while the average height of 5.5 cm was found in in the xanthan gum-treated sand condition

The effects of xanthan gum were not only on the height but also on the root system of the ryegrass (Fig. 6.4b) (Tran et al. 2019a). The root actively developed within the untreated sands due to proper aeration conditions. Meanwhile, the root system in the xanthan gum-treated sand was much shorter. The hard surface of the soil (i.e., the high compressive strength) and water near the soil surface (i.e., high water retention) might be important factors for the root lengths observed

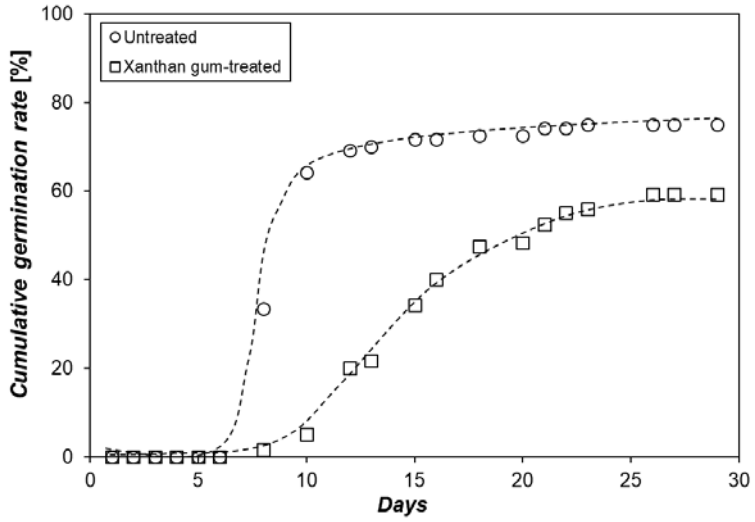

Figure 6.3 Seed germination rate on xanthan gum-treated sand (referred to Tran et al., 2019a)

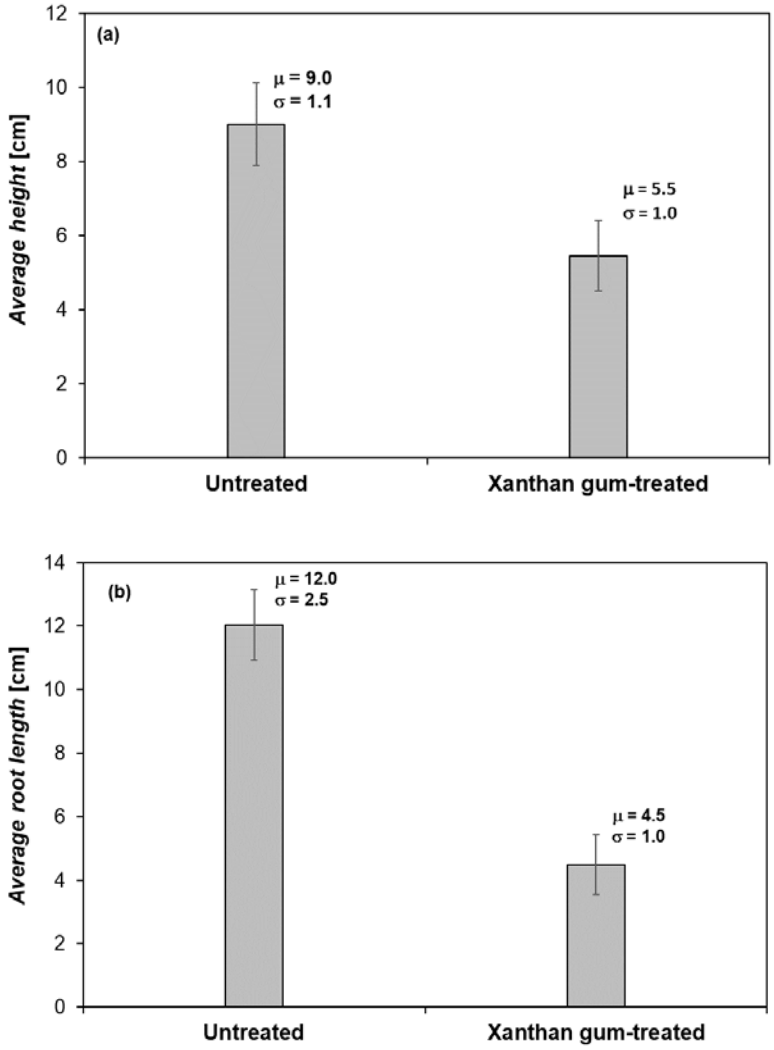

Figure 6.4 Vegetation height (a) and root growth (b) in xanthan gum-treated sand (referred to Tran et al., 2019a)

6.1.3.3 Effect of xanthan gum on the survivability of vegetation under drought conditions

Under the drought condition, the ryegrass started wilting due to water loss. The wilting rate of the ryegrass is shown in Fig. 6.5 (Tran et al. 2019a). For the untreated sand, the wilting started for one day and on the 4th day, all of the grasses in the untreated sand wilted. While it happened slowly for the xanthan gum-treated sand. In the same cultural condition, the wilting of grass significantly depends on the amount of available water within the soil. It is because the xanthan gum-treated sand has higher water retention compared to untreated sand (Chapter 3). In other words, under drought conditions, xanthan gum fosters less water loss, which can explain why the xanthan gum biopolymer demonstrated the best performance in improving the survivability of grass under drought conditions.

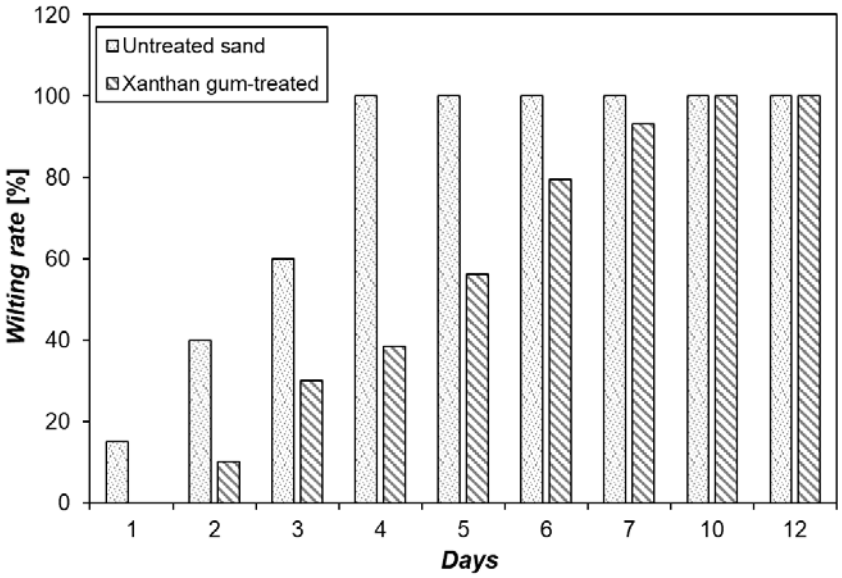

Figure 6.5 Effect of xanthan gum on the survivability of ryegrass (referred Tran et al., 2019a)

6.1.4 Discussion and summary

6.1.4.1 Discussion

The higher the amount of xanthan gum, the lower the free pore space within the soil. This is because the xanthan gum hydrogel absorbs the daily water, swells, and blocks the pore spaces. It is believed that the water-holding capacity of the biopolymer is an impacting factor when deciding what ratio of biopolymer concentration should be used to avoid waterlogging. Therefore, xanthan gum content lower than 0.5% is not suggested for vegetation purpose at a condition where water is supplied daily.

However, our results demonstrate that xanthan gum has a crucial role in the survivability of ryegrass owing to their high water-holding capacity during the first seven days of drought stress condition. More water contained in the pore spaces of the xanthan gum-treated sand provides water

more available to the ryegrass. Furthermore, the xanthan gum application method has a significant effect on increasing particle binding, which in turn can control the loss of fine soil particles subjected to wind or water erosion. The authors suggest that the amount of xanthan gum used should not be higher than 0.5% to control the softness and pore size of soil.

In conclusion, xanthan gum in sand from arid or semiarid regions can serve as essential tools for increasing water use efficiency and vegetation survivability and for reducing wind erosion and water erosion.

6.1.4.2 Summary

The presence of xanthan gum in soil control the root growth due to the high amount of water near the surface. Furthermore, xanthan gum also provides artificial water storage for the plant to improve its drought survivability, which is one of the most pressing issues in arid and semiarid areas. However, to avoid the waterlogging and have a better performance in the seed germination, lower than 0.5% xanthan gum should be used.

6.2 Slope surface treatment using biopolymer soils

6.2.1 Background

Section 3.3.2.3 provides the wetting parameters of 0.5% xanthan gum treated 20%kaolinite-sand mixture. The idea of evaluating the effect of xanthan gum on slope surface stability using a numerical modeling is brought up. Using a 2D finite element program (FLAC2D), which is effective for complex hydromechanical behavior consideration (Itasca 2011), the stability of a fictitious slope under a heavy rainfall is simulated.

6.2.2 Analytical method

The finite element method is an effective tool to consider the shear strength variation under transient unsaturated seepage (Cai and Ugai 2004; Fredlund et al. 1978). The yield criterion of the unsaturated soil is as follows (Fredlund et al. 1978).

$$\tau_{\max} = (\sigma - u_a)\tan\phi' + \frac{S_w - S_r}{1 - S_r}(u_a - u_w)\tan\phi' + c' \tag{6.1}$$

where τ_{max} is the material shear strength, ϕ' is the effective friction angle of the soil, c' is the effective cohesion of the soil, S_w is the water saturation, and S_r is the residual saturation. Moreover, the shear strength parameters, cohesion (c^{trial}), and friction angle (ϕ^{trial}) are defined as follows.

$$c^{trial} = \frac{1}{F^{trial}} \cdot c' \tag{6.2}$$

$$\phi^{trial} = \arctan\left(\frac{1}{F^{trial}} \cdot \tan\phi'\right) \tag{6.3}$$

where F^{trial} is the trial factor of safety. The initial F^{trial} value is set sufficiently low to ensure that the system is stable. The value is incrementally increased until failure. The critical factor at which failure occurs is taken to be the factor of safety.

In FLAC2D, a set of closed–formed equations is commonly used to simulate the hydraulic characteristics of unsaturated soils (Itasca 2011):

$$S_e = \frac{S_w - S_r}{1 - S_r} = \left[\frac{1}{1 + (\alpha \cdot \psi)^n}\right]^m \tag{6.4}$$

$$\left|K(\theta)\right| = K_s \cdot K_r = K_s \cdot S_e^{1/2}\left[1 - \left(1 - S_e^{1/m}\right)^m\right]^2 \tag{6.5}$$

where S_e is the effective saturation, $m = 1 - 1/n$, $n > 1$; $K(\theta)$ is the permeability of the soil, and K_s and K_r are the saturated and relative permeabilities, respectively.

6.2.3 Geometry and input parameters for FLAC simulation

The geometry of a real slope (N 57° 46′ 19.6″, E 127° 16′ 46.4″; *Namyangju*, Republic of Korea) was considered for numerical simulation. The site slope (39 m in height, 22° in average inclination) was reconstructed to contain the S8K2 soil along its surface in this study. Table 6.2 summarizes the basic geotechnical engineering properties and soil–water characteristics of the soils. The effective cohesion values were taken as zero to avoid overestimating the factor of safety (*FS*), as the failure surface is shallow (Fell et al. 2005).

Figure 6.6 (Tran et al. 2019b) shows the geometry of the slope and its initial *FS*. Using FLAC2D, the weakest area along the slope surface is predicted to start at a 38-m distance from the left boundary of the slope and extend down to the toe of the slope with a length of 23 m (Fig. 6.6a). It is assumed that the predicted failure area of the slope is treated by 0.5% xanthan gum-treated S8K2 soil with a thickness of 6 cm along 38 m in length, which appropriately forms a biopolymer – soil layer over the weakest area (Fig. 6.6b). To characterize the treated area, the soil properties of the weakest area are replaced by those of the xanthan gum –treated soil listed in Table 6.2.

For precipitation simulation, a heavy downpour (intensity = 1,125 m/h) condition reported to have caused serious debris flow in 2011 (Mt. Umyeon, Seoul, Republic of Korea, on 27 July 2011) was employed (Jeong et al. 2015). The change in the pore water pressure with depth in the weakest area (A-A′) (Fig. 6.6b) was estimated for the treated and untreated slopes.

6.2.4 Effect of biopolymer-soil treatment on shallow slope stability

Figure 6.7 shows the negative pore pressure (i.e., the matric suction) distribution along the cross-section A–A′ before (a, b) and after (c, d) rainfall. Before rainfall, the negative pore pressure at 0.06m depth of untreated slope (5.30×10^3 kPa) (Fig. 6.7a, b). Therefore, there were not a considerable improvement in the shear strength of soil. However, after 40 hours of rainfall, the negative pore water pressure of the xanthan gum–treated slope was higher than that of the untreated slope (Fig. 6.7c, d) because xanthan gum treatment at the surface of the weakest area could retains surface infiltration into the ground via the lower permeability. Thus, the xanthan gum treatment allowed the entire slope to remain safe for a longer period than the untreated slope under continuous heavy rainfall (Fig. 6.8) (Tran et al. 2019b). The untreated slope failed after 40 hours under continuous rainfall, whereas the slope treated with the 0.5% xanthan gum –treated soil on its weakest area surface (for a depth of 0.06 m) remained safe up to 480 hours. Therefore, a small amount of xanthan gum biopolymer (even for a shallow depth of 0.06 m) can enhance the slope stability against heavy rainfall.

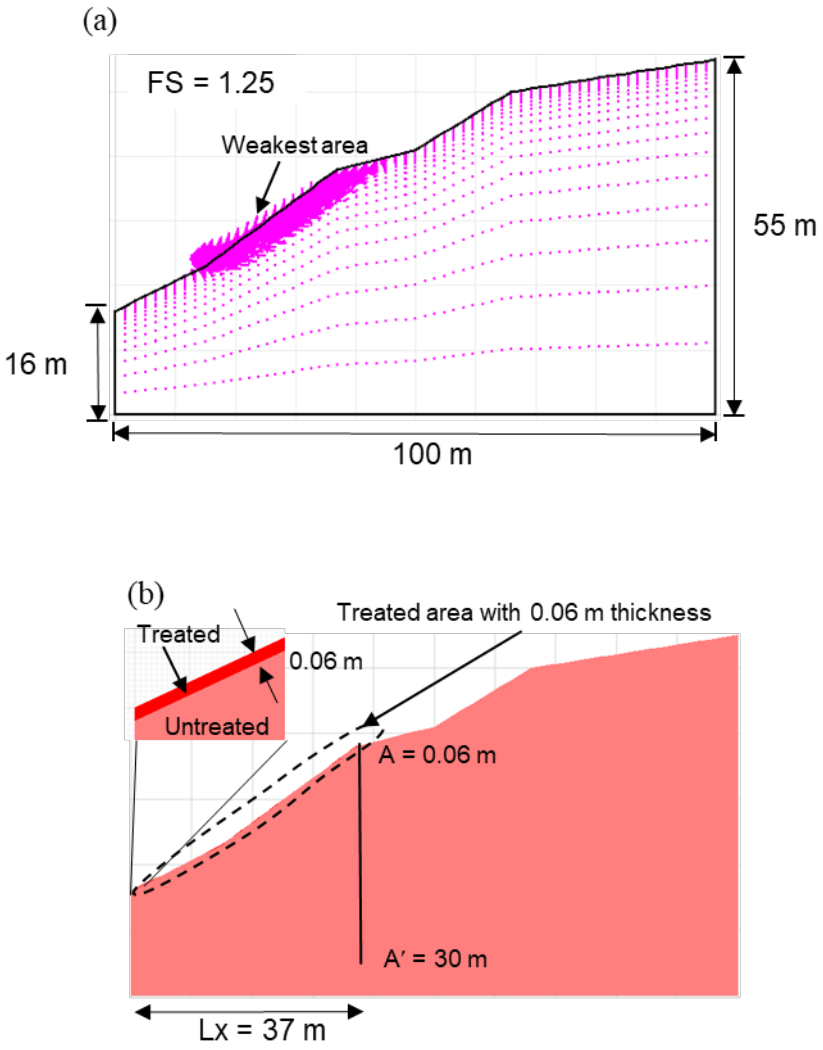

Figure 6.6 A Fictitious slope for numerical verification. (a) Overall geometry and weakest area of the slope. (b) Xanthan gum treatment simulation (0.06–m–thickness from the toe up to the entire weakest area) (Tran et al. 2019b)

Table 6.2. Input parameters for FLAC simulation (Tran et al. 2019b)

Parameters		Value		Unit
		Untreated S8K2	Xanthan gum -treated S8K2[1)]	
Dry density		1.55	1.55	g/cm^3
Cohesion (c')		0	0	kPa
Friction angle (ϕ')		35.7	34.6	°
Saturation		0.5	0.5	
Residual volumetric water content (θ_r)		0	0	
Van Genuchten parameters	α	0.46	0.54	kPa^{-1}
	m	0.45	0.55	
Saturated permeability of soil (K_{sat})		4.519×10^{-7}	1.573×10^{-9}	m/s

[1)] 0.5% xanthan gum (xanthan gum to soil ratio, in mass)

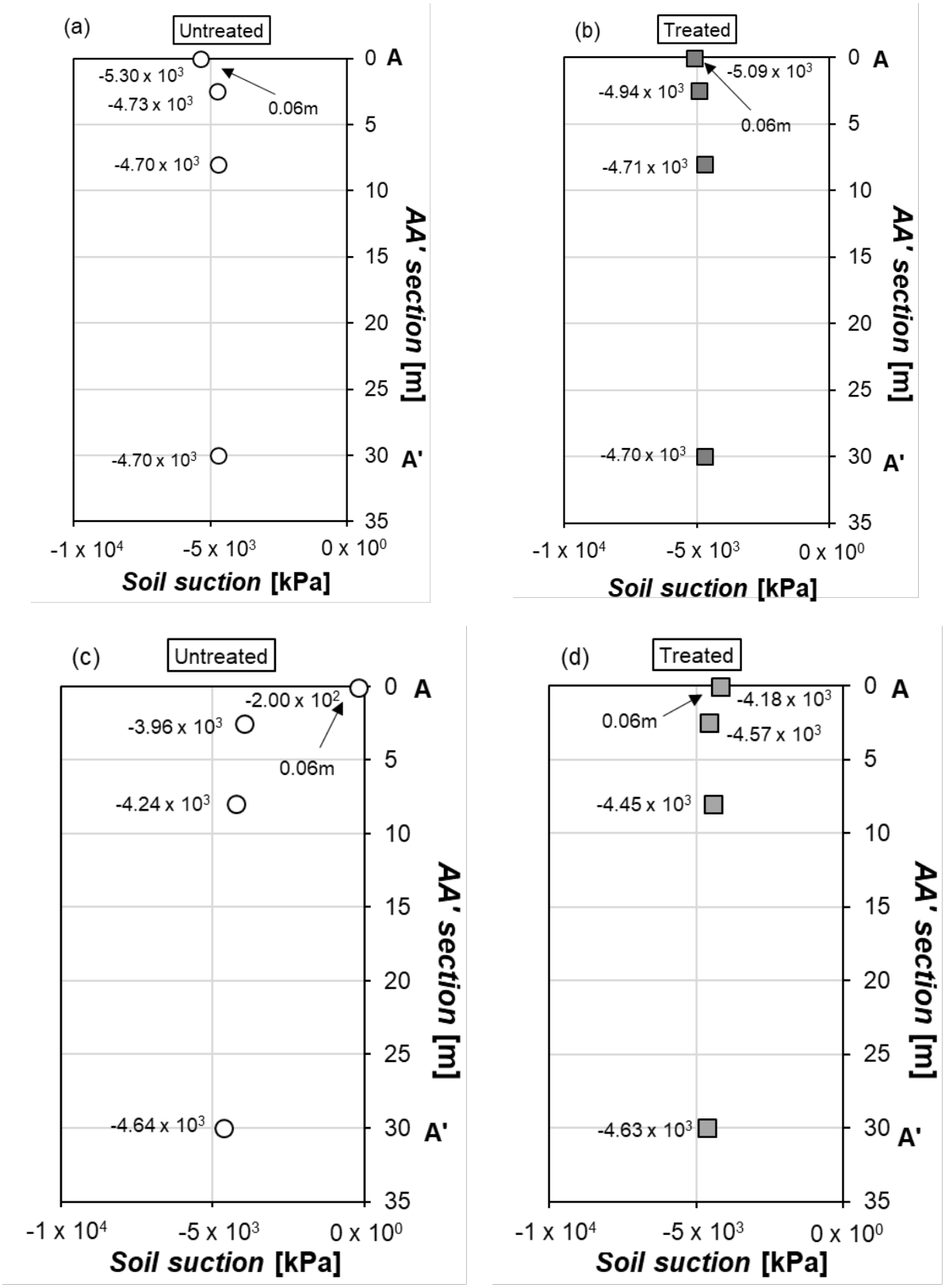

Figure 6.7. The pore pressure distribution along section AA′ before (a, b) and after 40–hours (c, d) of downpour simulation on untreated slope and xanthan-treated slope

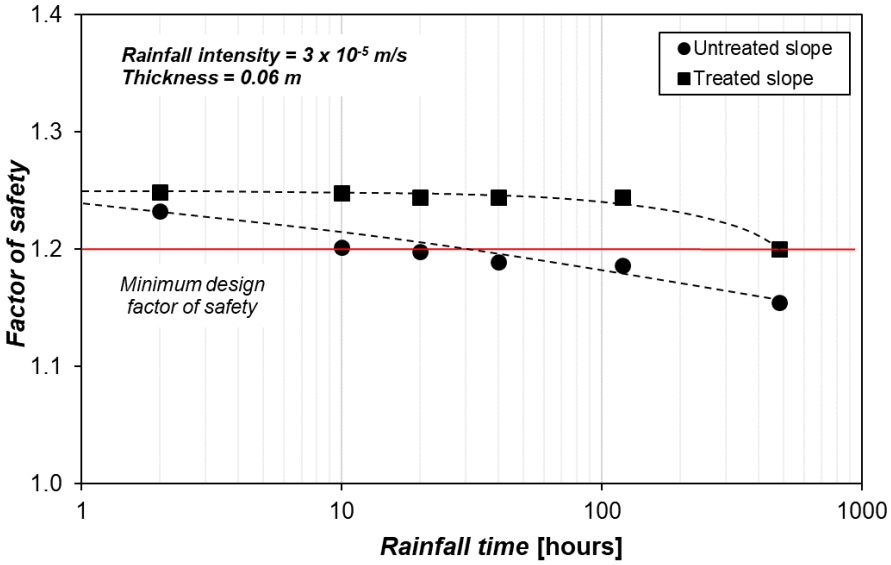

Figure 6.8. Variation of factor of safety against slope failure under continuous rainfall simulation (Tran et al. 2019b)

6.3 Potential for landfill materials using biopolymer-soil treatment

Increasing affluent lifestyles, continuing industrial and commercial growth in many countries around the world in the past decade has been accompanied by rapid increases in municipal solid waste production. Landfilling is the primary technology used for municipal solid waste management in middle and low-income countries (Townsend et al. 2015).

There are two main systems; liner and final cover, including many parts with different functions, which allows the landfill to storage wastes and serve to prevent contamination between the waste and the surrounding environment, especially groundwater. The liner system at the bottom of the landfill, besides pipe systems for leachate collection, removal and treatment, and foundation, has liners (i.e., barrier liner) is to prevent or minimize the migration of leachate to the environment. The final cover system has gas control, water drainage control, and liner that can prevent gases from escaping and water from entering and forming more leachate. Furthermore, most landfill caps include vegetation or grass layer of topsoil to prevent erosion. (Townsend et al. 2015)

To meet demands for a hydraulic/gas barrier liner, barrier materials such as inorganic adsorbents, organic adsorbents, and biosorbents need to have good performances in hydraulic conductivity reduction ($k < 10^{-10}$m/s) (Bouazza 2002), high shear strength and high contaminant removal abilities (Balkaya 2016; Prashanth 2001). Geosynthetic clay liners have been widely known

as a popular substitute for compacted clay liners in cover systems and composite bottom liners (Bouazza 2002).

The problem is that the development of vegetation root which is able to penetrate down to the liner of the final cover (Flower 1978; Hakonson et al. 1982), which in turn forms cracks in the cover system. To limit the root penetration, the use of heavy compaction of soils, which have small pore space and low oxygen supply for exhibits root growth, is suggested (Johnson and Urie 1985). However, this method can cause runoff due to the small pore space for water infiltration. Another problem to the liner is the effect of sunlight or temperature that can dry clay and destroy the workability of clay in liner and geomembrane system (BLM 1992)

Types of materials used for topsoil formation is essential for weathering erosion prevention such as rainwater and wind. If the low permeability materials are used, excess rainfall runs off the surface causing erosion (Johnson and Urie 1985). Wind erosion often occurs to landfills located in arid or semiarid regions where dry soil particles capable of being moved by velocity of the wind (Chepil 1958; Lutton et al. 1979). The use of vegetation layer provides excellent control for both wind and water erosion to landfill cover (Hauser 2016). Another problem that vegetation has to face is the competition for available space from surrounding shrubs or bushes (BLM 1992). To have effective performance, short root vegetation and dense vegetation layer are required for weathering erosion control (Johnson and Urie 1985).

With a quick look, the biopolymer-soil treatment seems to meet the requirements for a landfill liner and topsoil materials: (1) supplying a saturation zone for controlling the root growth and for preventing drying clay liner; (2) reducing water erosion via increasing infiltration and water holding capacity; (3) decreasing hydraulic conductivity and (4) increasing heavy metal removal via metal ion adsorption. However, different types of biopolymers show different effectiveness level for each application. From this study, we suggest using xanthan gum-treated sand as topsoil material, and gellan gum for liner material.

Chapter 7 Conclusions and future study

7.1 Conclusions

This dissertation focused on the water-related properties of biopolymer-soil treatment considering soil-water-hydrogel. Xanthan gum, and gellan gum, which have different strengthening behaviors to thermos-gelatin are used in this study.

Previous researchers have been suggested the use of xanthan gum for surface soil treatment such as anti-wind erosion, water retention improvement. SWCC results in this current study show that xanthan gum increases the remaining water and air entry values via water absorbing and holding capacity of xanthan gum hydrogel in soil. However, the swelling ability of xanthan gum is controlled by the pore size of soils. For instance, the xanthan gum content at 1% or higher does not show significant differences in water retention because during saturation 1% of xanthan gum hydrogel already fill the pore spaces of the soil in its entirety. No more water can be absorbed even at xanthan gum higher content. In other words, the pore size controls the amount of water absorbed. The pore size also controls the rate of change in water storage of xanthan gum-treated soil, which is reflected via the slope of the SWCC, as the air pressure increases. Therefore, the van Genuchten *n* parameter which indicates the slope of the SWCC shows an exponential decay relationship with xanthan gum content. The amount of xanthan gum lower than 1 % is suggested for the vegetation purpose in order to avoid the waterlogging impacts on vegetation germination and growth. As the soil pores are entirely filled by xanthan gum of contents higher than 1%, waterlogging can occur, which have an adverse aeration condition with respect to vegetation germination and growth.

Clay has the ability to form an active matrix with biopolymers via the presence of charges on both the clay and biopolymers. The presence of biopolymers renders different wetting behaviors of biopolymer-treated soils depending on the number of interaction between kaolinite and xanthan gum. At low xanthan gum content, the kaolinite-xanthan matrix acts as a water transferor. It is due to the water absorption capabilities of kaolinite and the biopolymer. As predominant properties of water absorption in xanthan gum occurs, xanthan-kaolinite mixture acts as a water barrier. Meanwhile, kaolinite-xanthan matrix serves as a water barrier as xanthan gum content of 0.5% or higher due to the predominant properties of water absorption in xanthan gum. This effect is only shown in kaolinite so far because kaolinite itself is known as less-swelling clay. For montmorillonite, due to the strong water absorption capacities of montmorillonite, the soil pore spaces are quickly blocked by swollen montmorillonite and xanthan gum.

If a hydrogel can form a strong and hard gel via heating and cooling process, the hydrogel is

classified as thermo gelatin hydrogel. Thermo-gelation properties allow gellan gum hydrogel to withstand high pressures such as effective stress and inlet water pressure. The pressurized hydraulic conductivity test shows that the effect of pore size and kaolinite admixture also appear in the performance of gellan gum on hydraulic conductivity control. The hydraulic conductivity of gellan gum-treated sand shows the exponential decay relationship with gellan gum content. The hydraulic conductivity converges at gellan gum higher than 1% content. The gellan-kaolinite matrix improves the performance of gellan gum in hydraulic conductivity reduction. Furthermore, the use of gellan gum helps control the loss of kaolinite induced by the high water pressure.

The ability of gellan gum in working under high pressure allows gellan gum-treated soil to become a hydraulic barrier. Via the pressurized upward flow system, a sand column containing a gellan-treated sand liner was used to treat a solution containing nickel which is shown as serve metal allergen. The results show that gellan gum, which can adsorb nickel via functional groups and cation exchange, enhances nickel adsorbability of sand. The nickel adsorbability increase with proportionally with gellan gum content. It is noted that the potassium cation exchange which is found in this study is only for nickel adsorption.

Based on the suggestion of xanthan gum content for vegetation purposes, 0.5% xanthan gum content is used to test the germination and growth of ryegrass. It is found that 0.5% xanthan gum reduces the seed germination due to the waterclogging of xanthan gum hydrogel. However, via providing a saturation zone near the surface, xanthan gum hydrogel can control the root growth, which can be useful for reducing the effect of plan root on membrane or liner below.

The numerical modeling using FLAC 2D shows that xanthan gum-treated soil can be used for water erosion reduction via quickly absorbing and holding water. During rainfall, the negative pore water pressure located near the surface of untreated slope decreases faster than that of xanthan gum-treated slope. It is because the amount of water that penetrates to the body of the treated slope can be controlled via 0.06 m xanthan gum-treated sand liner covering the weakest area of the slope. The slow decrease in negative pore water pressure, in turn, delays the strength reduction of the slope during rainfall. Therefore, the stability of the treated slope is longer than the untreated slope under the rainfall condition.

Generally, biopolymers through water absorbing and water holding processes can control the water distribution in soil, and the water flow through a soil. Besides, biopolymers with the functional groups such as carbonyl, methylol, methyl can enhance the ion interaction of soil particles; therefore, biopolymers can form a matrix with kaolinite and adsorb heavy metal ions. Depending on the desired engineering purpose of the use of biopolymers, the type, and concentration of biopolymers need to be considered. From this thesis, xanthan gum is suggested for surface treatment with purpose of water

erosion control, water storage for plants during drought conditions. Meanwhile, gellan gum can take advantage of its thermo-gelatin properties in urgent and deep applications such as grouting or hydraulic barrier.

7.2 Philosophy and Further Recommendations

Philosophy

It is known that the soil–water interactions, which are formed by the water content and soil physicochemical properties such as mineral composition, grain size distribution and soil organic matter content, determine the structural and hydrological properties of the soil. The presence of biopolymer-based hydrogel with its water absorbing and holding capacity will affect the soil-water-interaction by adding new interactions of hydrogel-soil particles, hydrogel-water to the original interaction.

A biopolymer-based hydrogel is a form of material between liquid and solid, so it has properties of both: viscosity and viscoelasticity. Therefore, to what extent biopolymer hydrogel can be considered to be a separated phase in soil, which has its properties that vary widely according to their water content.

Biopolymer soils are complex systems as they comprise two different porous frameworks: mineral soil constituents and swollen biopolymer hydrogel structures. Laboratory testing results show that the soil structure is a function of both biopolymer treatment (i.e., binding soil particles) and swelling ability of biopolymer between the soil particles.

The effects of biopolymer on soil rheology are keys for assessment of soil microstructural stability, which has been recognized. However, there is a limited number of existing studies dealing with the effects of soil-water-hydrogels interaction. Therefore, there is a need for further investigation.

Further recommendation

The research that has been undertaken for this thesis has highlighted several topics on which further research would be extended. The followings can help to enhance the understanding of water-related behaviors of bio-soil and applicability in engineering practice

Microscale: This study provides an understanding of water-related properties of biopolymer-treated soil considering soil-water-hydrogel interaction. However, providing information on the contact angle, surface tension, and viscosity of biopolymer-based hydrogel in soil surface is essential for having an insight into the performance of treated soil in microscale.

Macroscale: This study used laboratory SWCC data used for numerical modeling to evaluate the applicability of xanthan gum on reducing the rainfall-induced slope instability. Therefore, field monitoring data on pore water distribution and should be provided to check if there are a gap and connection between laboratory research and field application of biopolymer-soil treatment.

References

Aal, G.Z.A., Atekwana, E.A., and Atekwana, E.A. 2010. Effect of bioclogging in porous media on complex conductivity signatures. Journal of Geophysical Research: Biogeosciences **115**(G3). doi: https://doi.org/10.1029/2009JG001159.

Adachi, M., and Watanabe, S. 2007. Evaluation of combined deactivators-supplemented agar medium (CDSAM) for recovery of dermatophytes from patients with tinea pedis. Medical Mycology **45**(4): 347-349. doi: 10.1080/13693780601186531.

Agi, A., Junin, R., Gbonhinbor, J., and Onyekonwu, M. 2018. Natural polymer flow behaviour in porous media for enhanced oil recovery applications: a review. Journal of Petroleum Exploration and Production Technology **8**(4): 1349-1362. doi: https://doi.org/10.1007/s13202-018-0434-7.

Aider, M. 2010. Chitosan application for active bio-based films production and potential in the food industry. LWT-food science and technology **43**(6): 837-842.

Al-Darby, A. 1996a. The hydraulic properties of a sandy soil treated with gel-forming soil conditioner. Soil technology **9**(1-2): 15-28. doi: https://doi.org/10.1016/0933-3630(95)00030-5.

Al-Darby, A.M. 1996b. The hydraulic properties of a sandy soil treated with gel-forming soil conditioner. Soil Technology **9**(1–2): 15-28. doi: http://dx.doi.org/10.1016/0933-3630(95)00030-5.

Amundarain, J., Castro, L., Rojas, M., Siquier, S., Ramírez, N., Müller, A., and Saez, A.E. 2009. Solutions of xanthan gum/guar gum mixtures: shear rheology, porous media flow, and solids transport in annular flow. Rheologica acta **48**(5): 491-498. doi: https://doi.org/10.1007/s00397-008-0337-5.

Andry, H., Yamamoto, T., Irie, T., Moritani, S., Inoue, M., and Fujiyama, H. 2009. Water retention, hydraulic conductivity of hydrophilic polymers in sandy soil as affected by temperature and water quality. Journal of Hydrology **373**(1-2): 177-183. doi: https://doi.org/10.1016/j.jhydrol.2009.04.020.

Araki, C. 1966. Some recent studies on the polysaccharides of agarophytes. *In* Proceedings of the Fifth International Seaweed Symposium, Halifax, August 25–28, 1965. Elsevier. pp. 3-17.

Arnott, R. 1965. Particle sizes of clay minerals by small-angle x-ray scattering. American Mineralogist: Journal of Earth and Planetary Materials **50**(10): 1563-1575.

ASTM. 2016. D2166 / D2166M-16: Standard Test Method for Unconfined Compressive Strength of Cohesive Soil. ASTM International, West Conshohocken.

Auerbach, M., Witt, D., Toler, W., Fierstein, M., Lerner, R.G., and Ballard, H. 1988. Clinical use of the total dose intravenous infusion of iron dextran. Journal of Laboratory and Clinical Medicine **111**(5): 566-570.

Awan, M.A., Qazi, I.A., and Khalid, I. 2003. Removal of heavy metals through adsorption using sand. Journal of Environmental Sciences **15**(3): 413-416.

Ayeldeen, M., Negm, A., El-Sawwaf, M., and Kitazume, M. 2017. Enhancing mechanical behaviors of collapsible soil using two biopolymers. Journal of Rock Mechanics and Geotechnical Engineering **9**(2): 329-339.

Ayeldeen, M.K., Negm, A.M., and El Sawwaf, M.A. 2016. Evaluating the physical characteristics of biopolymer/soil mixtures. Arabian Journal of Geosciences **9**(5): 1-13. doi: https://doi.org/10.1007/s12517-016-2366-1.

Babbar, S.B., and Jain, R. 2006. Xanthan gum: an economical partial substitute for agar in microbial culture media. Current microbiology **52**(4): 287-292. doi: https://doi.org/10.1007/s00284-005-0225-5.

Balkaya, M. 2016. Evaluation of the use of alum sludge as hydraulic barrier layer and daily cover material in landfills: a finite element analysis study. Desalination and Water Treatment **57**(6): 2400-2412. doi: https://doi.org/10.1080/19443994.2015.1005154.

Barclay, W.R., and Lewin, R.A. 1985. Microalgal polysaccharide production for the conditioning of agricultural soils. Plant and Soil **88**(2): 159-169. doi: https://doi.org/10.1007/BF02182443.

Bassi, R., Prasher, S.O., and Simpson, B. 2000. Removal of selected metal ions from aqueous solutions using chitosan flakes. Separation Science and Technology **35**(4): 547-560. doi: https://doi.org/10.1081/SS-100100175.

Bear, J. 2012. Hydraulics of groundwater. Courier Corporation.

Bear, J. 2013. Dynamics of fluids in porous media. Courier Corporation.

Beard, J.B., and Green, R.L. 1994. The role of Turfgrasses in environmental protection and their benefits to Humans. Journal of Environmental Quality **23**(3): 452-460. doi: 10.2134/jeq1994.00472425002300030007x.

Bhardwaj, A.K., Shainberg, I., Goldstein, D., Warrington, D.N., and J.Levy, G. 2007. Water retention and hydraulic conductivity of cross-linked polyacrylamides in sandy soils. Soil Science Society of America Journal **71**(2): 406-412. doi: https://doi.org/10.2136/sssaj2006.0138.

Biot, M.A. 1941. General theory of three-dimensional consolidation. Journal of Applied Physics **12**(2): 155-164.

Bishop, A.W. 1959. The principle of effective stress. Teknisk ukeblad **39**: 859-863.

BLM, B.o.L.M. 1992. Eagle Mountain Landfill Project, Riverside County: Environmental Impact Statement. U.S. Department of The Interior.

Bohn, J.A., and BeMiller, J.N. 1995. (1→3)-β-d-Glucans as biological response modifiers: a review of structure-functional activity relationships. Carbohydrate Polymers **28**(1): 3-14. doi: https://doi.org/10.1016/0144-8617(95)00076-3.

Bolan, N.S., Naidu, R., Syers, J., and Tillman, R. 1999. Surface charge and solute interactions in soils. *In* Advances in agronomy. Elsevier. pp. 87-140.

Bolland, M.D.A., Posner, A., and Quirk, J. 1976. Surface charge on kaolinites in aqueous suspension. Soil Research **14**(2): 197-216.

Bouazza, A. 2002. Geosynthetic clay liner. Geotextiles and Geomembranes **20**(1): 3-17. doi: https://doi.org/10.1016/S0266-1144(01)00025-5.

Bouazza, A., Gates, W., and Ranjith, P. 2009. Hydraulic conductivity of biopolymer-treated silty sand. Géotechnique **59**(1): 71-72.

Bouhadir, K.H., Lee, K.Y., Alsberg, E., Damm, K.L., Anderson, K.W., and Mooney, D.J. 2001. Degradation of partially oxidized alginate and its potential application for tissue engineering. Biotechnology Progress **17**(5): 945-950. doi: doi:10.1021/bp010070p.

Brooks, R., and Corey, T. 1964. HYDRAU uc properties of porous media. Hydrology Papers, Colorado State University **24**: 37.

Brunk, D. 2008. Nickel is named contact allergen of the Year. Available from http://www.jfponline.com/fileadmin/content_pdf/ped/archive_pdf/vol42iss2/70075_main.pdf [accessed 5 June 2019].

Brutsaert, W. 1967. Some methods of calculating unsaturated permeability. Transactions of the ASAE **10**(3): 400-0404.

Bueno, V.B., Bentini, R., Catalani, L.H., and Petri, D.F.S. 2013. Synthesis and swelling behavior of xanthan-based hydrogels. Carbohydrate Polymers **92**(2): 1091-1099. doi: http://dx.doi.org/10.1016/j.carbpol.2012.10.062.

Burdine, N. 1953. Relative permeability calculations from pore size distribution data. Journal of Petroleum Technology **5**(3): 71-78.

Cabalar, A., Wiszniewski, M., and Skutnik, Z. 2017. Effects of Xanthan Gum Biopolymer on the Permeability, Odometer, Unconfined Compressive and Triaxial Shear Behavior of a Sand. Soil Mechanics and Foundation Engineering **54**(5): 356-361.

Cai, F., and Ugai, K. 2004. Numerical analysis of rainfall effects on slope stability. International Journal of Geomechanics **4**(2): 69-78. doi: https://doi.org/10.1061/(ASCE)1532-3641(2004)4:2(69).

Campbell, G.S. 1974. A simple method for determining unsaturated conductivity from moisture retention data. Soil science **117**(6): 311-314.

Candia, J.L.F., and Deckwer, W.D. 2002. Xanthan Gum. *In* Encyclopedia of Bioprocess Technology. John Wiley & Sons, Inc.

Cao, S. 2008. Why large-scale afforestation efforts in China have failed to solve the desertification problem. Environmental Science & Technology **42**(6): 1826-1831.

Castillo, N.A., Valdez, A.L., and Fariña, J.I. 2015. Microbial production of scleroglucan and downstream processing. Frontiers in microbiology **6**: 1106. doi: 10.3389/fmicb.2015.01106.

Çavuş, S., and Gürdağ, G. 2008. Competitive heavy metal removal by poly (2-acrylamido-2-methyl-1-propane sulfonic acid-co-itaconic acid). Polymers for Advanced Technologies **19**(9): 1209-1217. doi: https://doi.org/10.1002/pat.1113.

Chang, C., Duan, B., Cai, J., and Zhang, L. 2010. Superabsorbent hydrogels based on cellulose for smart swelling and controllable delivery. European Polymer Journal **46**(1): 92-100. doi: http://dx.doi.org/10.1016/j.eurpolymj.2009.04.033.

Chang, I., and Cho, G.-C. 2012. Strengthening of Korean residual soil with β-1,3/1,6-glucan biopolymer. Construction and Building Materials **30**(0): 30-35. doi: http://dx.doi.org/10.1016/j.conbuildmat.2011.11.030.

Chang, I., and Cho, G.-C. 2014. Geotechnical behavior of a beta-1,3/1,6-glucan biopolymer-treated residual soil. Geomechanics and Engineering **7**(6): 633-647. doi: http://dx.doi.org/10.12989/gae.2014.7.6.633

Chang, I., and Cho, G.-C. 2019. Shear strength behavior and parameters of microbial gellan gum-treated soils: from sand to clay. Acta Geotechnica **14**(2): 361-375. doi: https://doi.org/10.1007/s11440-018-0641-x.

Chang, I., Im, J., and Cho, G.-C. 2016. Geotechnical engineering behaviors of gellan gum biopolymer treated sand. Canadian Geotechnical Journal **53**(10): 1658-1670. doi: https://doi.org/10.1139/cgj-2015-0475.

Chang, I., Im, J., and Cho, G.C. 2016b. Introduction of microbial biopolymers in soil treatment for future environmentally-friendly and sustainable geotechnical engineering. Sustainability **8**(3): 251. doi: https://doi.org/10.3390/su8030251.

Chang, I., Im, J., Prasidhi, A.K., and Cho, G.-C. 2015a. Effects of Xanthan gum biopolymer on soil strengthening. Construction and Building Materials **74**(0): 65-72. doi: http://dx.doi.org/10.1016/j.conbuildmat.2014.10.026.

Chang, I., Jeon, M., and Cho, G.-C. 2015b. Application of microbial biopolymers as an alternative construction binder for earth buildings in underdeveloped countries. International Journal of Polymer Science **2015**: 9. doi: http://dx.doi.org/10.1155/2015/326745.

Chang, I., Kwon, Y.-M., Im, J., and Cho, G.-C. 2018. Soil consistency and inter-particle characteristics of xanthan gum biopolymer containing soils with pore-fluid variation. Canadian Geotechnical Journal. doi: https://doi.org/10.1139/cgj-2018-0254.

Chang, I., Prasidhi, A.K., Im, J., and Cho, G.-C. 2015c. Soil strengthening using thermo-gelation biopolymers. Construction and Building Materials **77**(0): 430-438. doi: http://dx.doi.org/10.1016/j.conbuildmat.2014.12.116.

Chang, I., Prasidhi, A.K., Im, J., Shin, H.-D., and Cho, G.-C. 2015d. Soil treatment using microbial biopolymers for anti-desertification purposes. Geoderma **253–254**(0): 39-47. doi: https://doi.org/10.1016/j.geoderma.2015.04.006.

Chang, S., Gupta, R., and Ryan, M. 1992. Effect of the adsorption of polyvinyl alcohol on the rheology and stability of clay suspensions. Journal of Rheology **36**(2): 273-287. doi: https://doi.org/10.1122/1.550345.

Chatterjee, S., Adhya, M., Guha, A., and Chatterjee, B. 2005. Chitosan from Mucor rouxii: production and physico-chemical characterization. Process Biochemistry **40**(1): 395-400. doi: https://doi.org/10.1016/j.procbio.2004.01.025.

Chauhan, K., Chauhan, G.S., and Ahn, J.-H. 2010. Novel polycarboxylated starch-based sorbents for Cu2+ ions. Industrial & Engineering Chemistry Research **49**(6): 2548-2556. doi: 10.1021/ie9009952.

Chen, C., and Wagenet, R. 1992. Simulation of water and chemicals in macropore soils Part 1. Representation of the equivalent macropore influence and its effect on soilwater flow. Journal of Hydrology **130**(1-4): 105-126. doi: https://doi.org/10.1016/0022-1694(92)90106-6.

Chen, R., Lee, I., and Zhang, L. 2015. Biopolymer stabilization of mine tailings for dust control. Journal of Geotechnical and Geoenvironmental Engineering **141**(2): 04014100. doi: doi:10.1061/(ASCE)GT.1943-5606.0001240.

Chen, R., Zhang, L., and Budhu, M. 2013a. Biopolymer stabilization of mine tailings. Journal of Geotechnical and Geoenvironmental Engineering **139**(10): 1802-1807. doi: https://doi.org/10.1061/(ASCE)GT.1943-5606.0000902.

Chen, X., Su, Z., Ma, Y., Yang, K., Wen, J., and Zhang, Y. 2013b. An improvement of roughness height parameterization of the Surface Energy Balance System (SEBS) over the Tibetan Plateau. Journal of applied meteorology and climatology **52**(3): 607-622.

Cheng, L., Cord-Ruwisch, R., and Shahin, M.A. 2013. Cementation of sand soil by microbially induced calcite precipitation at various degrees of saturation. Canadian Geotechnical Journal **50**(1): 81-90. doi: https://doi.org/10.1139/cgj-2012-0023.

Chenu, C. 1989. Influence of a fungal polysaccharide, scleroglucan, on clay microstructures. Soil Biology and Biochemistry **21**(2): 299-305. doi: http://dx.doi.org/10.1016/0038-0717(89)90108-9.

Chenu, C. 1993. Clay- or sand-polysaccharide associations as models for the interface between micro-organisms and soil: water related properties and microstructure. Geoderma **56**(1–4): 143-156. doi: http://dx.doi.org/10.1016/0016-7061(93)90106-U.

Chepil, W.S. 1958. Soil conditions that influence wind erosion. US Dept. of Agriculture.

Chirico, G.B., Borga, M., Tarolli, P., Rigon, R., and Preti, F. 2013. Role of Vegetation on Slope Stability under Transient Unsaturated Conditions. Procedia Environmental Sciences **19**: 932-941. doi: https://doi.org/10.1016/j.proenv.2013.06.103.

Chourasia, M., and Jain, S. 2004. Potential of guar gum microspheres for target specific drug release to colon. Journal of drug targeting **12**(7): 435-442.

Christensen, L.H., Breiting, V.B., Aasted, A., Jørgensen, A., and Kebuladze, I. 2003. Long-term effects of polyacrylamide hydrogel on human breast tissue. Plastic and reconstructive surgery **111**(6): 1883-1890. doi: 10.1097/01.prs.0000056873.87165.5a.

Chu, J., Varaksin, S., Klotz, U., and Mengé, P. 2009. Construction processes, State-of-the-art report. *In* 17th International conference on soil mechanics and geotechnical engineering, Alexandria, Egypt. pp. 3006-3135.

Chudzikowski, R. 1971. Guar gum and its applications. J. Soc. Cosmet. Chem **22**(323): 43-60.

Chung, C.-K., Kim, J.-H., Kim, J., and Kim, T. 2018. Hydraulic Conductivity Variation of Coarse-Fine Soil Mixture upon Mixing Ratio. Advances in Civil Engineering **2018**. doi: https://doi.org/10.1155/2018/6846584.

Crous, J.W. 2017. Use of hydrogels in the planting of industrial wood plantations. Southern Forests: a Journal of Forest Science **79**(3): 197-213. doi: 10.2989/20702620.2016.1221698.

D'Cunha, N.J., Misra, D., and Thompson, A.M. 2009. Experimental investigation of the applications of natural freezing and curdlan biopolymer for permeability modification to remediate DNAPL contaminated aquifers in Alaska. Cold Regions Science and Technology **59**(1): 42-50.

Das, B.M., and Sobhan, K. 2013. Principles of geotechnical engineering. Cengage learning.

Das, K., Das, S., and Dhundasi, S. 2008. Nickel, its adverse health effects & oxidative stress. Indian Journal of Medical Research **128**(4): 412. doi: https://doi.org/10.1016/j.jtemb.2012.01.002.

Davis, W.B. 1992. Unique bacterial polysaccharide polymer gel in cosmetics, pharmaceuticals and foods. Google Patents.

Dearfield, K.L., Abernathy, C.O., Ottley, M.S., Brantner, J.H., and Hayes, P.F. 1988. Acrylamide: its metabolism, developmental and reproductive effects, genotoxicity, and carcinogenicity. Mutation Research/Reviews in Genetic Toxicology **195**(1): 45-77. doi: https://doi.org/10.1016/0165-1110(88)90015-2.

DeJong, J.T., Mortensen, B.M., Martinez, B.C., and Nelson, D.C. 2010. Bio-mediated soil improvement. Ecological Engineering **36**(2): 197-210. doi: http://dx.doi.org/10.1016/j.ecoleng.2008.12.029.

DeJong, J.T., Soga, K., Kavazanjian, E., Burns, S., Paassen, L.A.V., Qabany, A.A., Aydilek, A., Bang, S.S., Burbank, M., Caslake, L.F., Chen, C.Y., Cheng, X., Chu, J., Ciurli, S., Esnault-Filet, A., Fauriel, S., Hamdan, N., Hata, T., Inagaki, Y., Jefferis, S., Kuo, M., Lalaoui, L., Larrahondo, J., Manning, D.A.C., Martinez, B., Montoya, B.M., Nelson, D.C., Palomino, A., Renforth, P., Santamarina, J.C., Seagren, E.A., Tanyu, B., Tsesarsky, M., and Weaver, T. 2013. Biogeochemical processes and geotechnical applications: progress, opportunities and challenges. Géotechnique **63**(4): 287-301. doi: 10.1680/geot.SIP13.P.017.

Du, C., Zhou, G., Wang, H., Chen, X., and Zhou, J. 2010. Depth profiling of clay–xanthan complexes using step-scan mid-infrared photoacoustic spectroscopy. Journal of Soils and Sediments **10**(5): 855-862. doi: https://doi.org/10.1007/s11368-010-0225-3.

Dumitriu, S. 2004. Polysaccharides: structural diversity and functional versatility. CRC press.

Ebina, T., Minja, R.J., Nagase, T., Onodera, Y., and Chatterjee, A. 2004. Correlation of hydraulic conductivity of clay–sand compacted specimens with clay properties. Applied clay science **26**(1-4): 3-12. doi: https://doi.org/10.1016/j.clay.2003.09.010.

Eliasson, A.-C. 2004. Starch in food: Structure, function and applications. CRC Press, Boca Raton, FL.

Etemadi, O., Petrisor, I.G., Kim, D., Wan, M.-W., and Yen, T.F. 2003. Stabilization of metals in subsurface by biopolymers: laboratory drainage flow studies. Soil and Sediment Contamination **12**(5): 647-661. doi: https://doi.org/10.1080/714037712.

Fan, T., Stewart, B.A., Payne, W.A., Yong, W., Luo, J., and Gao, Y. 2005. Long-term fertilizer and water availability effects on cereal yield and soil chemical properties in Northwest China. Soil Science Society of America Journal **69**(3): 842-855. doi: 10.2136/sssaj2004.0150.

Fell, R., MacGregor, P., Stapledon, D., and Bell, G. 2005. Geotechnical engineering of dams. CRC Press.

Flower, F.B. 1978. A study of vegetation problems associated with refuse landfills. Environmental Protection Agency, Office of Research and Development ….

Fourest, E., and Volesky, B. 1997. Alginate properties and heavy metal biosorption by marine algae. Applied Biochemistry and Biotechnology **67**(3): 215-226. doi: https://doi.org/10.1007/BF02788799.

Francis, H.P., DeBoer, E.D., and Wermers, V.L. 1987. High temperature drilling fluid component. *Edited by* A.M.-P. Company, US.

Fredlund, D. 2017. Role of the soil-water characteristic curve in unsaturated soil mechanics. *In* In Proceeding of the 19th International Conference on Soil Mechanics and Geotechnical Engineering. pp. 57-79.

Fredlund, D., Morgenstern, N.R., and Widger, R. 1978. The shear strength of unsaturated soils. Canadian geotechnical journal **15**(3): 313-321. doi: https://doi.org/10.1139/t78-029.

Fredlund, D.G., and Morgenstern, N.R. 1977. Stress state variables for unsaturated soils. Journal of Geotechnical and Geoenvironmental Engineering **103**(ASCE 12919).

Fredlund, D.G., Rahardjo, H., and Fredlund, M.D. 2012. Unsaturated soil mechanics in engineering practice. John Wiley & Sons.

Fredlund, D.G., and Xing, A. 1994. Equations for the soil-water characteristic curve. Canadian geotechnical journal **31**(4): 521-532.

Fredlund, M.D. 2000. The role of unsaturated soil property functions in the practice of unsaturated soil mechanics. University of Saskatchewan.

Free, E.E. 1911. Studies in soil physics, II. The movements of soil water. The Plant World **14**: 59-66.

Gaafer, M., Bassioni, H., and Mostafa, T. 2015. Soil Improvement Techniques. Int. J. Sci. Eng. Res **6**(12): 217-222.

Gallage, C.P.K., and Uchimura, T. 2010. Effects of dry density and grain size distribution on soil-water characteristic curves of sandy soils. Soil and Foundations **50**(1): 161-172. doi: https://doi.org/10.3208/sandf.50.161.

García-Ochoa, F., Santos, V.E., Casas, J.A., and Gómez, E. 2000. Xanthan gum: production, recovery, and properties. Biotechnology Advances **18**(7): 549-579. doi: https://doi.org/10.1016/S0734-9750(00)00050-1.

Gardner, W. 1956. Mathematics of isothermal water conduction in unsaturated soils. Highway research board special report **40**: 78-87.

Ghio, V.A., Monteiro, P.J.M., and Demsetz, L.A. 1994. The Rheology of Fresh Cement Paste Containing Polysaccharide Gums. Cement and Concrete Research **24**(2): 243-249.

Giavasis, I., Harvey, L.M., and McNeil, B. 2000. Gellan gum. Critical Reviews in Biotechnology **20**(3): 177-211.

Glicksman, M. 1969. Gum technology in the food industry. Academic Press, New York and London.

Greaves, G., Fontaine, A., Lagarde, P., Raoux, D., and Gurman, S. 1981. Local structure of silicate glasses. Nature **293**(5834): 611. doi: https://doi.org/10.1038/293611a0.

Guilherme, M.R., Aouada, F.A., Fajardo, A.R., Martins, A.F., Paulino, A.T., Davi, M.F., Rubira, A.F., and Muniz, E.C. 2015. Superabsorbent hydrogels based on polysaccharides for application in agriculture as soil conditioner and nutrient carrier: A review. European Polymer Journal **72**: 365-385. doi: https://doi.org/10.1016/j.eurpolymj.2015.04.017.

Gun'ko, V., Savina, I., and Mikhalovsky, S. 2017. Properties of water bound in hydrogels. Gels **3**(4): 37. doi: https://doi.org/10.3390/gels3040037.

Gupta, S.C., Hooda, K., Mathur, N., and Gupta, S. 2009. Tailoring of guar gum for desert sand stabilization.

Hakonson, T., White, G., and Karlen, E. 1982. Evaluation of geologic materials to limit biological intrusion of low-level waste site covers. *In* Proceedings of the ANS topical meeting on the treatment and handling of radioactive wastes.

Hatakeyama, H., and Hatakeyama, T. 1998. Interaction between water and hydrophilic polymers. Thermochimica Acta **308**(1–2): 3-22. doi: http://dx.doi.org/10.1016/S0040-6031(97)00325-0.

Hauser, V.L. 1978. Seepage control by particle size selection. Transactions of the ASAE **21**(4): 691-0695. doi: 10.13031/2013.35369.

Hauser, V.L. 2016. Evapotranspiration covers for landfills and waste sites. CRC Press.

Heath, D., and Tadros, T.F. 1983. Influence of pH, electrolyte, and poly (vinyl alcohol) addition on the rheological characteristics of aqueous dispersions of sodium montmorillonite. Journal of Colloid and Interface Science **93**(2): 307-319. doi: https://doi.org/10.1016/0021-9797(83)90415-0.

Heller, H., and Keren, R. 2002. Anionic polyacrylamide polymers effect on rheological behavior of sodium-montmorillonite suspensions. Soil Science Society of America Journal **66**(1): 19-25. doi: 10.2136/sssaj2002.1900.

Hirano, S., Kitaura, S., Sasaki, N., Sakaguchi, H., Sugiyama, M., Hashimoto, K., and Tanatani, A. 1996. Chitin biodegradation and wound healing in tree bark tissues. Journal of environmental polymer degradation **4**(4): 261-265. doi: 10.1007/bf02070695.

Hoare, T.R., and Kohane, D.S. 2008. Hydrogels in drug delivery: Progress and challenges. Polymer **49**(8): 1993-2007. doi: https://doi.org/10.1016/j.polymer.2008.01.027.

Hoffman, A.S. 2002. Hydrogels for biomedical applications. Advanced Drug Delivery Reviews **54**(1): 3-12. doi: http://dx.doi.org/10.1016/S0169-409X(01)00239-3.

Horace, B.L., Owen, J.W.L., and Owen, W.L. 1944. Production of mud-laden drilling fluids. Google Patents.

Hu, D.S.G., and Tsai, C.E. 1996. Correlation between interfacial free energy and albumin adsorption in poly (acrylonitrile–acrylamide–acrylic acid) hydrogels. Journal of applied polymer science **59**(12): 1809-1817. doi: https://doi.org/10.1002/(SICI)1097-4628(19960321)59:12<1809::AID-APP1>3.0.CO;2-U.

Huang, C., Chung, Y.-C., and Liou, M.-R. 1996. Adsorption of Cu (II) and Ni (II) by pelletized biopolymer. Journal of Hazardous Materials **45**(2-3): 265-277. doi: https://doi.org/10.1016/0304-3894(95)00096-8.

Huang, J.-p., Guan, X.-d., and Ji, F. 2012. Enhanced cold-season warming in semi-arid regions. Atmospheric Chemistry and Physics **12**(12): 5391-5398.

Huang, Z.-Q., Lu, J.-P., Li, X.-H., and Tong, Z.-F. 2007. Effect of mechanical activation on physico-chemical properties and structure of cassava starch. Carbohydrate polymers **68**(1): 128-135. doi: https://doi.org/10.1016/j.carbpol.2006.07.017.

Hufnagel, L., and Garamvölgyi, Á. 2014. Impacts of climate change on vegetation distribution No. 2 - Climate change induced vegetation shifts in the new world. Applied Ecology and Environmental Research **12**(2): 355-422. doi: 10.15666/aeer.

Igisu, H., Goto, I., Kawamura, Y., Kato, M., and Izumi, K. 1975. Acrylamide encephaloneuropathy due to well water pollution. Journal of Neurology, Neurosurgery & Psychiatry **38**(6): 581-584. doi: 10.1136/jnnp.38.6.581.

Imeson, A.P. 2012. Thickening and gelling agents for food. Springer Science & Business Media.

Islam, S., Bhuiyan, M.R., and Islam, M. 2017. Chitin and chitosan: structure, properties and applications in biomedical engineering. Journal of Polymers and the Environment **25**(3): 854-866. doi: https://doi.org/10.1007/s10924-016-0865-5.

Itasca. 2011. Fast Lagrangian analysis of continua. Version 7.0. Itasca Consulting Group Inc.,2011.

Ivanov, V., and Stabnikov, V. 2017. Construction Biotechnology. Biogeochemistry, Microbiology and Biotechnology of Construction Materials and Processes. Springer, Singapore.

Jansson, P.-E., Lindberg, B., and Sandford, P.A. 1983. Structural studies of gellan gum, an extracellular polysaccharide elaborated by Pseudomonas elodea. Carbohydrate Research **124**(1): 135-139. doi: https://doi.org/10.1016/0008-6215(83)88361-X.

Jeong, S., Kim, Y., Lee, J.K., and Kim, J. 2015. The 27 July 2011 debris flows at Umyeonsan, Seoul, Korea. Landslides **12**(4): 799-813. doi: https://doi.org/10.1007/s10346-015-0595-0.

Jhon, M.S., and Andrade, J.D. 1973. Water and hydrogels. Journal of biomedical materials research **7**(6): 509-522. doi: https://doi.org/10.1002/jbm.820070604.

Ji, F., Wu, Z., Huang, J., and Chassignet, E.P. 2014. Evolution of land surface air temperature trend. Nature Climate Change **4**: 462. doi: 10.1038/nclimate2223

https://www.nature.com/articles/nclimate2223#supplementary-information.

Jimtaisong, A., and Saewan, N. 2014. Utilization of carboxymethyl chitosan in cosmetics. International journal of cosmetic science **36**(1): 12-21. doi: https://doi.org/10.1111/ics.12102.

Johnson, D.I., and Urie, D.H. 1985. Landfill caps: Long term investments in need of attention. Waste management & research **3**(2): 143-148. doi: https://doi.org/10.1016/0734-242X(85)90072-2.

Kahr, G., and Madsen, F. 1995. Determination of the cation exchange capacity and the surface area of bentonite, illite and kaolinite by methylene blue adsorption. Applied Clay Science **9**(5): 327-336. doi: https://doi.org/10.1016/0169-1317(94)00028-O.

Kaplan, D.L. 1998. Introduction to biopolymers from renewable resources. *In* Biopolymers from renewable resources. Springer. pp. 1-29.

Karaborni, S., Smit, B., Heidug, W., Urai, J., and Van Oort, E. 1996a. The swelling of clays: molecular simulations of the hydration of montmorillonite. Science **271**(EPFL-ARTICLE-200818): 1102-1104. doi: 10.1126/science.271.5252.1102.

Karaborni, S., Smit, B., Heidug, W., Urai, J., and Van Oort, E. 1996b. The swelling of clays: molecular simulations of the hydration of montmorillonite. Science **271**(5252): 1102-1104. doi: 10.1126/science.271.5252.1102.

Karube, D. 1988. New Concept of Effective Stress in Unsaturated Soil and Its Proving Test. ASTM International. doi: 10.1520/STP29097S.

Karube, D., and Kawai, K. 2001. The role of pore water in the mechanical behavior of unsaturated soils. Geotechnical & Geological Engineering **19**(3-4): 211-241. doi: https://doi.org/10.1023/A:1013188200053.

Kato, A., Murata, K., and Kobayashi, K. 1988. Preparation and characterization of ovalbumin-dextran conjugate having excellent emulsifying properties. Journal of Agricultural and Food Chemistry **36**(3): 421-425. doi: 10.1021/jf00081a005.

Katzbauer, B. 1998. Properties and applications of xanthan gum. Polymer Degradation and Stability **59**(1–3): 81-84. doi: http://dx.doi.org/10.1016/S0141-3910(97)00180-8.

Kavazanjian, E., Iglesias, E., and Karatas, I. 2009. Biopolymer soil stabilization for wind erosion control. the 17th International Conference on Soil Mechanics and Geotechnical Engineering 881-884. doi: 10.3233/978-1-60750-031-5-881

Kawahara, S., Yoshikawa, A., Hiraoki, T., and Tsutsumi, A. 1996. Interactions of paramagnetic metal ions with gellan gum studied by ESR and NMR methods. Carbohydrate polymers **30**(2-3): 129-133.

Kazanskii, K., and Dubrovskii, S. 1992. Chemistry and physics of "agricultural" hydrogels. *In* Polyelectrolytes hydrogels chromatographic materials. Springer. pp. 97-133.

Khachatoorian, R., Petrisor, I.G., Kwan, C.-C., and Yen, T.F. 2003a. Biopolymer plugging effect: Laboratory-pressurized pumping flow studies. Journal of Petroleum Science and Engineering **38**(1-2): 13-21. doi: https://doi.org/10.1016/S0920-4105(03)00019-6.

Khachatoorian, R., Petrisor, I.G., Kwan, C.-C., and Yen, T.F. 2003b. Biopolymer plugging effect: laboratory-pressurized pumping flow studies. Journal of Petroleum Science and Engineering **38**(1–2): 13-21. doi: http://dx.doi.org/10.1016/S0920-4105(03)00019-6.

Khatami, H.R., and O'Kelly, B.C. 2012. Improving mechanical properties of sand using biopolymers. Journal of Geotechnical and Geoenvironmental Engineering **139**(8): 1402-1406. doi: https://doi.org/10.1061/(ASCE)GT.1943-5606.0000861.

Khayat, K., and Yahia, A. 1998. Simple field tests to characterize fluidity and washout resistance of structural cement grout. Cement, Concrete and Aggregates **20**(1): 145-156. doi: 10.1520/CCA10448J.

Khayat, K.H. 1998. Viscosity-enhancing admixtures for cement-based materials - An overview. Cement & Concrete Composites **20**(2-3): 171-188.

Khayat, K.H., and Yahia, A. 1997. Effect of welan gum high-range water reducer combinations on rheology of cement grout. Aci Materials Journal **94**(5): 365-372.

Khullar, P., Khar, R.K., and Agarwal, S.P. 1998. Evaluation of guar gum in the preparation of sustained-release matrix tablets. Drug development and industrial pharmacy **24**(11): 1095-1099.

Klute, A. 1965. Laboratory measurement of hydraulic conductivity of saturated soil. Methods of soil analysis. Part 1. Physical and mineralogical properties, including statistics of measurement and sampling(methodsofsoilana): 210-221.

Kolla, P., Köhler, J., and Schomburg, G. 1987. Polymer-coated cation-exchange stationary phases on the basis of silica. Chromatographia **23**(7): 465-472. doi: https://doi.org/10.1007/BF02309412.

Koupai, J.A., Eslamian, S.S., and Kazemi, J.A. 2008. Enhancing the available water content in unsaturated soil zone using hydrogel, to improve plant growth indices. Ecohydrology & Hydrobiology **8**(1): 67-75. doi: https://doi.org/10.2478/v10104-009-0005-0.

Krishnan, K.A., Sreejalekshmi, K., and Baiju, R. 2011. Nickel (II) adsorption onto biomass based activated carbon obtained from sugarcane bagasse pith. Bioresource Technology **102**(22): 10239-10247. doi: https://doi.org/10.1016/j.biortech.2011.08.069.

Kulicke, W.-M., Lettau, A.I., and Thielking, H. 1997. Correlation between immunological activity, molar mass, and molecular structure of different (1→ 3)-β-D-glucans. Carbohydrate Research **297**(2): 135-143.

Kulshreshtha, Y., Schlangen, E., Jonkers, H., Vardon, P., and Van Paassen, L. 2017. CoRncrete: A corn starch based building material. Construction and Building Materials **154**: 411-423.

Lagaly, G. 1989. Principles of flow of kaolin and bentonite dispersions. Applied Clay Science **4**(2): 105-123. doi: https://doi.org/10.1016/0169-1317(89)90003-3.

Laliberte, G. 1969. A mathematical function for describing capillary pressure-desaturation data. Hydrological Sciences Journal **14**(2): 131-149. doi: https://doi.org/10.1080/02626666909493724.

Lapasin, R. 2012. Rheology of industrial polysaccharides: theory and applications. Springer Science & Business Media.

Larson, S.L., Newman, J.K., Griggs, C.S., Beverly, M., and Nestler, C.C. 2012. Biopolymers as an alternative to petroleum-based polymers for soil modification, ESTCP ER-0920: Treatability studies. ARMY CORPS OF ENGINEERS VICKSBURG MS ENGINEER RESEARCH AND DEVELOPMENT CENTER.

Latifi, N., Horpibulsuk, S., Meehan, C.L., Abd Majid, M.Z., Tahir, M.M., and Mohamad, E.T. 2016. Improvement of problematic soils with biopolymer—an environmentally friendly soil stabilizer. Journal of Materials in Civil Engineering **29**(2): 04016204.

Lázaro, N., Sevilla, A.L., Morales, S., and Marqués, A.M. 2003. Heavy metal biosorption by gellan gum gel beads. Water research **37**(9): 2118-2126. doi: https://doi.org/10.1016/S0043-1354(02)00575-4.

Lee, C.S., Robinson, J., and Chong, M.F. 2014. A review on application of flocculants in wastewater treatment. Process Safety and Environmental Protection **92**(6): 489-508. doi: https://doi.org/10.1016/j.psep.2014.04.010.

Lee, W.-K., Lim, Y.-Y., Leow, A.T.-C., Namasivayam, P., Abdullah, J.O., and Ho, C.-L. 2017. Biosynthesis of agar in red seaweeds: A review. Carbohydrate polymers **164**: 23-30. doi: https://doi.org/10.1016/j.carbpol.2017.01.078.

Lehrsch, G., Sojka, R., Reed, J., Henderson, R., and Kostka, S. 2011. Surfactant and irrigation effects on wettable soils: runoff, erosion, and water retention responses. Hydrological Processes **25**(5): 766-777. doi: https://doi.org/10.1002/hyp.7866

Lejcuś, K., Śpitalniak, M., and Dąbrowska, J. 2018. Swelling behaviour of superabsorbent polymers for soil amendment under different loads. Polymers **10**(3): 271. doi: https://doi.org/10.3390/polym10030271.

Lentz, R.D., Sojka, R.E., Carter, D.L., and Shainberg, I. 1992. Preventing irrigation furrow erosion with small applications of polymers. Soil Science Society of America Journal **56**(6): 1926-1932. doi: 10.2136/sssaj1992.03615995005600060046x.

Leong, E.C., and Rahardjo, H. 1997. Review of soil-water characteristic curve equations. Journal of geotechnical and geoenvironmental engineering **123**(12): 1106-1117.

Lévesque, S.G., Lim, R.M., and Shoichet, M.S. 2005. Macroporous interconnected dextran scaffolds of controlled porosity for tissue-engineering applications. Biomaterials **26**(35): 7436-7446. doi: https://doi.org/10.1016/j.biomaterials.2005.05.054.

Liu, X.D., Tokura, S., Haruki, M., Nishi, N., and Sakairi, N. 2002. Surface modification of nonporous glass beads with chitosan and their adsorption property for transition metal ions. Carbohydrate Polymers **49**(2): 103-108.

Lourenco, S., Gallipoli, D., Augarde, C.E., Toll, D.G., Fisher, P.C., and Congreve, A. 2012. Formation and evolution of water menisci in unsaturated granular media. Géotechnique **62**(3): 193-199. doi: http://dx.doi.org/10.1680/geot.11.P.034.

Lu, N., and Likos, W.J. 2004. Unsaturated soil mechanics. J. Wiley.

Lutton, R.J., Regan, G., and Jones, L.W. 1979. Design and construction of covers for solid waste landfills. Environmental Protection Agency, Office of Research and Development ….

Maghchiche, A., Haouam, A., and Immirzi, B. 2010. Use of polymers and biopolymers for water retaining and soil stabilization in arid and semiarid regions. Journal of Taibah University for Science **4**: 9-16. doi: https://doi.org/10.1016/S1658-3655(12)60022-3.

Makusa, G.P. 2012. Soil stabilization methods and materials. Lulea, Sweden: sn.

Mani, S., Khabaz, F., Godbole, R.V., Hedden, R.C., and Khare, R. 2015. Structure and hydrogen bonding of water in polyacrylate gels: Effects of polymer hydrophilicity and water concentration. The Journal of Physical Chemistry B **119**(49): 15381-15393. doi: 10.1021/acs.jpcb.5b08700.

Marcotte, M., Hoshahili, A.R.T., and Ramaswamy, H. 2001. Rheological properties of selected hydrocolloids as a function of concentration and temperature. Food Research International **34**(8): 695-703. doi: https://doi.org/10.1016/S0963-9969(01)00091-6.

Marinari, S., Masciandaro, G., Ceccanti, B., and Grego, S. 2000. Influence of organic and mineral fertilisers on soil biological and physical properties. Bioresource Technology **72**(1): 9-17. doi: https://doi.org/10.1016/S0960-8524(99)00094-2.

Marten, D.A., and Frankenberger, W.T. 1992. Modification of infiltration rates in an organic-amended irrigated. Agronomy Journal **84**(4): 707-717. doi: 10.2134/agronj1992.00021962008400040032x.

Mazumder, M., Sriraman, V., Kim, H.H., and Lee, S.-J. 2016. Quantifying the environmental burdens of the hot mix asphalt (HMA) pavements and the production of warm mix asphalt (WMA). International Journal of Pavement Research and Technology **9**(3): 190-201.

McKee, C., and Bumb, A. 1987. Flow-testing coalbed methane production wells in the presence of water and gas. SPE formation Evaluation **2**(04): 599-608. doi: https://doi.org/10.2118/14447-PA.

Mitchell, J., and Santamarina, J. 2005. Biological Considerations in Geotechnical Engineering. Journal of Geotechnical and Geoenvironmental Engineering **131**(10): 1222-1233. doi: 10.1061/(ASCE)1090-0241(2005)131:10(1222).

Mitchell, J.K. 1993. Fundamentals of soil behavior. John Wiley and Sons, Inc.

Mitchell, J.K., and Soga, K. 2005. Fundamentals of soil behavior. 3rd ed. John Wiley & Sons, Hoboken, N.J.

Miyoshi, E., and Nishinari, K. 1999. Non-Newtonian flow behaviour of gellan gum aqueous solutions. Colloid and Polymer Science **277**(8): 727-734. doi: https://doi.org/10.1007/s0039600504.

Mogollon, L., Rodriguez, R., Larrota, W., Ramirez, N., and Torres, R. 1998. Biosorption of nickel using filamentous fungi. Biotechnology for Fuels and Chemicals: 593-601. doi: https://doi.org/10.1007/978-1-4612-1814-2_54.

Mualem, Y. 1976a. A new model for predicting the hydraulic conductivity of unsaturated porous media. Water resources research **12**(3): 513-522. doi: https://doi.org/10.1029/WR012i003p00513

Mualem, Y. 1976b. Hysteretical models for prediction of the hydraulic conductivity of unsaturated porous media. Water resources research **12**(6): 1248-1254. doi: https://doi.org/10.1029/WR012i006p01248.

Mudgil, D., Barak, S., and Khatkar, B.S. 2014. Guar gum: processing, properties and food applications—a review. Journal of food science and technology **51**(3): 409-418.

Mukherjee, S., Mukhopadhyay, S., Zafri, M.Z.B., Zhan, X., Hashim, M.A., and Gupta, B.S. 2018. Application of guar gum for the removal of dissolved lead from wastewater. Industrial Crops and Products **111**: 261-269. doi: https://doi.org/10.1016/j.indcrop.2017.10.022.

Mulqueen, J. 2005. The flow of water through gravels. Irish Journal of Agricultural and Food Research **44**(1): 83-94.

Mustafa, M.A., Al-Darby, A.M., Al-Omran, A.M., and Mursi, M. 1989. Impact of a gel conditioner and water quality upon soil infiltration. Irrigation Science **10**(3): 169-176. doi: https://doi.org/10.1007/BF00257950.

Myriam, N., An, C., Wim, S., and J, V.E. 2005. Leuconostoc dextransucrase and dextran: production, properties and applications. Journal of Chemical Technology & Biotechnology **80**(8): 845-860. doi: doi:10.1002/jctb.1322.

Nachtergaele, W. 1989. The Benefits of Cationic Starches for the Paper Industry. Starch - Stärke **41**(1): 27-31. doi: doi:10.1002/star.19890410108.

Nagy, E., and Deák, Á.J. 2013. Investigation of water capillary rise in soil columns made from clay mineral mixtures pretreated with cationic surfactants. Communications in soil science and plant analysis **44**(1-4): 749-757. doi: https://doi.org/10.1080/00103624.2013.748130.

Nakano, M., Nakamura, Y., Takikawa, K., Kouketsu, M., and Arita, T. 1979. Sustained release of sulphamethizole from agar beads. Journal of Pharmacy and Pharmacology **31**(12): 869-872.

Narjary, B., Aggarwal, P., Singh, A., Chakraborty, D., and Singh, R. 2012. Water availability in different soils in relation to hydrogel application. Geoderma **187**: 94-101. doi: https://doi.org/10.1016/j.geoderma.2012.03.002.

Nasser, M., and James, A. 2007. Effect of polyacrylamide polymers on floc size and rheological behaviour of kaolinite suspensions. Colloids and Surfaces A: Physicochemical and Engineering Aspects **301**(1-3): 311-322. doi: https://doi.org/10.1016/j.colsurfa.2006.12.080.

Neethu, T., Dubey, P., and Kaswala, A. 2018. Prospects and Applications of Hydrogel Technology in Agriculture. Int. J. Curr. Microbiol. App. Sci **7**(5): 3155-3162. doi: https://doi.org/10.20546/ijcmas.2018.705.369.

Nugent, R.A., Zhang, G., and Gambrell, R.P. 2009. Effect of exopolymers on the liquid limit of clays and its engineering implications. Transportation Research Record **2101**(1): 34-43. doi: https://doi.org/10.3141/2101-05.

Oliveira, J.T., Martins, L., Picciochi, R., Malafaya, P.B., Sousa, R.A., Neves, N.M., Mano, J.F., and Reis, R.L. 2010. Gellan gum: a new biomaterial for cartilage tissue engineering applications. J Biomed Mater Res A **93**(3): 852-863. doi: 10.1002/jbm.a.32574.

Oller, A.R., Costa, M., and Oberdörster, G. 1997. Carcinogenicity assessment of selected nickel compounds. Toxicology and applied pharmacology **143**(1): 152-166.

Orts, W., Roa-Espinosa, A., Sojka, R., Glenn, G., Imam, S., Erlacher, K., and Pedersen, J. 2007. Use of synthetic polymers and biopolymers for soil stabilization in agricultural, construction, and military applications. Journal of Materials in Civil Engineering **19**(1): 58-66. doi: https://doi.org/10.1061/(ASCE)0899-1561(2007)19:1(58).

Orts, W.J., Sojka, R.E., and Glenn, G.M. 2000. Biopolymer additives to reduce erosion-induced soil losses during irrigation. Industrial Crops and Products **11**(1): 19-29. doi: https://doi.org/10.1016/S0926-6690(99)00030-8.

Osacky, M., Geramian, M., Ivey, D.G., Liu, Q., and Etsell, T.H. 2015. Influence of Nonswelling Clay Minerals (Illite, Kaolinite, and Chlorite) on Nonaqueous Solvent Extraction of Bitumen. Energy & Fuels **29**(7): 4150-4159. doi: 10.1021/acs.energyfuels.5b00269.

Osmałek, T., Froelich, A., and Tasarek, S. 2014. Application of gellan gum in pharmacy and medicine. International Journal of Pharmaceutics **466**(1): 328-340. doi: https://doi.org/10.1016/j.ijpharm.2014.03.038.

Ottenbrite, R.M., Park, K., Okana, T., and Peppas, N.A. 2010. Biomedical Application of Hydrogels Handbook. Springer, New York.

Pacheco-Torgal, F., and Jalali, S. 2011. Nanotechnology: advantages and drawbacks in the field of construction and building materials. Construction and building materials **25**(2): 582-590. doi: https://doi.org/10.1016/j.conbuildmat.2010.07.009.

Palaniraj, A., and Jayaraman, V. 2011. Production, recovery and applications of xanthan gum by Xanthomonas campestris. Journal of Food Engineering **106**(1): 1-12. doi: http://dx.doi.org/10.1016/j.jfoodeng.2011.03.035.

Panda, G., Das, S., Bandopadhyay, T., and Guha, A. 2007. Adsorption of nickel on husk of Lathyrus sativus: behavior and binding mechanism. Colloids and Surfaces B: Biointerfaces **57**(2): 135-142. doi: https://doi.org/10.1016/j.colsurfb.2007.01.022.

Panda, G., Das, S., Chatterjee, S., Maity, P., Bandopadhyay, T., and Guha, A. 2006. Adsorption of cadmium on husk of Lathyrus sativus: Physico-chemical study. Colloids and Surfaces B: Biointerfaces **50**(1): 49-54. doi: https://doi.org/10.1016/j.colsurfb.2006.03.022.

Parija, S., Misra, M., and Mohanty, A. 2001. Studies of natural gum adhesive extracts: an overview. Journal of Macromolecular Science, Part C: Polymer Reviews **41**(3): 175-197.

Pasqui, D., De Cagna, M., and Barbucci, R. 2012. Polysaccharide-based hydrogels: the key role of water in affecting mechanical properties. Polymers **4**(3): 1517-1534. doi: https://doi.org/10.3390/polym4031517.

Peng, X.-W., Zhong, L.-X., Ren, J.-L., and Sun, R.-C. 2012. Highly effective adsorption of heavy metal ions from aqueous solutions by macroporous xylan-rich hemicelluloses-based hydrogel. Journal of agricultural and food chemistry **60**(15): 3909-3916. doi: 10.1021/jf300387q.

Pham, H.Q., Fredlund, D.G., and Barbour, S.L. 2005. A study of hysteresis models for soil-water characteristic curves. Canadian Geotechnical Journal **42**(6): 1548-1568. doi: https://doi.org/10.1139/t05-071.

Pierre, C., Demangeon, F., and Yves, H. 1993. Bituminous binder emulsion with a viscosity controlled by addition of scleroglucan. Google Patents.

Pini, R., Canarutto, S., and Guidi, G.V. 1994. Soil microaggregation as influenced by uncharged organic conditioners. Communications in Soil Science and Plant Analysis **25**(11-12): 2215-2229. doi: 10.1080/00103629409369183.

Plaster, E. 2013. Soil science and management. Cengage learning.

Poli, A., Di Donato, P., Abbamondi, G.R., and Nicolaus, B. 2011. Synthesis, production, and biotechnological applications of exopolysaccharides and polyhydroxyalkanoates by archaea. Archaea **2011**. doi: 10.1155/2011/693253.

Prashanth, J.P., Sivapullaiah, P. V., & Sridharan, A. 2001. Pozzolanic fly ash as a hydraulic barrier in land fills. Engineering Geology **60**(1-4): 245-252. doi: https://doi.org/10.1016/S0013-7952(00)00105-8.

Preocanin, T., Abdelmonem, A., Montavon, G., and Luetzenkirchen, J. 2016. Charging Behavior of Clays and Clay Minerals in Aqueous Electrolyte Solutions—Experimental Methods for Measuring the Charge and Interpreting the Results. *In* Clays, Clay Minerals and Ceramic Materials Based on Clay Minerals. IntechOpen.

Rathor, G., Chopra, N., & Adhikari, T. . 2014. Nickel as a pollutant and its management. Int. Res. J. Environ. Sci **3**: 94-98.

Razakamanantsoa, A., Djeran-Maigre, I., and Barast, G. 2014. Characterisation of bentonite polymer for bottom liner use. Environmental Geotechnics **3**(1): 28-35. doi: https://doi.org/10.1680/envgeo.13.00095.

Renault, F., Sancey, B., Badot, P.M., and Crini, G. 2009. Chitosan for coagulation/flocculation processes – An eco-friendly approach. European Polymer Journal **45**(5): 1337-1348. doi: https://doi.org/10.1016/j.eurpolymj.2008.12.027.

Risica, D., Dentini, M., and Crescenzi, V. 2005. Guar gum methyl ethers. Part I. Synthesis and macromolecular characterization. Polymer **46**(26): 12247-12255.

Ritzema, H. 2006. Drainage principles and applications. ILRI.

Rodrigues, A., and Emeje, M. 2012. Recent applications of starch derivatives in nanodrug delivery. Carbohydrate Polymers **87**(2): 987-994. doi: https://doi.org/10.1016/j.carbpol.2011.09.044.

Roering, J.J., Schmidt, K.M., Stock, J.D., Dietrich, W.E., and Montgomery, D.R. 2003. Shallow landsliding, root reinforcement, and the spatial distribution of trees in the Oregon Coast Range. Canadian Geotechnical Journal **40**(2): 237-253. doi: 10.1139/t02-113.

Rong, H., Qian, C., and Wang, R. 2011. A cementation method of loose particles based on microbe-based cement. Science China Technological Sciences **54**(7): 1722-1729. doi: https://doi.org/10.1007/s11431-011-4408-y.

Rydh, C.J., and Karlström, M. 2002. Life cycle inventory of recycling portable nickel–cadmium batteries. Resources, Conservation and Recycling **34**(4): 289-309. doi: https://doi.org/10.1016/S0921-3449(01)00114-8.

Sällfors, G., and Öberg-Högsta, A.-L. 2002. Determination of hydraulic conductivity of sand-bentonite mixtures for engineering purposes. Geotechnical & Geological Engineering **20**(1): 65-80. doi: https://doi.org/10.1023/A:1013857823676.

Seilkop, S.K., and Oller, A.R. 2003. Respiratory cancer risks associated with low-level nickel exposure: an integrated assessment based on animal, epidemiological, and mechanistic data. Regulatory Toxicology and Pharmacology **37**(2): 173-190.

Seki, K. 2007. SWRC fit - a nonlinear fitting program with a water retention curve for soils having unimodal and bimodal pore structure. Hydrology and Earth System Sciences Discussions **4**(1): 407-437. doi: https://doi.org/10.5194/hessd-4-407-2007.

Shaikh, S.M., Nasser, M.S., Hussein, I., Benamor, A., Onaizi, S.A., and Qiblawey, H. 2017. Influence of polyelectrolytes and other polymer complexes on the flocculation and rheological behaviors of clay minerals: A comprehensive review. Separation and Purification Technology **187**: 137-161. doi: https://doi.org/10.1016/j.seppur.2017.06.050.

Sivapullaiah, P., Sridharan, A., and Stalin, V. 2000. Hydraulic conductivity of bentonite-sand mixtures. Canadian geotechnical journal **37**(2): 406-413. doi: https://doi.org/10.1139/t99-120.

Smitha, S., and Sachan, A. 2016. Use of agar biopolymer to improve the shear strength behavior of sabarmati sand. International Journal of Geotechnical Engineering **10**(4): 387-400. doi: 10.1080/19386362.2016.1152674.

Sonebi, M. 2006. Rheological properties of grouts with viscosity modifying agents as diutan gum and welan gum incorporating pulverised fly ash. Cement and Concrete Research **36**(9): 1609-1618.

Soon, N., Lee, L., Khun, T., and Ling, H. 2013. Improvements in engineering properties of soils through microbial-induced calcite precipitation. KSCE Journal of Civil Engineering **17**(4): 718-728. doi: 10.1007/s12205-013-0149-8.

Stabnikov, V., Ivanov, V., and Chu, J. 2015. Construction Biotechnology: a new area of biotechnological research and applications. World J Microbiol Biotechnol **31**(9): 1303-1314. doi: 10.1007/s11274-015-1881-7.

Stojakovic, D., Milenkovic, J., Daneu, N., and Rajic, N. 2011. A study of the removal of copper ions from aqueous solution using clinoptilolite from Serbia. Clays and Clay Minerals **59**(3): 277-285. doi: https://doi.org/10.1346/CCMN.2011.0590305.

Survase, S.A., Saudagar, P.S., Bajaj, I.B., and Singhal, R.S. 2007. Scleroglucan: fermentative production, downstream processing and applications. Food Technology and Biotechnology **45**(2): 107.

Takahashi, N., and Kuroda, K. 2011. Materials design of layered silicates through covalent modification of interlayer surfaces. Journal of Materials Chemistry **21**(38): 14336-14353. doi: 10.1039/C1JM10460H.

Takanabe, H., Kiba, A., and Kodama, K. 2001. Cosmetic composition. Google Patents.

Tami, D., Rahardjo, H., and Leong, E.-C. 2004. Effects of hysteresis on steady-state infiltration in unsaturated slopes. Journal of Geotechnical and Geoenvironmental Engineering **130**(9): 956-967. doi: https://doi.org/10.1061/(ASCE)1090-0241(2004)130:9(956).

Tanaka, Y., Uryu, T., and Yaguchi, M. 1996. Cement compositions containing a sulfated polysaccharide and method. Google Patents.

Tang, Y., Hu, X., Zhang, X., Guo, D., Zhang, J., and Kong, F. 2016. Chitosan/titanium dioxide nanocomposite coatings: Rheological behavior and surface application to cellulosic paper. Carbohydrate polymers **151**: 752-759. doi: https://doi.org/10.1016/j.carbpol.2016.06.023.

Tao, H., Chen, C., Jiang, P., and Tang, L. 2017. Soil water characteristic curves based on particle analysis. Procedia engineering **174**: 1289-1295. doi: https://doi.org/10.1016/j.proeng.2017.01.273.

Terzaghi, K. 1943. Theoretical Soil Mechanics. John Wiley, New York.

Tirtaatmadja, V., Dunstan, D.E., and Boger, D.V. 2001. Rheology of dextran solutions. Journal of Non-Newtonian Fluid Mechanics **97**(2-3): 295-301. doi: https://doi.org/10.1016/S0377-0257(00)00226-3.

Townsend, T.G., Powell, J., Jain, P., Xu, Q., Tolaymat, T., and Reinhart, D. 2015. Sustainable practices for landfill design and operation. Springer.

Tran, A.T.P., Chang, I., and Cho, G.-C. 2019a. Soil water retention and vegetation survivabiity improvement using microbial biopolymers in drylands. Geomechanics and Engineering **17**(5): 475-483. doi: http://dx.doi.org/10.12989/gae.2019.17.5.475.

Tran, A.T.P., Chang, I., and Cho, G.-C. 2019b. Wetting soil-water characteristics of xanthan gum biopolymer-treated soils. Canadian Geotechnical Journal: NRC research Press, (under review).

Tsutsumi, A., Ya, D., Hiraoki, T., Mochiku, H., Yamaguchi, R., and Takahashi, N. 1993. ESR studies of Mn (II) binding to gellan and carrageenan gels. Food hydrocolloids **7**(5): 427-434. doi: https://doi.org/10.1016/S0268-005X(09)80238-5.

van Genuchten, M.T. 1980. A closed-form equation for predicting the hydraulic conductivity of unsaturated soils. Soil science society of America journal **44**(5): 892-898. doi: 10.2136/sssaj1980.03615995004400050002x.

van Genuchten, M.T., and Nielsen, D. 1985. On describing and predicting the hydraulic properties. *In* Annales Geophysicae. pp. 615-628.

Vanapalli, S., Fredlund, D., Pufahl, D., and Clifton, A. 1996. Model for the prediction of shear strength with respect to soil suction. Canadian Geotechnical Journal **33**(3): 379-392.

Velimirovic, M., Tosco, T., Uyttebroek, M., Luna, M., Gastone, F., De Boer, C., Klaas, N., Sapion, H., Eisenmann, H., Larsson, P.-O., Braun, J., Sethi, R., and Bastiaens, L. 2014. Field assessment of guar gum stabilized microscale zerovalent iron particles for in-situ remediation of 1,1,1-trichloroethane. Journal of Contaminant Hydrology **164**: 88-99. doi: https://doi.org/10.1016/j.jconhyd.2014.05.009.

Viñarta, S.C., François, N.J., Daraio, M.E., Figueroa, L.I., and Fariña, J.I. 2007. Sclerotium rolfsii scleroglucan: The promising behavior of a natural polysaccharide as a drug delivery vehicle, suspension stabilizer and emulsifier. International journal of biological macromolecules **41**(3): 314-323.

Vishnuvarthanan, M., and Rajeswari, N. 2013. Additives for enhancing the drying properties of adhesives for corrugated boards. Alexandria Engineering Journal **52**(1): 137-140. doi: https://doi.org/10.1016/j.aej.2012.10.002.

Wang, X., Zheng, Y., and Wang, A. 2009. Fast removal of copper ions from aqueous solution by chitosan-g-poly (acrylic acid)/attapulgite composites. Journal of Hazardous Materials **168**(2-3): 970-977. doi: https://doi.org/10.1016/j.jhazmat.2009.02.120.

Wang, Y., Lauten, R.A., and Peng, Y. 2016. The effect of biopolymer dispersants on copper flotation in the presence of kaolinite. Minerals Engineering **96**: 123-129. doi: https://doi.org/10.1016/j.mineng.2016.05.010.

Whiffin, V.S., van Paassen, L.A., and Harkes, M.P. 2007. Microbial carbonate precipitation as a soil improvement technique. Geomicrobiology Journal **24**(5): 417-423. doi: 10.1080/01490450701436505.

Whistler, R.L., and Hymowitz, T. 1979. Guar: agronomy, production, industrial use, and nutrition. Purdue University Press.

Williams, P.J. 1982. The surface of the earth: an introduction to geotechnical science. Addison-Wesley Longman Ltd.

Wu, A., Sun, Y., and Liu, X.-p. 2008. Granular dynamic theory and its applications. Springer.

Yang, H., Rahardjo, H., Leong, E.-C., and Fredlund, D.G. 2004. Factors affecting drying and wetting soil-water characteristic curves of sandy soils. Canadian Geotechnical Journal **41**(5): 908-920. doi: https://doi.org/10.1139/t04-042.

Yang, J., Wang, F., Fang, L., and Tan, T. 2007. Synthesis, characterization and application of a novel chemical sand-fixing agent-poly (aspartic acid) and its composites. Environmental Pollution **149**(1): 125-130.

Yaseen, E., Herald, T., Aramouni, F., and Alavi, S. 2005. Rheological properties of selected gum solutions. Food Research International **38**(2): 111-119. doi: https://doi.org/10.1016/j.foodres.2004.01.013.

Yvin, J.C., Cruz, F., Joubert, J.M., Cloarec, B., Richard, C., Plesse, B., Kopp, M., and Fritig, B. 2002. Method for stimulating natural control system of plants. Laboratories Goemar S.A. p. 8.

Zemmouri, H., Drouiche, M., Sayeh, A., Lounici, H., and Mameri, N. 2013. Chitosan Application for Treatment of Beni-Amrane's Water Dam. Energy Procedia **36**: 558-564. doi: https://doi.org/10.1016/j.egypro.2013.07.064.

Zhan, X.-B., Lin, C.-C., and Zhang, H.-T. 2012. Recent advances in curdlan biosynthesis, biotechnological production, and applications. Applied microbiology and biotechnology **93**(2): 525-531.

Zhang, H., Fang, B., Lu, Y., Qiu, X., Jin, H., Liu, Y., Wang, L., Tian, M., and Li, K. 2016. Rheological Properties of Water-Soluble Crosslinked Xanthan Gum. Journal of Dispersion Science and Technology: null-null. doi: https://doi.org/10.1080/01932691.2016.1169929.

Zhang, L., Zeng, Y., & Cheng, Z. 2016. Removal of heavy metal ions using chitosan and modified chitosan: A review. Journal of Molecular Liquids **214**: 175-191. doi: https://doi.org/10.1016/j.molliq.2015.12.013.

Zhou, Z., and Gunter, W.D. 1992. The nature of the surface charge of kaolinite. Clays and Clay minerals **40**(3): 365-368. doi: https://doi.org/10.1346/CCMN.1992.0400320.

Acknowledgment

It is hard to express my gratitude to those who have been with me through the previous five years. There were many times I wondered if I could ever complete my degree, and they were there for me to give spiritual supports

I would first like to express my gratitude to my supervisor, Professor Gye-Chun Cho, and Professor Ilhan Chang from UNSW for guiding me, encouraging me, and strengthening my focus during the entire process. I greatly appreciate your understanding and kindness.

I also appreciate all the help I received from my labmates. Thank you for making my research life smoother. Thank you Chang-Ho Hong, YoHan Cha, Joo-Young Im, Ji-Won Kim, Jung-Tae Kim, Chul-Whan Kang, Yeong-Man Kwon, Min-Hyeong Lee, Seok-Jun Kang, Jun Beom An, Hyun-Joong Hwang, and Jin Kim. Moreover, I want to thank my senior Ah-Ram Kim who gave me helpful advice on my studies.

I would like to especially thank my special sister, Munsuk. She takes care of me as well as all of the members with the love of a true sister. She gives me life tips, encourages me, and helps me as much as she can. She is my special treasure that makes my life in Korea much pleasant.

I would like to acknowledge my close friend Hoon Cho for making sure that my life at KAIST included research, sports, and fantastic food. I appreciate you and the many years of friendship you have provided.

I have been fortunate to have a close family to provide me their friendships, their loves. Thank you for always loving me.

I would like to thank Hue University of Sciences, and colleagues of the Hydrogeology and Engineering Geological Department for encouraging me to study abroad.

Special thanks do to my committee member Prof. Gye-Chun Cho, Prof. Seung-Rae Lee, Prof. Dong-Soo Kim, Prof. Tae-Hyuk Kwon, Dr. Mun-Kyeong Chung, and Prof. Ilhan Chang for their recommendations that helped shape my thesis.

The acknowledgments would not be complete without thanking Jesus Christ for the uncountable prayers that have been answered for over four years.

CURRICULUM VITAE

TRAN THI PHUONG AN

Nationality: Vietnamese

Date of birth: March 31st, 1987

EDUCATION

Korean Advanced Institute of Science and Technology (KAIST) 2014~ now
Ph.D. student

Yamaguchi University, Japan MA Civil Engineering 2012-2014
Graded: GPA 3.35/4.0
Thesis: *Effect of creep on consolidation behavior of saturated clay under cyclic loading*

Hue University of Sciences, Vietnam BA Geology 2005-2009
Graded: Distinction (8.08/10)
Thesis: "*Evaluation of Geological Engineering condition for high rise Danang Center, and proper suggestions for foundation solution.*"

EXPERIENCES

Lecturer at Hue University of Sciences 2011-2012
Faculty of Hydrogeology and Engineering Geological Department,
Hue University of Sciences

Teaching Assistant at Hue University of Sciences 2009-2011
Faculty of Hydrogeology and Engineering Geological Department,
Hue University of Sciences

LIST OF PUBLICATION

International journal

1. Im, Jooyoung, **An TP Tran**, Ilhan Chang, and Gye-Chun Cho (2017). Dynamic properties of gel-type biopolymer-treated sands evaluated by Resonant Column (RC) tests. *Geomechanics and Engineering* 12(5), 815-830.
2. **Tran, A.T.P**, Chang, I., and Cho, G.-C. (2019). Soil water retention and vegetation survivability improvement using microbial biopolymers in drylands. *Geomechanics and Engineering* 17(5), 475-483, doi: http://dx.doi.org/10.12989/gae.2019.17.5.475.
3. **Tran, An T.P**., Ah-Ram Kim, and Gye-Chun Cho (2019). Numerical modeling on the stability

of slope with foundation during rainfall. *Geomechanics and Engineering* 17(1), 109-118**,** https://doi.org/10.12989/gae.2019.17.1.109

4. **Tran, A.T.P**, Chang, I., and Cho, G.-C. 2019b. Wetting soil-water characteristics of xanthan gum biopolymer-treated soils. Canadian Geotechnical Journal: NRC research Press, (under review)

Conferences

1. Cho, G. C., **Tran, A.T.P**, Kim, A. R., & Kim, D. H. (2015, November). Numerical Modeling on the Stability of A Pile-Reinforced Slope. In the 28th KKHTCNN symposium on Civil Engineering, Thailand.
2. Im, Jooyoung, **Tran, A.T.P**, Park, Jin-Won, Chang, Ilhan, Cho, Gye-Chun (2016). Introduction of a slope surface protection method using biopolymer based bio-soil compound. KSCE 2016 CONVENTION PROGRAM, 2016.10, 163-164
3. **Tran, A.T.P**, Sim, Y., Kim, A.R., Cho, G.C., & Kim, D. H (2016). Numerical Modeling of Rainfall-induced Slope Failure. The 2016 World Congress on Advances in Civil, Environmental, and Materials Research (ACEM16)
4. **An T.P. Tran**, Jooyoung Im, Ilhan Chang, Gye-Chun Cho (2017). Numerical analysis on stability of a biopolymer – treated cut slope. KGS Spring National Conference 2017 / March 16-17, 2017 / Seoul / Korea, Page 52
5. **Tran, T. P. A.**, Im, J., Cho, G. C., & Chang, I. (2017) Soil–water characteristics of xanthan gum biopolymer containing soils. Proceedings of the 19th International Conference on Soil Mechanics and Geotechnical Engineering, Seoul 2017, pp 1091 – 1094
6. **An T.P. Tran**, Ilhan Chang, Jooyoung Im, Gye-Chun Cho (2017). Capillary conductivity of xanthan gum treated clayey soils at low soil suction. In the 30th KKHTCNN symposium on Civil Engineering, November 2-4, Taiwan.
7. **Tran, T. P. A.**, Cho, G. C., Chang, I., & Lee, S. (2018). Effect of xanthan gum biopolymer on the water retention characteristics of unsaturated sand. In International Conference on Unsaturated Soil. International Society for Soil Mechanics and Geotechnical Engineering.
8. **Tran, An TP**, Ilhan Chang, Jooyoung Im, and Gye-Chun Cho (2018). "Biopolymer application for soil moisture retention and vegetation growth improvement in sand." In ACEM18. International Association of Structural engineering and mechanics.
9. Lee, S., **Tran, T. P. A.**, Chang, I., & Cho, G. C. (2018). Introduction of a vegetation–friendly bio-based soil binder. In 11ICG. Korean Geosynthetics Society.
10. **Tran, T. P. A.**, Cho, H., Im, J., Chang, I., Cho, G. C., & Han, J. I. (2018). Removal of heavy metal ion using biopolymers-soils. In 31st KKHTCNN Symposium on Civil Engineering. Kyoto University.
11. Chang, I., **Tran, T.P.A.**, and Cho, G.C. (2019). Introduction of biopolymer-based materials for ground hydraulic conductivity control". WTC2019, ITA-AITES General Assembly and World Tunnel Congress, 3rd – 9th May, 2019, Naples.